QUANTIFYING THE FREQUENCY OF FLASH DROUGHT IN THE SOUTHEASTERN UNITED STATES AND ESTIMATING ITS EFFECT ON CROP YIELDS

by

JASIA JANNAT

(Under the Direction of George Vellidis)

ABSTRACT

Flash drought is the rapid onset or intensification of short-term agricultural drought. This research aimed to quantify the frequency and duration of flash drought and its effect on rainfed maize (*Zea mays*) and cotton (*Gossypium hirsutum L.*) yields in the southeastern United States. For this study, a flash drought event was defined as when root zone plant-available soil water was less than 40% of field capacity for 15 consecutive days during the growing season. The SmartIrrigation (SI) CropFit App was used to quantify flash drought events at 40 virtual rainfed cotton and 61 virtual rainfed maize fields in Florida and Georgia from 2003-2022 during the growing season and the crops' reproductive phase. Overall, Georgia experienced more flash droughts than Florida. The Decision Support System for Agrotechnology Transfer (DSSAT) CSM-CERES-Maize and CSM-CROPGRO-Cotton crop simulation models were then used to simulate yield reductions resulting from a 15-day flash drought during different phenological stages of cotton and maize at selected virtual fields. Simulated maize yield reductions exceeded 40%-50% in Coastal Plain regions in Georgia and Florida for a 15-day flash drought event during the first half of June. The maximum cotton yield reductions were approximately 25% for events occurring

from mid-July to mid-August. For SI CropFit to be used to quantify flash drought for forage grass as was done for cotton and maize, it requires a forage grass model with a region-specific crop coefficient (K_C) curve. The DSSAT CSM-CROPGRO-Perennial-Forage model was applied to develop a K_C curve for rainfed forage bermudagrass in southern Georgia. The model was evaluated using three years of field data and then used to simulate daily K_C values for three years. A K_C was developed by fitting a polynomial curve to the simulated K_C values. This curve can be integrated into SI CropFit as it represents the expected crop water use patterns of optimally managed rainfed forage bermudagrass in southern Georgia. Overall, this entire study, for the first time, quantified the frequency of flash drought and its effects on crop yield in the southeastern U.S. and provides a methodology for capturing the occurrence of flash drought in real time.

INDEX WORDS: Flash drought, Maize, Cotton, Bermudagrass, Yield reduction, DSSAT-CSM, CSM-CERES-Maize, CSM-CROPGRO-Cotton, CSM-CROPGRO-Perennial-Forage, Crop coefficient curve.

QUANTIFYING THE FREQUENCY OF FLASH DROUGHT IN THE SOUTHEASTERN UNITED STATES AND ESTIMATING ITS EFFECT ON CROP YIELDS

by

JASIA JANNAT

B.S., University of Dhaka, Bangladesh, 2017

M.S., University of Dhaka, Bangladesh, 2019

A Dissertation Submitted to the Graduate Faculty of The University of Georgia in Partial Fulfillment of the Requirements for the Degree

DOCTOR OF PHILOSOPHY

ATHENS, GEORGIA

2025

QUANTIFYING THE FREQUENCY OF FLASH DROUGHT IN THE SOUTHEASTERN UNITED STATES AND ESTIMATING ITS EFFECT ON CROP YIELDS

by

JASIA JANNAT

Major Professor:	George Vellidis
Committee:	Lisa Baxter Corey J. Bryant Gerrit Hoogenboom John L. Snider

Electronic Version Approved:

Ron Walcott
Vice Provost for Graduate Education and Dean of the Graduate School
The University of Georgia
August 2025

ACKNOWLEDGEMENTS

I would like to express my gratitude to the following people for their crucial support and assistance during my Ph.D. research, which has made this academic journey much easier. This project would not be possible without the funding of the National Oceanic and Atmospheric Administration (NOAA) Weather Program Office (Award No NA20OAR4590498) and immense support from the Department of Crop and Soil Sciences, University of Georgia. I would like to express my deepest gratitude to my advisor, Dr. George Vellidis, for his unwavering support, guidance, and patience throughout my Ph.D. journey. His insightful advice and encouragement have been instrumental in shaping this research and my growth as a scholar. My heartfelt appreciation goes out to Dr. Gerrit Hoogenboom, whose knowledge and expertise in the subject matter guided me in my research. I extend my sincere appreciation to my committee members, Dr. Corey J. Bryant, Dr. John L. Snider, and Dr. Lisa Baxter, for their valuable feedback, constructive criticism, and thought-provoking discussions that have strengthened my work. I would like to acknowledge the assistance of Jose H. Andreis, Michasia Dowdy, Stephen Allen, Dr. William Anderson, Matthew A. Gruver, John Paulk, all the graduate students, and student workers during the field and lab work. I am extremely grateful to my husband, Md Ariful Islam Sohag, who gave me mental strength and supported me wholeheartedly throughout every step of my journey. I am thankful to my parents and sister for their unconditional love, patience, and support. Their belief in me has been my greatest source of motivation.

TABLE OF CONTENTS

Page

LIST OF TABLES

Page

LIST OF FIGURES

Page

CHAPTER 1

INTRODUCTION AND LITERATURE REVIEW

Introduction

Flash drought is a short-term agricultural drought characterized by rapid onset and intensification (Otkin et al., 2018, 2022; Li et al., 2020; Chen et al., 2020; Woloszyn et al., 2021) due to lower-than-normal precipitation rates, high temperatures, winds, and solar radiation (Otkin et al., 2018; Woloszyn et al., 2021). Based on the physical mechanisms associated with flash droughts, they are sometimes classified as heat wave-driven (caused by above-normal temperatures) and precipitation deficit-driven (caused by below-normal precipitation) (Mo and Lettenmaier, 2015, Wang and Yung, 2018). These conditions can deplete soil moisture in the root zone, particularly in sandy soils, causing damage to rainfed crops, local economies, and ecosystem goods and services (Mozny et al., 2012; Otkin et al., 2018; NOAA, 2022).

Occurrence of flash drought

North American agricultural lands are expected to experience a 53% rise from the 32% annual probability of flash droughts by the end of this century (Basara and Christian, 2023; Yuan et al., 2023), with the southeastern United States (U.S.) experiencing more frequent episodes (Lesinger and Tian, 2022). One of the factors leading to the higher incidence of flash drought is that the southeastern Coastal Plain (sometimes referred to as the Gulf Atlantic Coastal Plain), the region's dominant crop production area, contains mostly sandy soil with low water holding capacity in addition to atmospheric pressure pattern, high temperature and lower precipitation Deepa and Vijayan, 2025; Voiland, 2019). During the summer growing season, precipitation events are associated with localized thunderstorms, frequently resulting in some areas receiving

daily precipitation while nearby areas may not receive precipitation for two or three weeks. This pattern can result in very localized flash drought events (Fortin, 2019; NIDIS, 2024). Generally, the mean maize growing season precipitation in the Valley and Ridge, Blue Ridge, and Piedmont regions of Georgia was 537 mm, while in the Coastal Plain regions of Georgia and Florida, it was 495 mm and 632 mm, respectively, over 20-year record. In the Coastal Plain region of Florida, the mean cotton growing season precipitation was 829 mm, while in Georgia, it was 581 mm. It is visible how precipitation pattern varies within different ecoregions. If regular precipitation events do not replenish soil moisture, flash droughts develop rapidly, leading to water stress for rainfed crops, especially during their reproductive phase (Ingrao et al., 2023). In Georgia and Florida, the reproductive phase of maize, cotton, and bermudagrass occurs mostly during June-July, July-August, and May-October, respectively, depending on the planting dates.

Observations of soil moisture content in the root zone and evaporative demand are important factors in identifying flash drought at a particular time (Otkin et al., 2018; Christian et al., 2019; Noguera et al., 2020). On the other hand, flash droughts are typically short-lived, lasting from 10 to 20 days (a set of five days) (Walker et al., 2023). Ten or more days with soil moisture of less than 30% of field capacity were considered to be a flash drought event by Wang and Yuan (2018). Pendergrass et al. (2019) considered a flash drought as a rapid onset when a two-category change was observed in the U.S. Drought Monitor (USDM) in 14 days and sustained for at least another two weeks. Although the USDM is an effective tool for quantifying regional and prolonged drought, weekly USDM forecasts might not reflect how quickly drought conditions are changing (Tyagi et al., 2022) nor how they may be affecting rainfed crops.

Operation of SmartIrrigation CropFit

The SmartIrrigation CropFit App (hereafter referred to as SI CropFit) is a smartphone-based irrigation scheduling tool for managing irrigation in four agronomic crops – maize, cotton, peanut, and soybean. SI CropFit evolved from standalone apps for these crops that were part of a suite of SmartIrrigation Apps released beginning in 2014 (https://smartirrigationapps.org/) (Migliaccio et al., 2015a; 2015b; Vellidis et al., 2016; Miller et al., 2018a; 2018b; Ayankojo et al., 2018; Gallios et al., 2023). Plot-scale and on-farm research in Alabama, Florida, Georgia, and Mississippi has shown that using SI CropFit for scheduling irrigation for maize, cotton, peanut, and soybean results in 5-15% increase in yield and up to 40% greater irrigation water use efficiency than those achieved with traditional calendar-based irrigation scheduling methods (Vellidis et al., 2016; Vellidis, 2022; Gallios et al., 2023).

SI CropFit operates using a soil water balance model. It estimates daily crop water use using the FAO 56 method (Jensen, 1968; Allen et al., 1998), which is widely accepted for irrigation scheduling. The model uses meteorological data to calculate daily reference evapotranspiration (ET_O) and then applies the appropriate daily crop coefficient (K_C) to estimate daily crop water use (ET_C). The crop coefficient changes with the phenological stage and typically begins with small values after emergence and increases to 1.0 or above when the crop has the greatest water demand. The crop coefficient value decreases as crops reach maturity and begin to senesce (Vellidis et al., 2016). The model then uses daily ET_C, precipitation received, irrigation applied, and the soil's plant available water holding capacity (AWHC) to estimate a daily root zone soil water deficit (RZSWD) in terms of the percent of plant available soil water. Plant available soil water is defined as the water held by the soil matrix between field capacity and the wilting point. A 50% RZSWD or depletion of 50% of plant-available soil water is a commonly accepted irrigation threshold for

agronomic crops. Because the soil water balance model in SI CropFit has been shown to perform well, in this study, SI CropFit was used to determine the daily RZSWD for 61 virtual rainfed maize and 40 cotton fields in Georgia and Florida.

Maize

Maize (*Zea mays*) is a multipurpose crop grown under different agroclimatic conditions around the world. By area, it is the most commonly grown crop in the U. S. with 377.6 million tonnes produced in 2024, including 1.26 million tonnes in Georgia and 0.17 million tonnes in Florida (USDA-ERS, 2025). Maize is a crucial row crop in Florida for grain, silage, dairy, and livestock (Hand et al., 2024). In Georgia, maize is essential for row crop rotations, and it's the third-largest row crop, which has an economic value of $509.1 million, making it vital for the livestock and ethanol industries (Tubbs et al., 2024). Around 90% of the maize in the Georgia Coastal Plain is irrigated, although only around 50% and 10% of the maize in the Piedmont and Mountain areas, respectively, are irrigated (Tubbs et al., 2024), while 44% of the maize in Florida is irrigated (USDA-NASS, 2022).

Effects of water stress on maize

Maize is sensitive to water stress, particularly during its reproductive phase. Yield losses can reach 8% daily, based on the stress level experienced during silk and pollen formation (Kim and Lee, 2023), as those are the most susceptible growth stages for maize (Aslam et al., 2015; Sah et al., 2020). Liu et al. (2022) observed that maize under water stress during the flowering stage completed the basal kernel filling process faster without increasing the kernel filling rate, reducing kernel weight. Under drought conditions, the reproductive phase of maize resulted in a considerable decrease in grain number and weight and ultimately higher yield losses due to ovary abortion, mostly happening after silking (Oury et al., 2016a; Oury et al., 2016b).

Cotton

Upland cotton (*Gossypium hirsutum*) is widely grown in the southeastern U.S., with production reaching 3 million tonnes during the 2024 marketing year. This was approximately 11.5% of the total global production (USDA-ERS, 2025). In 2024, Georgia produced 0.42 million tonnes of cotton, while Florida produced 0.03 million tonnes. In terms of irrigation practice, out of 5,08,652 ha, cotton is produced under irrigation in 1,64,219 ha of land in Georgia (USDA-NASS, 2022) while 3,431 ha out of 39,889 ha of cotton land is irrigated in Florida (USDA-NASS, 2017).

Effects of water stress on cotton

Compared to other important crops, cotton, being glycophytic, exhibits a greater resilience to abiotic stressors than maize (Ullah et al., 2017). However, the impact of drought stress on cotton's physiological processes and yield is significant, which was observed in different studies (Snowden et al. 2014; Hejnák et al., 2015; Iqbal et al., 2017; Zonta et al., 2017; Khan et al., 2018; Gao et al., 2020, and Tokel et al., 2022). The length of a drought, as well as other environmental stressors, all affect the severity of these impacts. Water stress during flowering can cause flower abortion, affecting fruit growth and structure (Snowden et al. 2014; Iqbal et al. 2017; Zonta et al., 2017; Khan et al., 2018). It also affects fiber quality by altering the metabolism of sucrose in fibers (Gao et al., 2020). Long-term water stress can impair photosynthetic electron transport, causing a reduction in the photosynthesis of cotton (Sekmen et al., 2014; Parkash et al., 2024). Total dry weight of cotton was decreased by 8% under drought conditions in a study (Hejnák et al., 2015). In another study, seed cotton yield was reduced by 11%-17% depending on the cultivars, under ambient temperature (31.0/26.4°C) and soil relative water content level at 60% (Gao et al., 2020).

Bermudagrass

Bermudagrass is a warm-season perennial grass that is produced as a forage crop across the globe. It is both grazed and cut for hay and is an important nutrient source for livestock (Huang et al., 2011; Rouquette et al., 2011; Daniel et al., 2016). In Georgia, it is grown on approximately 1.2 million ha (Baxter et al., 2023). "Alicia", "Coastal", "Tifton 44", "Tifton 78", and "Tifton 85" are bermudagrass cultivars commonly used in the Coastal Plain physiographic region of the southeastern U.S. Because "Tifton 85" produces higher hay yields and has higher digestibility than most other cultivars (Lee et al., 2017), it is a popular selection among growers. In Georgia, approximately 15,374 ha of hay fields out of 2,26,511 ha are irrigated (USDA-NASS, 2022), which highlights the regional importance of irrigation practices in forage production.

Effects of water stress on bermudagrass

Bermudagrass is drought-tolerant (Husmoen et al. 2012; Baxter et al., 2022) due to its deep rooting system (Zhou et al., 2014; Gopinath et al., 2022), rapid stomatal closure (Zhou et al., 2013), and its large rhizome system (Zhou et al., 2014). However, adequate soil moisture is vital for bermudagrass growth. Without adequate soil moisture, plant uptake of soil water and nutrients is reduced, adversely affecting photosynthesis and respiration (Khan et al., 2018; Seleiman et al., 2021; Bijalwan et al., 2022), leaf water potential (Goche et al., 2020; Hemati et al., 2022), and stomatal conductance (Kumar et al., 2023). Stomatal closure results in a decrease in the crop's photosynthetic rate (Huang et al., 2014), ultimately affecting crop yield. Studies on drought stress in turf bermudagrass cultivars have been done; however, there aren't many studies on forage bermudagrass. For example, Steinke et al. (2011) found that some turf cultivars lost 50% of their green ground cover in 20 days without rain or irrigation, while other cultivars survived a full 60-day dry period without experiencing cover loss. Jespersen et al. (2019) found that drought stress

reduced membrane stability and respiration rates in some turf cultivars, which slowed the growth of the grasses.

Bermudagrass crop coefficient curve (K_C) development

Daily crop water, which is also referred to as crop evapotranspiration or ET_C, is a complex process influenced by several meteorological variables, including relative humidity, solar radiation, wind speed, and air temperature (Allen et al., 2005). Crop parameters such as variety and phenological stage also play key roles in determining ET_C values. The United Nations Food and Agriculture Organization (FAO)'s Irrigation and Drainage Paper No. 56, commonly referred to as FAO-56 (Jensen, 1968; Allen et al., 1998), provides guidelines for estimating crop water requirements using reference ET (ET_O) and daily crop coefficient (K_C). Different studies in different regions have developed bermudagrass crop coefficient curves under various environmental and climatic conditions using different ET methods such as weighing lysimeter, eddy covariance systems, etc. Weighing lysimeters determine ET_C by assessing daily changes in soil and crop mass and are considered the standard for Kc curve development (Ghiat et al., 2021). However, this approach requires substantial investment in the construction and operation of the lysimeters. Observing changes in soil moisture within the root zone with soil moisture sensors and from those data estimating ET_C is another approach that has been recently applied (Vellidis et al., 2016; Maktabi et al., 2022; Bedwell et al., 2025). The eddy covariance approach uses the vertical flux of water vapor to measure ET directly, but it is also expensive and difficult to implement (Ghiat et al., 2021).

Crop coefficient curves for forage and turf grass have been developed using weighing lysimeters and soil moisture sensors. Weighing lysimeters were used in a study conducted in São Paulo State, Brazil, to develop ET_C values and a Kc curve for forage bermudagrass (*Cynodon* spp.)

(Sanches et al., 2019). The bermudagrass was single-cropped (only crop in the field) for a year and overseeded with ryegrass and black oats in the autumn and winter. ET_C was calculated using weighing lysimeters, and Kc values were estimated from those data using ET_O calculated with the Penman-Monteith equation. A Kc curve was developed from the daily Kc values. Forage bermudagrass K_C values and daily water use are not well documented in the literature, especially for rainfed production, whereas few studies have been conducted on turf bermudagrass. In a study using weighing lysimeters, Kc curves were developed for turfgrass bermudagrass and tall fescue in North Carolina, U.S. (Pinnix and Miller, 2019). In this study, tall fescue had higher Kc values than bermudagrass. In a study conducted in Florida, U.S., K_C curves for four warm-season turfgrass species- "Tifway" bermudagrass (*Cynodon dactylon* (L.) Pers. *x Cynodon transvaalensis* Burtt-Davy), "Empire" zoysiagrass (*Zoysia japonica* Steud.), "Floratam" St. Augustinegrass (*Stenotaphrum secundatum* (Walter) Kuntze), and "Argentine" bahiagrass (*Paspalum notatum* Flugge) were developed by measuring ET_C using weighing lysimeters and calculating ET_O with the American Society of Civil Engineers (ASCE)-Environmental & Water Resources Institute (EWRI) standardized method (Wherley et al., 2015). Using the FAO-56 dual crop coefficient technique for ET_O and a weighing lysimeter to estimate ET_C, Crookston (2016) developed seasonal Kc curves for ten turfgrasses in Colorado, U.S. All the above-mentioned studies were conducted under optimal soil moisture conditions.

Crop modeling simulations

In agricultural contexts, process-based models have become frequently used to evaluate the effects of climate change and investigate the links between environmental or phenological factors and crop productivity (Wang et al., 2011). Photosynthesis, respiration, soil water balance, and energy balance of the plant-soil-atmosphere system are all converted into mathematical

equations by crop models, which then combine them to create a computer program that simulates crop development (Luo et al., 2023). Crop growth simulation models can be used in many ways. For example, they can guide plant scientists and breeders toward the necessary traits in improved varieties, they can be used to evaluate cropping systems management practices to reduce the effects of climate change (Fodor et al., 2017), and they can be used to evaluate ET dynamics under different crop management scenarios. The latter is particularly relevant to the work reported here because conducting field experiments to understand and quantify ET dynamics under various crop management scenarios is expensive, labor intensive, and time consuming. In contrast, once a crop growth simulation is calibrated and validated, it can be used to evaluate various crop management scenarios with relatively little additional effort. Some of the most frequently used crop modeling systems are the AquaCrop model (Steduto et al., 2009), the Agricultural Production Systems Simulator (APSIM) model (Keating et al., 2003), and the Decision Support System for Agrotechnology Transfer (DSSAT) model (Jones et al., 2003).

DSSAT is one of the most widely used crop modeling systems (Jones et al., 2003; Koo, 2016; Ma et al., 2020) and has been proven to be reliable for crop growth simulation under different agricultural scenarios and management practices. In more than 198 countries throughout the world, 30,000 academics, educators, consultants, and others from various fields have utilized it (Hoogenboom et al., 2024). If long meteorological data records are available, simulations can be run for many years in DSSAT (Hoogenboom et al., 2023) from which the yearly variation of crop productivity can be observed under long-term climatic changes, and a mean annual K_C curve can be developed that is representative of a region. These factors led to the selection of the DSSAT application for this research.

Decision Support System for Agrotechnology Transfer (DSSAT)

The DSSAT is a universally used decision support tool that includes dynamic crop growth simulation models for over 42 crops (Hoogenboom et al., 2019) to evaluate the changes in soil water, carbon, and nitrogen over time within the cropping system and to estimate crop yield and growth (Abayechaw, 2021). DSSAT Cropping System Model (CSM)-CERES-Maize, which is one of the most popular and widely used crop models within DSSAT-CSM (Yakoub et al., 2017), provides a framework to conduct research for understanding the effect of various management practices and changes in environmental conditions on the growth and yield of maize by evaluating the relative response of different scenarios-such as for irrigation management (Kaur and Arora, 2018; Malik and Dechmi, 2019); climate change (Ngwira et al., 2014; Farhangfar et al., 2015), etc. The CSM-CERES-Maize model's module structure makes it possible to measure drought stress and its possible effects on crop development, production, and growth (Amiri et al., 2022).

The CSM-CROPGRO-Cotton has been used in the southeastern U.S. to study irrigation water use, climate variability, and ENSO impact on cotton yield (Garcia et al., 2010; Paz et al., 2012). The model has also been used to simulate cotton production under various water stress scenarios. Modala et al. (2015) experimented with the evaluation of the model to predict cotton growth and yield in comparison with the observed data from 2008-2010 and 2012 under different irrigation strategies in the Texas Rolling Plains. Although the evapotranspiration (ET) simulation in the model was not satisfactory under deficit irrigation (0% and 33% ET replacements) during dry seasons, the model showed significant potential to predict cotton growth and yield in arid conditions under different irrigation management to conserve water during different seasons. In another study conducted in the Texas High Plains, the CSM-CROPGRO-Cotton was used to

evaluate the impacts of deficit irrigation on irrigation water use efficiency and seed cotton output in dry, normal, and wet years over the past 41 years (Himanshu et al., 2021).

DSSAT-CSM includes the CSM-CROPGRO-Perennial-Forage model (Rymph et al., 2004), which provides for species adaptations and data files for three perennial forages – bermudagrass, bahiagrass, and brachiariagrass (Hoogenboom et al., 2023). In this study, the CSM-CROPGRO-Perennial-Forage (CROPGRO-PFM) (4.8.2 version) was used to estimate daily ET_C and develop a K_C curve for rainfed forage bermudagrass. Several studies have used DSSAT-CSM to measure ET_C under different scenarios for crops such as maize (Marek et al., 2017; Menefee et al., 2021), cotton (Dejonge & Thorp et al., 2017; Thorp et al., 2020), and sweet corn (Hailegnaw et al., 2024). However, little has been published on using crop growth models to estimate the ET_C of forage grasses. Castaño-Sánchez et al. (2020) used the CSM-CROPGRO-Perennial-Forage model to forecast ET_C and yield of alfalfa under an elevated CO_2 environment.

Project description

The flash drought and its consequences prompted this study, whose aim was to estimate the frequency of flash drought events and their effect on rainfed crops in the southeastern U.S. The SI CropFit mobile app was used to identify flash drought events during the maize and cotton growing seasons in Georgia and Florida. Flash drought frequency maps were developed for cotton and maize growing areas of each state as well. Additionally, the DSSAT-CSM suite of crop models is used to assess the impact of flash drought on rainfed crops in selected locations in Georgia and Florida. Also, the CSM-CROPGRO-Perennial-Forage model was applied to predict crop water use and develop a crop coefficient ($K_{C\text{-}DSSAT}$) curve for rainfed forage bermudagrass in southern Georgia with the objective of incorporating the K_C curve into the SI CropFit for flash drought prediction.

Goals and objectives

The overall goal of this study is to identify the flash drought events and understand the impact of flash drought on rainfed crops in the Southeast U.S., as well as generate the crop coefficient growth curve of bermudagrass as a part of developing the SI CropFit forage app. Specific objectives are-

a. To quantify the frequency and duration of flash drought in the major agronomic crop-growing areas of Florida and Georgia,
b. To simulate the yield response of rainfed maize and cotton to the occurrence of flash drought during different phenological stages,
c. To evaluate the four ET estimation methods available in the CSM-CROPGRO-Perennial-Forage model for use in developing a bermudagrass Kc curve to be incorporated into SI CropFit.

CHAPTER 2

QUANTIFYING THE FREQUENCY AND DURATION OF GROWING SEASON FLASH DROUGHT IN THE SOUTHEASTERN UNITED STATES[1]

[1]Jannat, J., J. Andreis, L. Baxter, C. J. Bryant, G. Hoogenboom, P. Knox, X. Lu, W. R. Lusher, J. L. Snider, and G. Vellidis. To be submitted to *Field Crops Research*.

Abstract

Flash drought is defined as the rapid onset or intensification of short-term agricultural drought, which is characterized by lower precipitation rates and higher temperatures, winds, and solar radiation, all of which act to negatively affect the growth and yield of crops. The goal of this study was to quantify the frequency and duration of flash drought for rainfed maize (*Zea mays*) and cotton (*Gossypium hirsutum L.*) in Florida and Georgia. For this study, a flash drought event was defined as a period when plant-available soil water in the root zone was less than 40% of field capacity for 15 consecutive days during the growing season. The SmartIrrigation (SI) CropFit App was used to quantify the occurrence of flash drought events at 61 virtual field locations in Florida and Georgia over a 20-year period (2003-2022) for the entire growing season as well as during the crops' reproductive phase. Overall, Georgia experienced more flash droughts than Florida. Rainfed maize in Georgia on average experienced a flash drought on average at least once per growing season, and at least 50% of the flash drought events for maize occurred during the crop's reproductive phase. In Florida, this figure was as low as 12%. Although the overall number of cotton flash drought events in both states was lower than for maize, 75% of flash drought events for cotton in Georgia and 50% in Florida occurred during the crop's reproductive phase. Simulations with the Decision Support System for Agrotechnology Transfer (DSSAT) CSM-CERES-Maize and CSM-CROPGRO-Cotton crop growth models demonstrated that the flash drought events identified with SI CropFit coincided with periods of crop water stress in the DSSAT-CSM models. A web-based Flash Drought Interactive Map Tool was developed to allow users to explore and visualize frequency maps of flash drought events for the study regions under scenarios with different combinations of crops (cotton or maize), flash drought periods, and either the entire growing season or the reproductive phase of the crop. This study, for the first time,

quantifies the frequency of flash drought associated with agronomic crops in the southeastern U.S. and provides a methodology for capturing the occurrence of flash drought in real time.

Introduction

Overview of flash drought

Adequate soil moisture is vital for plant growth. Without it, plant uptake of soil water and nutrients is reduced, adversely affecting photosynthesis, respiration (Khan et al., 2018; Seleiman et al., 2021; Bijalwan et al., 2022), leaf water potential (Goche et al., 2020; Hemati et al., 2022), and stomatal conductance, ultimately affecting crop yield (Kumar et al., 2023). As a result, drought can have serious effects on rainfed crop production and local economies (Manuel et al., 2008; Price et al., 2017; Kuwayama et al., 2019). Nguyen et al. (2023) showed that between 1979-2019, crop yield losses varied between 27%–30% because of prolonged drought events in the southeastern United States (U.S.).

In contrast to prolonged drought, flash drought is the rapid onset and intensification of relatively short-term agricultural drought (Otkin et al., 2018, 2022; Li et al., 2020; Chen et al., 2021; Woloszyn et al., 2021). Like prolonged drought, it occurs because of lower-than-normal precipitation rates and abnormally high temperatures, winds, and solar radiation (Otkin et al., 2018; Woloszyn et al., 2021). Based on the physical mechanisms associated with flash droughts, they are sometimes classified as heat wave-driven (caused by above-normal temperatures) and precipitation deficit-driven (caused by below-normal precipitation) (Mo and Lettenmaier, 2015, Wang and Yung, 2018). When these conditions continue for several days, soil moisture in the root zone can be depleted rapidly, especially in sandy soil, resulting in damage to rainfed crops (Mozny et al., 2012; Otkin et al., 2018; NOAA, 2022).

The southeastern U.S. typically experiences more flash drought episodes compared to the rest of the continent (Lesinger and Tian, 2022). Flash droughts, which accounted for 9.8% of all U.S. droughts between 2000 and 2019, were more likely to occur over southern U.S. states (Leeper et al., 2022). One of the factors leading to the higher incidence of flash drought is that the southeastern Coastal Plain (sometimes referred to as the Gulf Atlantic Coastal Plain), the region's dominant crop production area, is characterized by sandy soils with low water holding capacity. During the summer growing season, precipitation events are associated with localized thunderstorms, frequently resulting in some areas receiving daily precipitation while nearby areas may not receive precipitation for two or three weeks. This pattern can result in very localized flash drought events (Fortin, 2019; NIDIS, 2024). If regular precipitation events do not replenish soil moisture, flash droughts develop rapidly, and rainfed crops may undergo periods of water stress, especially if they are in their reproductive phase (Ingrao et al., 2023). Although the U.S. Drought Monitor (USDM) is an effective tool for quantifying regional and prolonged drought, weekly USDM forecasts might not reflect how quickly drought conditions are changing (Tyagi et al., 2022) nor how they may be affecting rainfed crops. For example, a significant flash drought event that resulted in severe damage to rainfed cotton, hay, and other forage crops in the southeastern U.S. occurred in September 2019 (Voiland, 2019; Ford et al., 2023; Gibbons et al., 2023) and was not captured by the USDM.

Duration of flash drought

Flash drought events are typically short-lived, lasting from 10 to 20 days (Walker et al., 2023). Ten or more days with soil moisture of less than 30% of field capacity was defined as a flash drought event by Wang and Yuan (2018). Observations of soil moisture content in the root

zone and evaporative demand are important factors in identifying the occurrence of flash drought (Otkin et al., 2018; Christian et al., 2019; Noguera et al., 2020; Basara and Christian, 2023).

Soil moisture data collected by the authors during the 2024 growing season in the Coastal Plain of Georgia are emblematic of how rapidly soil moisture can be depleted in the soil profile of rainfed crops grown in sandy soil. Figure 2.1 shows soil water tension in rainfed cotton from a field in southwestern Georgia (Figure 2.1a) and rainfed peanut from a field in south-central Georgia (Figure 2.1b) for a period of about five weeks. Soil water tension is the absolute value of soil matric potential. In both the cotton and peanut fields, soil water tension increased from the optimal range for those crops (shown by the blue area in the graphs) to the point of visible wilting (shown by the red area of the graphs) within seven days and stayed dry for at least seven more days. Figure 2.1c shows the season-long soil water tension for the field shown in Figure 2.1b, with two periods of 14 or more days with very low soil moisture, both of which may be characterized as flash drought events.

Goals and objectives

Because of its rapid onset and timing, the impact of the well-documented flash drought event that occurred during September 2019 on rainfed crops was not effectively captured by the USDM or other tools used to document drought events. As a result, growers whose crops were damaged by the flash drought were not eligible for state and federal disaster assistance programs.

The 2019 flash drought and its consequences prompted a study to estimate the frequency of flash drought events and the effect of flash drought events on the yield of rainfed crops in the southeastern U.S. Specific objectives of this study were: (1) to quantify the frequency and duration of flash drought in the major agronomic crop growing areas of Florida and Georgia and (2) to

develop web-based flash drought interactive map tool for visualizing the frequency of flash drought events for rainfed cotton and maize under different scenarios.

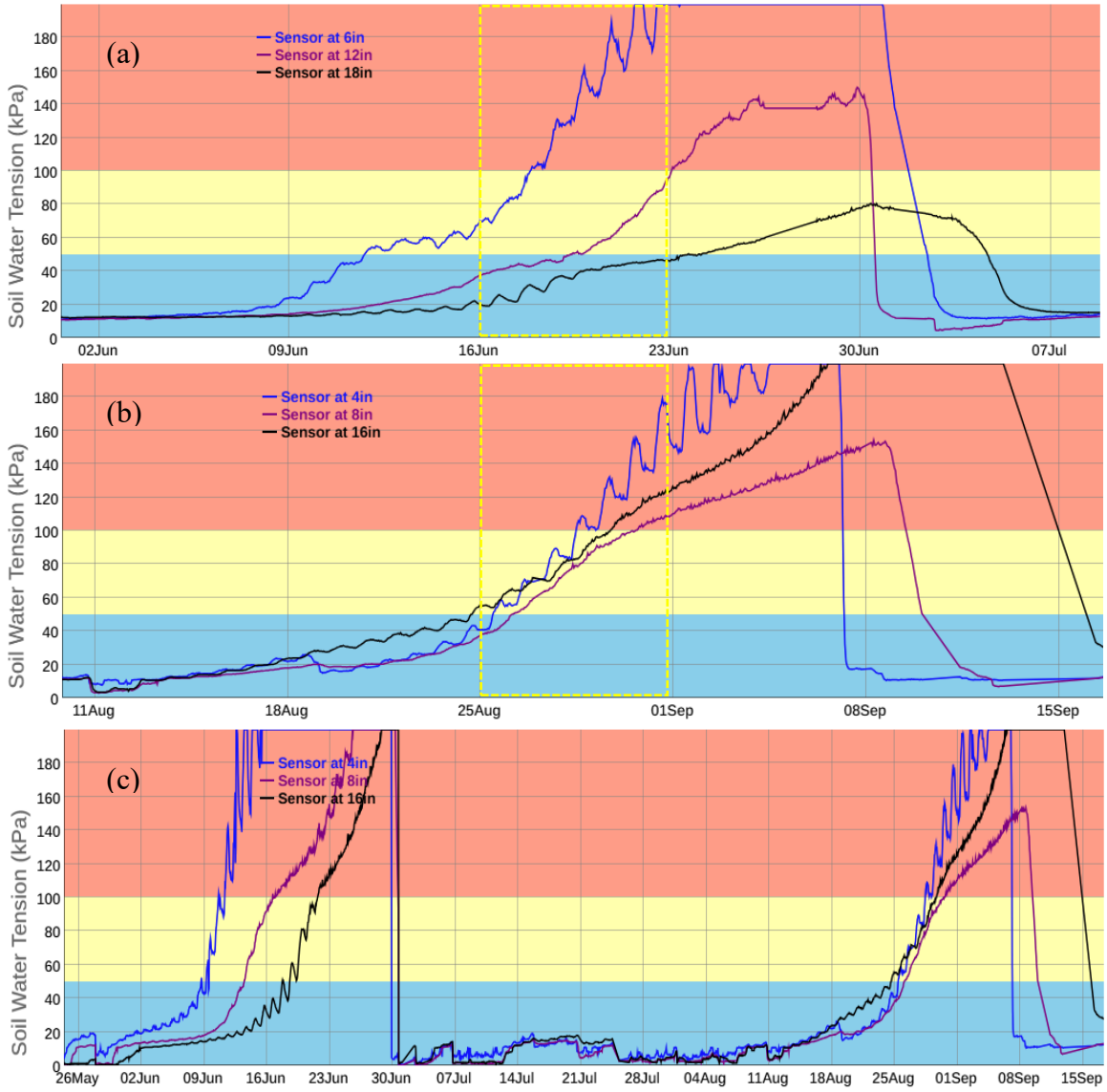

Figure 2.1 Soil water tension in rainfed cotton (a) and rainfed peanut (b) grown in the sandy soils typical of the Coastal Plain during the 2024 growing season. In both cases, soil water tension increased from the optimal range for those crops (shown by the blue area in the graphs) to the wilting point (shown by the red area of the graphs) within seven days and stayed dry for at least seven more days. The season-long soil moisture for the field shown in (b) with two extended periods with very low soil moisture, both of which can be characterized as flash drought, is shown in (c).

Materials and methods

SmartIrrigation CropFit

SmartIrrigation CropFit (hereafter referred to as SI CropFit) is a smartphone-based irrigation scheduling platform for four agronomic crops – maize, cotton, peanut, and soybean. SI CropFit evolved from standalone apps that were part of a suite of SmartIrrigation Apps released beginning in 2014 (https://smartirrigationapps.org/) (Migliaccio et al., 2015a; 2015b; Vellidis et al., 2016; Miller et al., 2018a; 2018b; Ayankojo et al., 2018; Gallios et al., 2023). Plot-scale and on-farm research in Alabama, Florida, Georgia, and Mississippi has shown that using SI CropFit for scheduling irrigation for maize, cotton, peanut, and soybean results in 5-15% increase in yield and up to 40% greater irrigation water use efficiency than those achieved with traditional calendar-based irrigation scheduling methods (Vellidis et al., 2016; Vellidis, 2022; Gallios et al., 2023).

SI CropFit operates using a soil water balance model. It estimates daily crop water use using the FAO-56 method (Jensen, 1968; Allen et al., 1998), which is widely accepted for irrigation scheduling (Eq. 2.1).

$$ET_C = ET_O \times K_C \quad (2.1)$$

where,

ET_C = daily crop water use (mm day^{-1}),

ET_O = reference evapotranspiration (ET) calculated using the Penman-Monteith equation (mm day^{-1}), and

K_C = a daily crop coefficient.

The model uses meteorological data to calculate daily ET_O and then applies the appropriate K_C to estimate daily ET_C. The crop coefficient changes with the phenological stage and typically

begins with small values after emergence and increases to 1.0 or above when the crop has the greatest water demand. The crop coefficient value decreases as crops reach maturity and begin to senesce (Vellidis et al., 2016; Chapter 2). For all the agronomic crops, changes in phenology and associated changes in K_C are driven by accumulated heat units commonly referred to as growing degree days.

The model then uses daily ET_C, precipitation received, irrigation applied, and the soil's plant available water holding capacity (AWHC) to maintain a soil water balance and estimate a daily root zone soil water deficit (RZSWD) in terms of percent of plant available soil water. Plant available soil water is defined as the water held by the soil matrix between field capacity and the wilting point. A 50% RZSWD or depletion of 50% of plant available soil water is a commonly accepted irrigation threshold for agronomic crops (Peters et al., 2013; Sharma, 2019) and is sometimes referred to as the minimum allowable depletion (Scherer and Steele, 2024). In the soil water balance model, today's plant-available soil water is calculated by subtracting yesterday's ET_C from yesterday's plant-available soil water and adding precipitation received or irrigation applied. The root zone used by the soil water balance model begins with a rooting depth of 15 cm and increases by 0.75 cm per day until it reaches a maximum depth, which is crop dependent. For cotton, the maximum rooting depth is 76 cm and for maize, it is 61 cm. Each layer of soil that is added has a soil water content of 85% of field capacity. Consequently, the soil profile acts as a reservoir of soil water in the soil water balance model.

SI CropFit pulls meteorological data from several sources – state weather station networks (mesonets), Apple Weather (Apple Inc., Cupertino, CA, U.S.), a commercial provider of meteorological data, and five commercial automated rain gauge brands using Application Programming Interfaces (APIs). Users in U.S. states with participating mesonets can select a

weather station as their primary provider of meteorological data. The closest weather station is selected based on the field's coordinates. Users elsewhere utilize Apple Weather, which provides meteorological data on a 4 km grid, as their primary provider of meteorological data. The field's coordinates are used to select the appropriate source grid. When SI CropFit is used for irrigation scheduling, an automated on-farm rain gauge that provides hyper-local precipitation data is highly recommended. The model operates primarily on a cloud server with daily updates of user-need information to the smartphone platform. Figure 2.2 shows the operating principles of SI CropFit.

One of the functionalities of SI CropFit is that users can define the perimeter of their field using dropped pins. The perimeter is then used to extract soil information, including soil type, field

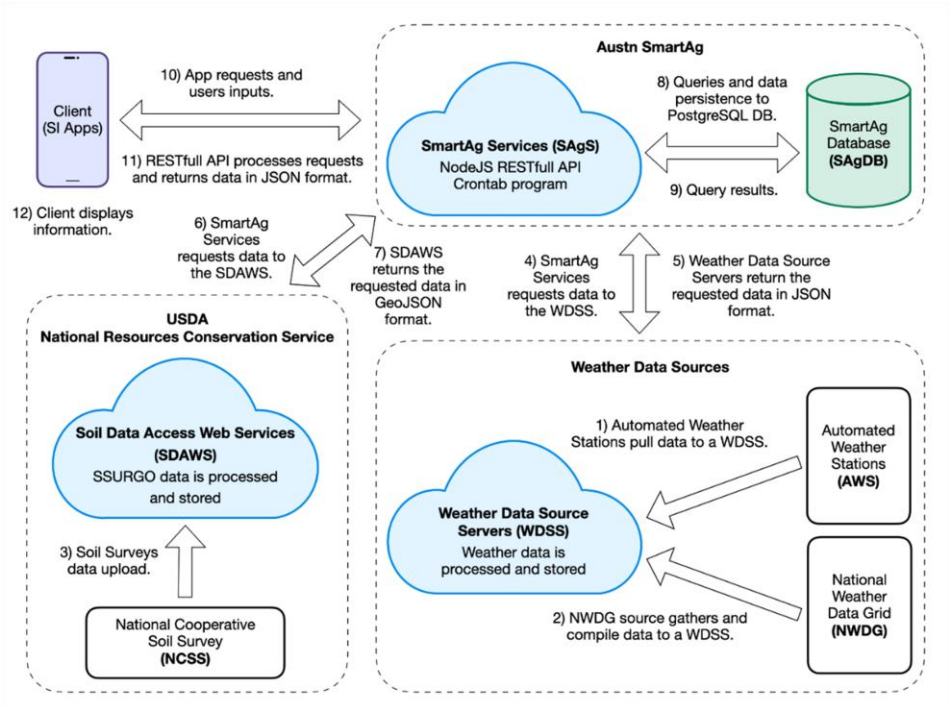

Figure 2.2 Schematic showing the operating principles of SmartIrrigation CropFit (SI CropFit), including interaction among client, cloud server (Austn SmartAg), weather data sources services, and soil data access and web services. The cloud-shaped sections indicate dynamic, service-oriented components and stand in for online services or data servers, such as Weather Data Source Servers (WDSS), Soil Data Access Web Services (SDAWS), and SmartAg Services (SAgS). Using a PostgreSQL database, the cylinder form represents the SmartAg Database (SAgDB), which stands for durable storage.

capacity (FC), and wilting point (WP) from the USDA Natural Resources and Conservation Services (NRCS) Web Soil Survey (https://websoilsurvey.sc.egov.usda.gov/App/). The soil's plant available water holding capacity (AWHC) is calculated by subtracting WP from FC. If there is more than one soil type within the field perimeter, an area-weighted average AWHC is calculated, and that value is subsequently used in the soil water balance model (Figure 2.3).

Because the soil water balance model in SI CropFit has been shown to perform well, in this study, SI CropFit was used to determine the daily RZSWD for virtual rainfed maize and cotton fields established at the locations of the Florida Automated Weather Network (FAWN) (https://fawn.ifas.ufl.edu) and the University of Georgia Weather Network (UGAWN) (http://weather.uga.edu) weather stations (Figure 2.4). In each state, areas in which maize and cotton are grown at a moderate to large scale were delineated. For cotton and maize in Florida, this

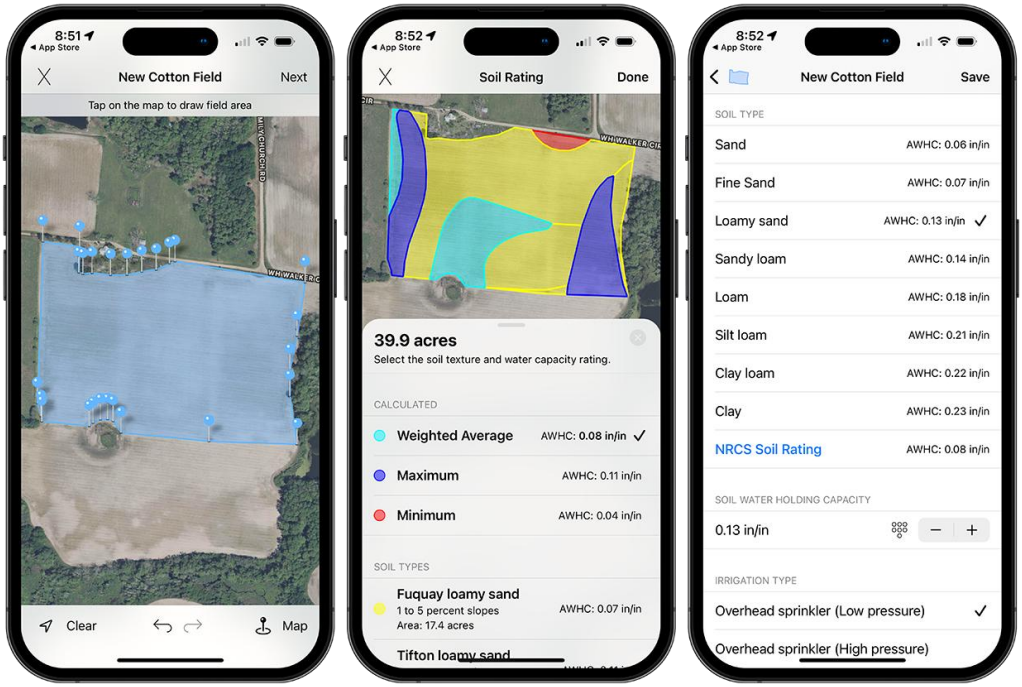

Figure 2.3 Screenshots from SmartIrrigation CropFit (SI CropFit) showing how a field is delineated (left) and how an area-weighted average available water holding capacity (AWHC) (middle) is determined from the USDA Natural Resources and Conservation Services (NRCS) Web Soil Survey. The screenshot at the right also shows additional options for selecting an appropriate AWHC for a field.

was north of 28.9° N (approximately just south of the city of Ocala) and east of 87.6° W (just east of Pensacola). In Georgia, this included the entire state for maize and the Coastal Plain for cotton (Figure 2.4). Only weather stations within this region and with at minimum a 20-year record of meteorological data were used. This resulted in using a total of 61 weather stations / virtual fields for maize (14 in Florida and 47 in Georgia) and 40 weather stations / virtual fields for cotton (14 in Florida and 26 in Georgia) (Figure 2.4). Each virtual field was 0.1 ha in size (32 × 32 m) and

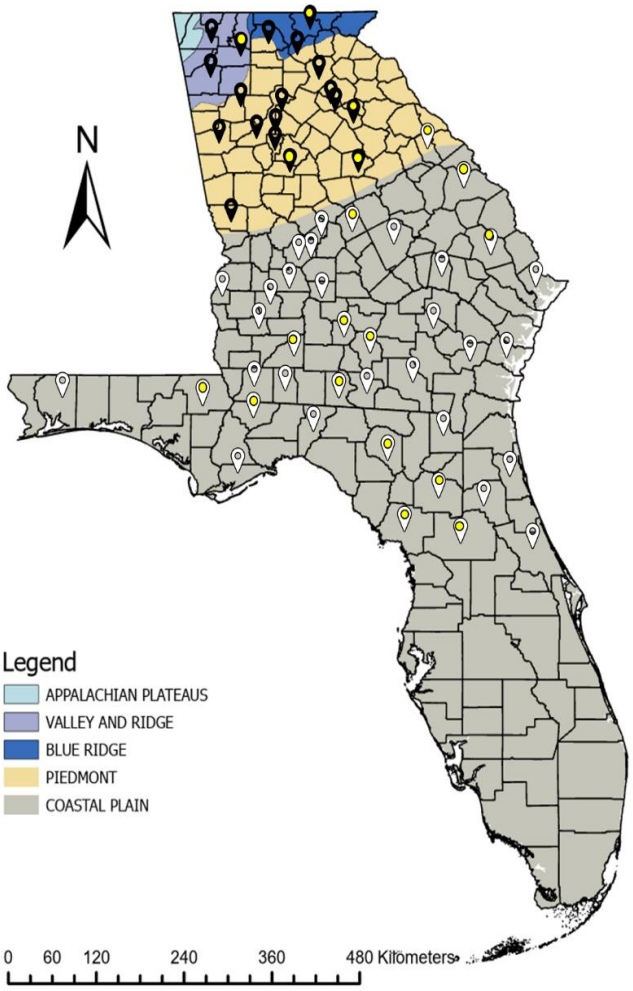

Figure 2.4 The pins on the map show the location of the 61 virtual fields used in this study. Color-coding indicates which crops were simulated at each virtual field as well as what type of simulations were conducted. Black pins indicate virtual fields used for maize. White pins indicate virtual fields used for both maize and cotton. Pins with a yellow dot indicate virtual fields selected as examples to show the number of flash drought events that occurred during the entire growing season and the reproductive phase of maize and cotton (Tables 2.1 and 2.2).

centered on the geographic coordinates of the weather station. The perimeter of each virtual field was used to extract soil information (AWHC) from the Web Soil Survey (Figure 2.3).

The virtual fields were in four distinct ecoregions (Figure 2.4). The Valley and Ridge and Blue Ridge ecoregions are in northern Georgia and are mountainous. They are characterized by clay and loamy soils. The Piedmont ecoregion is in central Georgia and is a transitionary area between the mountains and the Coastal Plain. Piedmont is characterized by rolling hills and clay soil. The Coastal Plain is the primary agronomic crop production area of Georgia and Florida and is characterized by sandy soils with little elevation change. There were three virtual fields in the Valley and Ridge, two in the Blue Ridge, 17 in Piedmont, and 38 in the Coastal Plain. For simplicity, virtual fields in the Valley and Ridge, Blue Ridge, and Piedmont ecoregions were grouped (22 total) when evaluating results.

Although maize planting dates vary across Florida and Georgia from year to year and by location, an average planting date of April 15 was selected for Florida and April 01 for Georgia based on discussions with Extension specialists in both states. The planting date for rainfed maize in Florida is later than that of irrigated maize, so that the reproductive phase coincides with the beginning of the summer rainy season in June (Wright et al., 2020). Planting dates for rainfed and irrigated maize do not vary in Georgia (Tubbs et al., 2024). Cotton planting dates in Florida and Georgia depend on the location, time of year, and several factors such as soil temperature, moisture content, and climate, and range from early April to early June. After consulting with Extension personnel, an average planting date of May 15 was selected for both states (Hand et al., 2024, and Wright et al., 2003).

Frequency of flash drought occurrence

For this study, flash drought was defined as occurring when RZSWD was greater than or equal to 60% (≥60%) for a minimum of 15 continuous days during the growing season. This was based on studies from the literature which defined flash drought as events of between 10 and 20 days in duration with soil moisture of less than 30% of field capacity (Walker et al., 2023; Wang and Yuan, 2018). This period length was also supported by a study mentioned in Chapter 3 of this dissertation in which a crop growth simulation model was used to estimate the impact of 15-day flash drought events on the yield of rainfed cotton and maize in the southeastern Coastal Plain. Modeling results indicated yield reductions as high as 40-50% for maize and as high as 25% for cotton if flash drought occurred during the reproductive phase of the crops. RZSWD ≥60% was selected based on studies from the literature indicating that, depending on the soil type, when soil water depletion exceeds 50% of AWHC, most agronomic crops generally begin to experience water stress (Peters et al., 2013; Sharma, 2019). Scenarios during which RZSWD ≥70% and ≥80% were also evaluated. RZSWD ≥70% is the same as soil moisture of less than 30% of field capacity.

A server-side system called SmartAg Services (written in NodeJS) and a server-side database called SmartAg Database (PostgreSQL) were used to automate the process of running SI CropFit for maize and cotton separately at all the virtual field sites for the 20 growing seasons of each crop between 2003-2022. RZSWD was calculated daily, and the number of 15-day periods for which RZSWD ≥60%, ≥70%, and ≥80% during each growing season at each location was aggregated. For an event to fall within one of these three categories, all 15 days were required to be greater than or equal to the threshold. If, for example, we had 14 days with RZSWD ≥70% and 1 day ≥60% but < 70% during the 15 days, the event would be considered a RZSWD ≥60% event. If there were 30 consecutive days of RZSWD exceeding one of the thresholds, it was counted as

two events. For example, if there were 15 days when RZSWD ≥60% and then 15 days when RZSWD ≥70%, it was counted as one RZSWD ≥60% event and one RZSWD ≥70% event. If a 15-day period exceeded these thresholds, it was recorded as a flash drought event.

Confirming flash drought events with a crop growth model

The Decision Support System for Agrotechnology Transfer (DSSAT) is a universally used decision support tool that includes dynamic crop growth simulation models for over 42 crops (Hoogenboom et al., 2019). In this project, the DSSAT Cropping System Model (CSM)-CERES-Maize and CSM-CROPGRO-Cotton models (v.4.8.2) (Hoogenboom et al., 2023) were primarily used to simulate the effect of flash drought on rainfed maize and cotton yields respectively (Chapter 3). In the study reported here, the two models were used to assess whether the flash drought events identified by SI CropFit coincided with periods of crop water stress identified by DSSAT-CSM. Both the maize and cotton models simulate several physiological parameters, including two crop water stress indices – the water deficit stress index for photosynthesis (WSPD) and the water deficit stress index for growth (WSGD). These two indices were used to assess whether the flash drought events identified by SI CropFit coincided with periods of crop water stress in DSSAT-CSM simulations.

Both indices assume that when root water uptake is not able to meet the plant's water needs, photosynthesis and transpiration are reduced proportionally to match decreased water uptake (Woli, 2010). WSPD accounts for water deficit effects resulting from stomatal closure. When potential root uptake is less than the potential transpiration rate, the actual transpiration rate is reduced by closed stomata, which in turn proportionally reduces potential photosynthesis and potential biomass production (Ritchie, 1998). WSGD accounts for water deficit effects on plant physiological processes affected by turgor pressure, such as leaf expansion, branching, and

tillering, that are more sensitive to water stress than stomata controlled processes (Ritchie, 1998). Consequently, in the DSSAT-CSM models, WSGD is the initial indicator of crop water stress. The range for both indices is 0-1, with 1 indicating maximum stress (Hoogenboom et al., 2023; Ritchie, 1998). Both indices are often used as a means of benchmarking other water stress indicators. For example, Woli et al. (2012) used WSPD to benchmark the response of eight drought stress indices in rainfed maize in the southeastern U.S.

For optimal performance, DSSAT-CSM models must be calibrated and evaluated using field data. Calibration entails adjusting the parameters of the model so that values of key simulated variables, such as leaf area and mass, above-ground biomass, and yield, compare favorably to field observations of the variables. The calibration of the two models was described in Chapter 3 of this dissertation.

Thirteen of the 61 virtual fields (four in Florida and nine in Georgia) were used for confirming flash drought events with DSSAT-CSM. The fields were selected to be representative of the major cotton and maize growing areas of Florida and Georgia. Five were in the Valley and Ridge, Blue Ridge, and Piedmont ecoregions (Blairsville, Calhoun, Eatonton, Griffin, Watkinsville) and used only for maize simulations, four were in the Georgia Coastal Plain (Camilla, Midville, Plains, Tifton), and four were in the Florida Coastal Plain (Citra, Live Oak, Marianna, Quincy). The eight Coastal Plain fields were used for cotton and maize simulations. The soils, planting dates, and meteorological data used for the 1 ha virtual fields during the SI CropFit analyses were used in the DSSAT-CSM simulations. The 13 virtual fields were weather station sites located at the University of Georgia and University of Florida research and education centers, where detailed soil data (particle size analysis, soil pH, cation exchange capacity, bulk density, etc.) needed for DSSAT-CSM simulations were available.

For this study, WSPD and WSGD were simulated daily for each virtual field during the maize and cotton growing seasons under rainfed conditions for the 20-year period (2003-2022) described earlier. Because the literature does not provide clear thresholds for the level of water stress indicated by increasing WSPD and WSGD values, all simulated days during which the indices >0 were considered water stress periods. These periods were then compared to the days when SI CropFit RZSWD was ≥60%. The comparison was conducted from 01 May to 31 July for maize and 01 July to 30 September for cotton, periods which generally bracket the reproductive phase for these crops based on the planting dates used. The statistical relationship between the number of flash drought days per month identified using the SI CropFit RZSWD method and the number of crop water stress days determined using the DSSAT-CSM WSPD and WSGD method was evaluated using the coefficient of determination (R^2) from the Linear Regression method in the R statistical software (R Core Team, 2023) at the 13 virtual maize field and 8 virtual cotton fields.

Flash drought frequency maps

The Flash Drought Interactive Map Tool, a web-based frontend application, was developed using Vue.js (https://vuejs.org), which provided a component-based structure for user interaction and retrieves data from the SmartAg Services through dedicated API (Application Programming Interface) endpoints. Spatial data visualization was implemented using Mapbox© (Mapbox, Inc., San Francisco, California, USA) with map tiles from OpenStreetMap© (OpenStreetMap Foundation, Cambridge, United Kingdom) to allow users to explore and visualize the frequency of flash droughts using contour maps of the study regions under scenarios with different combinations of crops, i.e., cotton or maize, flash drought periods (10 or 15 days), RZSWD (≥60%, ≥70%, and ≥80%), and either the entire growing season or the reproductive phase of the crop. The

contour maps were developed by interpolating the flash drought results from the individual virtual fields using the inverse distance weighting (IDW) method, implemented with the Turf.js (https://turfjs.org/) library on the SmartAg Services. In addition to the maps, the portal displays the maximum and minimum number of events under the selected scenario. The URL of the Flash Drought Interactive Map Tool is https://sicropfit.austn.co/mapView.

Results and discussion

Precipitation and ET

The mean cumulative precipitation, ET_O, and ET_C during the growing season and reproductive phase of maize and cotton, respectively, between 2003-2022 in each of the ecoregions described earlier are shown in Figures 2.5 and 2.6. Precipitation data were extracted from the records of the FAWN and UGAWN weather stations associated with each virtual field, while ET_O and ET_C were calculated with SI CropFit using data from the weather stations. For all three regions and both the entire growing season and the reproductive phase of the growing season, the mean cumulative ET_C was less than the mean cumulative precipitation. This demonstrates that over the period of records, more precipitation is received than the amount of water required to meet the crops' ET demands (ET_C). However, these data do not show the distribution of precipitation during the growing season and further demonstrate the importance of quantifying the frequency of flash drought occurrence as well as the impact of flash drought on crop yield.

Flash drought occurrence in virtual fields

SI CropFit generated reports on the number of flash drought events for each maize and cotton growing season at each of the virtual fields from 2003 to 2022. Examples of how annual results were visualized are presented for maize in Marianna, FL (Figure 2.7). In this virtual field, between June 10 and July 10, 2022, there were 32 consecutive days when RZSWD exceeded 60%

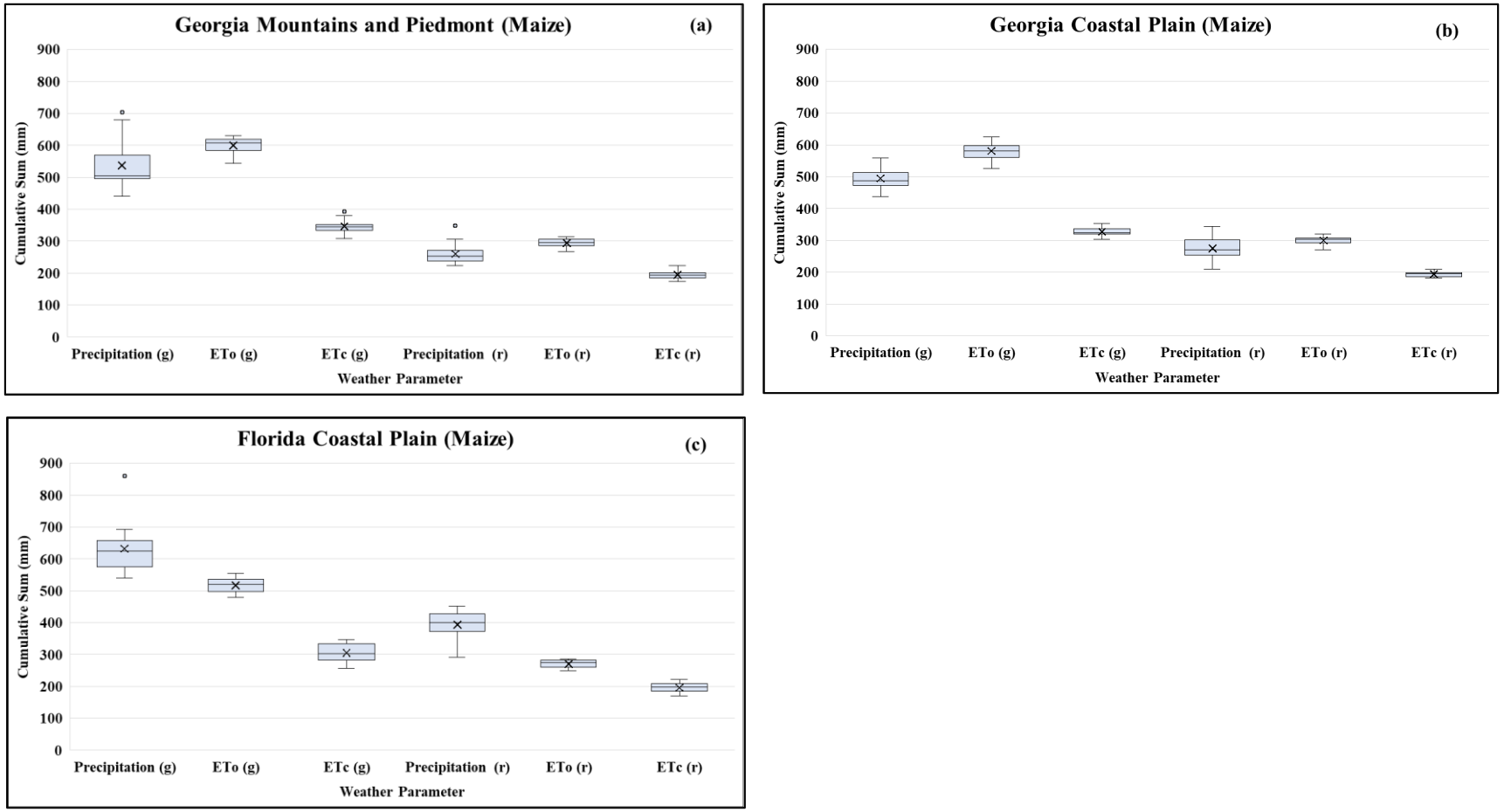

Figure 2.5 Mean cumulative sum of precipitation, reference evapotranspiration (ET_O), and daily crop water use (ET_C) by geographic region: (a) Mountains and Piedmont in Georgia, (b) Georgia Coastal Plain, and (c) Florida Coastal Plain during the growing season and reproductive phase of maize for 2003-2022. In each graph, (g) represents the growing season, (r) represents the reproductive phase, the box represents the distribution of 50% of the data, the whiskers represent the distribution of the other 50% of the data, the horizontal line in each box represents the median, and the X represents the mean.

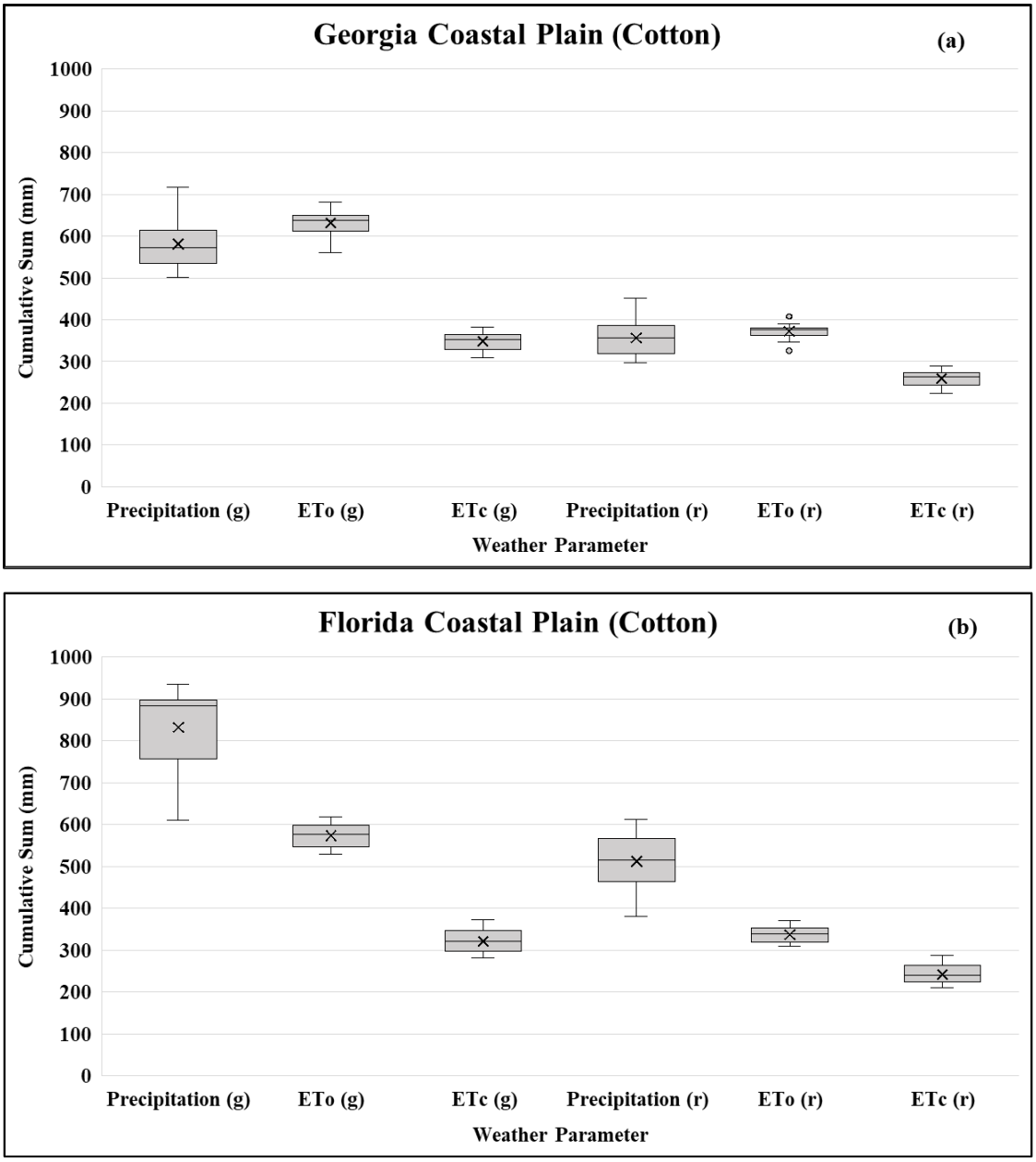

Figure 2.6. Mean cumulative precipitation, reference evapotranspiration (ET_O), and daily crop water use (ET_C) by geographic region: (a) Georgia Coastal Plain and (b) Florida Coastal Plain during the growing season and reproductive stages of cotton for 2003-2022. In each graph, (g) represents the growing season, (r) represents the reproductive phase, the box represents the distribution of 50% of the data, the whiskers represent the distribution of the other 50% of the data, the horizontal line in each box represents the median, and the X represents the mean.

and 17 days in that period when RZSWD exceeded 80%. As described earlier, a flash drought event was recorded when RZSWD exceeded 60% for 15 consecutive days. In the Marianna example, two flash drought events were recorded – the first one characterized as RZSWD ≥60% and the second as RZSWD ≥70%. These periods of flash drought coincided with the reproductive phase of maize (R1–R5 growth), which is the most sensitive to water stress (Figure 2.7). Based on the simulations with the CSM-CERES-Maize and CSM-CROPGRO-Cotton models, these two periods of flash drought may have resulted in yield losses of 53% when compared to the 20-year

Smartirrigation Corn

User: support@austn.co

Field: Field Corn Marianna | Planting date: Apr-15-2022 | Lat: 30.85, Lon: -85.16516 | Weather Data Source: FAWN - Marianna

Date	Days After Planting (DAP)	Acc. Heat Units (GDD 50F)	Phenological Stage	Evapotranspiration Eto (in)	Crop Coeff. (KC)	Evapotranspiration. (Et*KC in)	Effective Rain (in)	RZSWD (in)	RZSWD (%)
Jun-02-2022	48	1129	V9	0.2211	1.05	0.23216	0	1.0848	57
Jun-03-2022	49	1161	V9	0.2254	1.05	0.23667	0	1.3215	69
Jun-04-2022	50	1192	V9	0.2083	0.84	0.17497	0	1.4965	78
Jun-05-2022	51	1222	V9	0.2317	0.63	0.14597	0.3238	1.3187	69
Jun-06-2022	52	1247	V9	0.1553	0.84	0.13045	0.0088	1.4403	75
Jun-07-2022	53	1276	Tasseling	0.1785	0.63	0.11246	0	1.5527	81
Jun-08-2022	54	1307	Tasseling	0.2201	0.42	0.09244	0.0181	1.627	85
Jun-09-2022	55	1339	R1	0.1797	0.42	0.07547	0.675	1.0275	54
Jun-10-2022	56	1366	R1	0.1402	1.05	0.14721	0	1.1747	61
Jun-11-2022	57	1395	R1	0.2023	0.84	0.16993	0	1.3446	70
Jun-12-2022	58	1426	R1	0.2143	0.63	0.13501	0	1.4796	77
Jun-13-2022	59	1460	R1	0.2193	0.63	0.13816	0	1.6178	84
Jun-14-2022	60	1494	R1	0.2128	0.42	0.08938	0.0538	1.6534	86
Jun-15-2022	61	1526	R1	0.2071	0.42	0.08698	0	1.7404	91
Jun-16-2022	62	1561	R1	0.2195	0.42	0.09219	0.3238	1.5088	79
Jun-17-2022	63	1597	R1	0.2423	0.63	0.15265	0	1.6614	87
Jun-18-2022	64	1629	R2	0.2306	0.42	0.09685	0	1.7583	92
Jun-19-2022	65	1667	R2	0.2626	0.42	0.11029	0	1.8686	97
Jun-20-2022	66	1701	R2	0.2529	0.42	0.10622	0	1.92	100
Jun-21-2022	67	1737	R2	0.2536	0.42	0.10651	0	1.92	100
Jun-22-2022	68	1771	R2	0.2282	0.42	0.09584	0	1.92	100
Jun-23-2022	69	1809	R3	0.2913	0.42	0.12235	0	1.92	100
Jun-24-2022	70	1847	R3	0.2746	0.42	0.11533	0	1.92	100
Jun-25-2022	71	1885	R3	0.272	0.42	0.11424	0.0538	1.8662	97
Jun-26-2022	72	1912	R3	0.1208	0.42	0.05074	0	1.9169	100
Jun-27-2022	73	1946	R3	0.2311	0.42	0.09706	0	1.92	100
Jun-28-2022	74	1980	R4	0.234	0.42	0.09828	0	1.92	100
Jun-29-2022	75	2011	R4	0.1929	0.42	0.08102	0	1.92	100
Jun-30-2022	76	2041	R4	0.1914	0.42	0.08039	0	1.92	100
Jul-01-2022	77	2070	R4	0.1647	0.42	0.06917	0	1.92	100
Jul-02-2022	78	2102	R4	0.1814	0.42	0.07619	0.0538	1.8662	97
Jul-03-2022	79	2133	R4	0.1444	0.42	0.06065	0.0181	1.9019	99
Jul-04-2022	80	2162	R4	0.1552	0.42	0.06518	0.5669	1.3531	70
Jul-05-2022	81	2191	R5	0.1793	0.63	0.11296	0	1.466	76
Jul-06-2022	82	2223	R5	0.2214	0.63	0.13948	0	1.6055	84
Jul-07-2022	83	2259	R5	0.2412	0.4195	0.10118	0	1.7067	89
Jul-08-2022	84	2295	R5	0.2444	0.4094	0.10006	0	1.8068	94
Jul-09-2022	85	2331	R5	0.2486	0.3993	0.09927	0.1619	1.7442	91
Jul-10-2022	86	2363	R5	0.1632	0.3904	0.06371	0.0088	1.7991	94
Jul-11-2022	87	2396	R5	0.1953	0.3811	0.07443	1.0169	0.8566	45

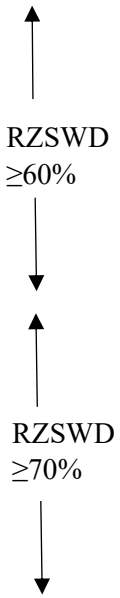

Figure 2.7 SmartIrrigation CropFit (SI CropFit) report showing root zone soil water deficit (RZSWD) for the Marianna, FL, virtual field during the 2022 maize growing season. Red cells indicate days when RZSWD ≥80%, orange cells indicate RZSWD ≥70%, and yellow cells indicate days when RZSWD ≥60%. Flash drought events that occurred during the growing season are indicated in the figure with the arrows.

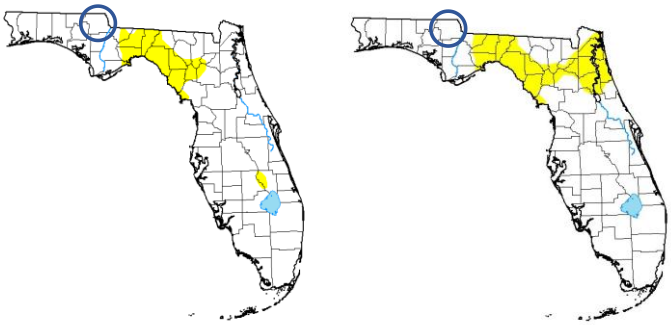

June 14, 2022 June 21, 2022

Figure 2.8 U.S. Drought Monitor maps for Florida from the weeks of June 14 and June 21, 2022, indicating normal conditions (white) in most of the state with some areas characterized as being abnormally dry (yellow). The map indicates normal conditions around Marianna (circled).

rainfed maize yield (Chapter 3). In stark contrast to the SI CropFit results, the USDM did not capture drought conditions in either Marianna (Figure 2.8) during these two periods. This juxtaposition in results was observed for multiple years at many of the virtual fields. Because of the difference in variables used by the USDM, it is not effective at identifying the rapid intensification of short-term agricultural drought (Ford et al., 2023; Walker et al., 2023). These differences emphasize the importance of developing alternative tools to quantify the effects of flash drought.

Flash drought occurrence over the period of record

To gain perspective on the prevalence of flash drought over the 20-year period of record (2003-2022), the total number and the mean annual number of 15-day flash drought events were quantified for the entire growing season as well as for the reproductive phase of cotton and maize at each of the virtual fields. Figure 2.9 shows the mean annual flash drought events observed during the 20-year period of record for RZSWD ≥60%, RZSWD ≥70%, and RZSWD ≥80% during the entire growing season and the reproductive phase for maize. Figure 2.10 shows these results for cotton. In each graph, the box represents the distribution of 50% of the flash drought events

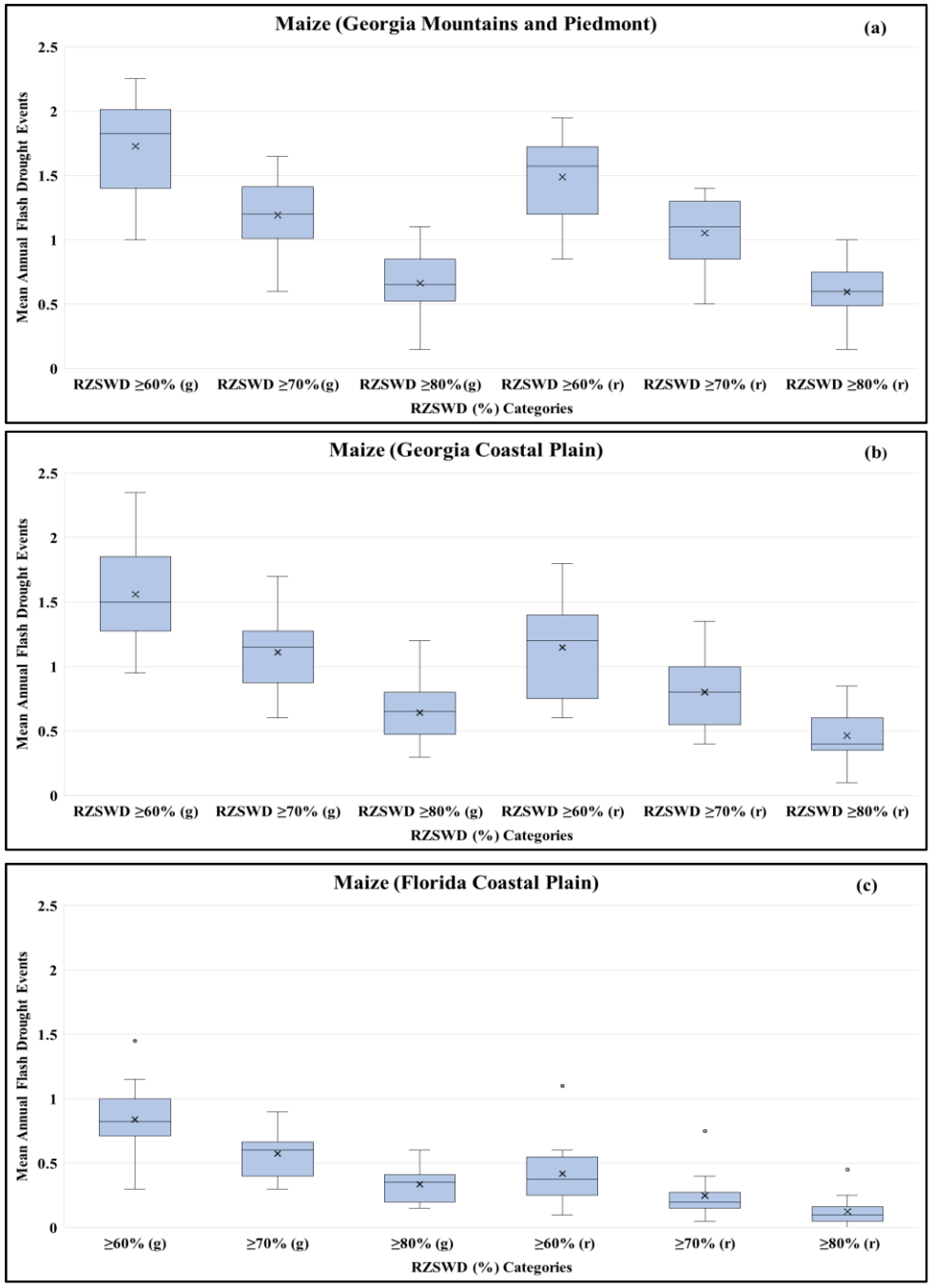

Figure 2.9 Mean annual flash drought events observed during the 20-year period of record for root zone soil water deficit- RZSWD ≥60%, RZSWD ≥70%, and RZSWD ≥80% by geographic region: (a) Georgia Mountains and Piedmont, (b) Georgia Coastal Plain and (c) Florida Coastal Plain, during the entire growing season and the reproductive phase for maize. In each graph, (g) represents the growing season, (r) represents the reproductive phase, the box represents the distribution of 50% of the observed flash drought events, the whiskers represent the distribution of the other 50% of the events, the horizontal line represents the median, and the X represents the mean. Circles represent outliers.

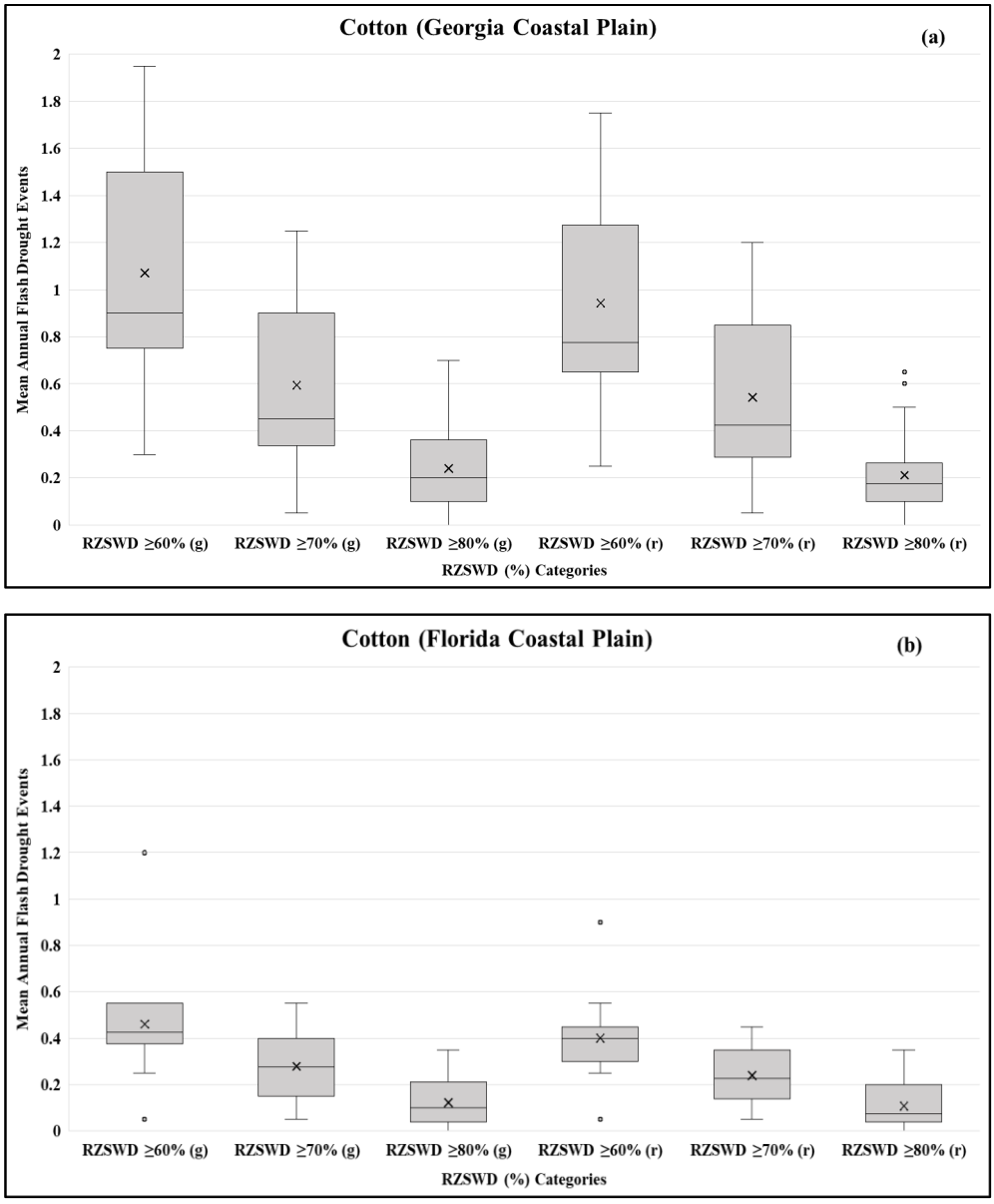

Figure 2.10 Mean annual flash drought events observed during the 20-year period of record for root zone soil water deficit- RZSWD ≥60%, RZSWD ≥70%, and RZSWD ≥80% by geographic region during the entire growing season and the reproductive phase for cotton. In each graph, (g) represents the growing season, (r) represents the reproductive phase, the box represents the distribution of 50% of the observed flash drought events, the whiskers represent the distribution of the other 50% of the events, the horizontal line represents the median, and the X represents the mean. Circles represent outliers.

that were observed in the virtual fields, the whiskers represent the distribution of the other 50% of the events, the horizontal line represents the median, the X represents the mean, and the circles represent outliers. Across all regions and for both crops, the number of events decreased as the threshold for characterizing a flash drought increased from RZSWD ≥60 to RZSWD ≥80.

There were substantially fewer maize flash drought events in the Florida Coastal Plain than in the Georgia mountains and Piedmont, and the Georgia Coastal Plain (Figures 2.9a, 2.9b, and 2.9c). In the Georgia mountains and Piedmont region, the maize reproductive phase mean annual precipitation is less than ET_O and only slightly higher than ET_C (Figure 2.5), making the occurrence of flash drought more likely. Similarly, there were fewer flash drought events in the Florida Coastal Plain than in the Georgia Coastal Plain for cotton (Figure 2.10). This is most likely the result of the growing season rains (Figure 2.6) associated with the summer rainy season in Florida (Wright et al., 2020). In Florida, the mean number of events during the growing seasons and reproductive phase of the growing seasons is similar, indicating that most flash drought events occurred during the reproductive phase (Figure 2.10b).

Table 2.1 presents the maize results in more detail for selected virtual fields. The selected fields span the geographic regions that were simulated and are included in the virtual fields shown by pins with yellow dots in Figure 2.4. The number of growing season flash drought events was generally greater in Georgia than in Florida, with substantially more RZSWD ≥60% events occurring than RZSWD ≥80% events. The virtual field with the fewest RZSWD ≥60% events (6) and RZSWD ≥80% events (3) was in Alachua, FL, and the field with the most RZSWD ≥60% (47) and RZSWD ≥80% (19) events were in Plains, GA. In Georgia, there were large differences in the number of events between virtual fields, with the smallest number of events occurring in the mountain region in the northeast of the state. The largest number of events occurred in the Coastal

Table 2.1 Period of record (2003-2022) total and mean annual number of 15-day flash drought events with root zone soil water deficit- RZSWD ≥60%, ≥70%, and ≥80% as identified by SmartIrrigation CropFit (SI CropFit) for maize at selected virtual fields in Georgia and Florida. The number of flash drought events is shown for the entire growing season and the reproductive phase of maize. The mean number of events is shown in parentheses. The virtual fields above the broken line are in the mountain and Piedmont region, while the virtual fields below the broken line are in the Coastal Plain region of Georgia.

Virtual Field Name	Period of Record Total and Mean Annual Flash Drought Events for Maize					
	Growing Season			Reproductive Phase		
	RZSWD ≥60%	RZSWD ≥70%	RZSWD ≥80%	RZSWD ≥60%	RZSWD ≥70%	RZSWD ≥80%
Georgia						
Blairsville	20 (1.00)	12 (0.60)	3 (0.15)	17 (0.85)	10 (0.50)	3 (0.15)
Calhoun	37 (1.85)	24 (1.20)	9 (0.45)	34 (1.70)	23 (1.15)	9 (0.45)
Eatonton	30 (1.50)	24 (1.20)	13 (0.65)	26 (1.30)	22 (1.10)	11 (0.55)
Griffin	39 (1.95)	28 (1.40)	13 (0.65)	33 (1.65)	25 (1.25)	13 (0.65)
Watkinsville	44 (2.20)	32 (1.60)	17 (0.85)	39 (1.95)	28 (1.40)	16 (0.80)
Camilla	25 (1.25)	18 (0.90)	13 (0.65)	15 (0.75)	11 (0.55)	7 (0.35)
Midville	37 (1.85)	26 (1.30)	12 (0.60)	31 (1.55)	23 (1.15)	12 (0.60)
Plains	47 (2.35)	34 (1.70)	19 (0.95)	35 (1.75)	27 (1.35)	16 (0.80)
Tifton	39 (1.95)	25 (1.25)	12 (0.60)	30 (1.50)	18 (0.90)	8 (0.40)
Florida						
Alachua	6 (0.30)	6 (0.30)	3 (0.15)	4 (0.20)	4 (0.20)	2 (0.10)
Citra	20 (1.00)	11 (0.55)	4 (0.20)	9 (0.45)	5 (0.25)	1 (0.05)
Live Oak	12 (0.60)	8 (0.40)	4 (0.20)	7 (0.35)	4 (0.20)	2 (0.10)
Marianna	29 (1.45)	18 (0.90)	11 (0.55)	22 (1.10)	15 (0.75)	9 (0.45)
Quincy	15 (0.75)	8 (0.40)	5 (0.25)	8 (0.40)	5 (0.25)	3 (0.15)

Plain area in the southwest of the state. In contrast, the number of events that occurred in the virtual fields located in Florida had a smaller range (Table 2.1).

Because water stress during the reproductive phase is most likely to affect yield (Chapter 3), examining the number of events during this period is important. For maize, the reproductive phase was defined from R1 to Maturity. For the virtual fields in Georgia, between 50% and 100% of flash drought events occurred during the reproductive phase (Table 2.1, Figure 2.9). For more

than half the virtual fields in Georgia, the number of flash drought events of RZSWD ≥70% exceeded 20, indicating that such an event is likely to occur each year (Table 2.1).

In contrast to Georgia, reproductive phase flash drought events in Florida for maize occurred approximately half as frequently as growing season flash drought events (Figure 2.9c). This is likely because the planting date for rainfed maize in Florida is scheduled so that the reproductive phase coincides with the beginning of the summer rainy season in June (Wright et al., 2020).

Table 2.2 shows the growing season and reproductive phase flash drought events for selected virtual cotton fields in Florida and Georgia. The selected fields are included in the virtual fields shown by pins with yellow dots in Figure 2.4. As with maize, Georgia experienced significantly more flash drought events than Florida (Figures 2.10a and 2.10b). There were large differences in the number of flash drought events among the virtual fields in Georgia, with the smallest number of events occurring at Dixie, located in the southwestern area of the state, and the largest number of events occurring at Dearing on the eastern side of the state. In Florida, the difference in flash drought event occurrence between virtual fields was smaller (Figure 2.10b). The reproductive phase of cotton was defined from the first flower to 60% open bolls. For the virtual fields in Georgia, between 75% and 100% of flash drought events occurred during the reproductive phase. For more than half the virtual fields in Georgia, the number of flash drought events of RZSWD ≥60% exceeded 15, indicating that such an event is likely to occur frequently (Table 2.2). Flash drought events in Florida during the cotton growing season were about half of those for maize, but most flash drought events occurred during the reproductive phase. The virtual field in Marianna was an outlier, with double the number of reproductive phase flash drought events compared to the other Florida virtual fields (Figure 2.10b). The lower number of flash

Table 2.2 Period of record (2003-2022) total and mean annual number of 15-day flash drought events with root zone soil water deficit- RZSWD ≥60%, ≥70%, and ≥80% as identified by SmartIrrigation CropFit (SI CropFit) for cotton at selected virtual fields in Georgia and Florida. The number of flash drought events is shown for the entire growing season and the reproductive phase of cotton. The mean number of events is shown in parentheses.

Virtual Field Name	Period of Record Total and Mean Annual Flash Drought Events for Cotton					
	Growing Season			Reproductive Phase		
	RZSWD ≥60%	RZSWD ≥70%	RZSWD ≥80%	RZSWD ≥60%	RZSWD ≥70%	RZSWD ≥80%
Georgia						
Camilla	16 (0.80)	7 (0.35)	3 (0.15)	14 (0.70)	7 (0.35)	3 (0.15)
Dearing	39 (1.95)	24 (1.20)	14 (0.70)	35 (1.75)	24 (1.20)	13 (0.65)
Dixie	6 (0.30)	1 (0.05)	0 (0.00)	5 (0.25)	1 (0.05)	0 (0.00)
Jeffersonville	36 (1.80)	24 (1.20)	13 (0.65)	32 (1.60)	22 (1.10)	12 (0.60)
Midville	34 (1.70)	21 (1.05)	8 (0.40)	28 (1.40)	18 (0.90)	5 (0.25)
Plains	22 (1.10)	9 (0.45)	6 (0.30)	21 (1.05)	8 (0.40)	5 (0.25)
Statesboro	27 (1.35)	18 (0.90)	8 (0.40)	25 (1.25)	17 (0.85)	8 (0.40)
Tifton	21 (1.05)	13 (0.65)	6 (0.30)	20 (1.00)	13 (0.65)	5 (0.25)
Florida						
Citra	5 (0.25)	3 (0.15)	2 (0.10)	5 (0.25)	3 (0.15)	2 (0.10)
Live Oak	11 (0.55)	6 (0.30)	1 (0.05)	9 (0.45)	5 (0.25)	1 (0.05)
Marianna	24 (1.20)	11 (0.55)	7 (0.35)	18 (0.9)	9 (0.45)	7 (0.35)
Ocklawaha	8 (0.40)	6 (0.30)	2 (0.10)	8 (0.40)	6 (0.30)	2 (0.10)
Quincy	8 (0.40)	3 (0.15)	1 (0.05)	8 (0.40)	3 (0.15)	1 (0.05)

drought events in Florida is directly related to the later planting date selected for cotton compared to maize (April 15 vs May 15), which resulted in most of the reproductive phase of cotton coinciding with the rainy season in Florida.

Comparison of SI CropFit flash drought events to DSSAT-CSM water stress indices

As described earlier, the relationship between the occurrence of crop water stress periods determined with the DSSAT-CSM WSPD and WSGD indices and flash drought events identified with the SI CropFit RZSWD ≥60% method was evaluated. This was done both visually and

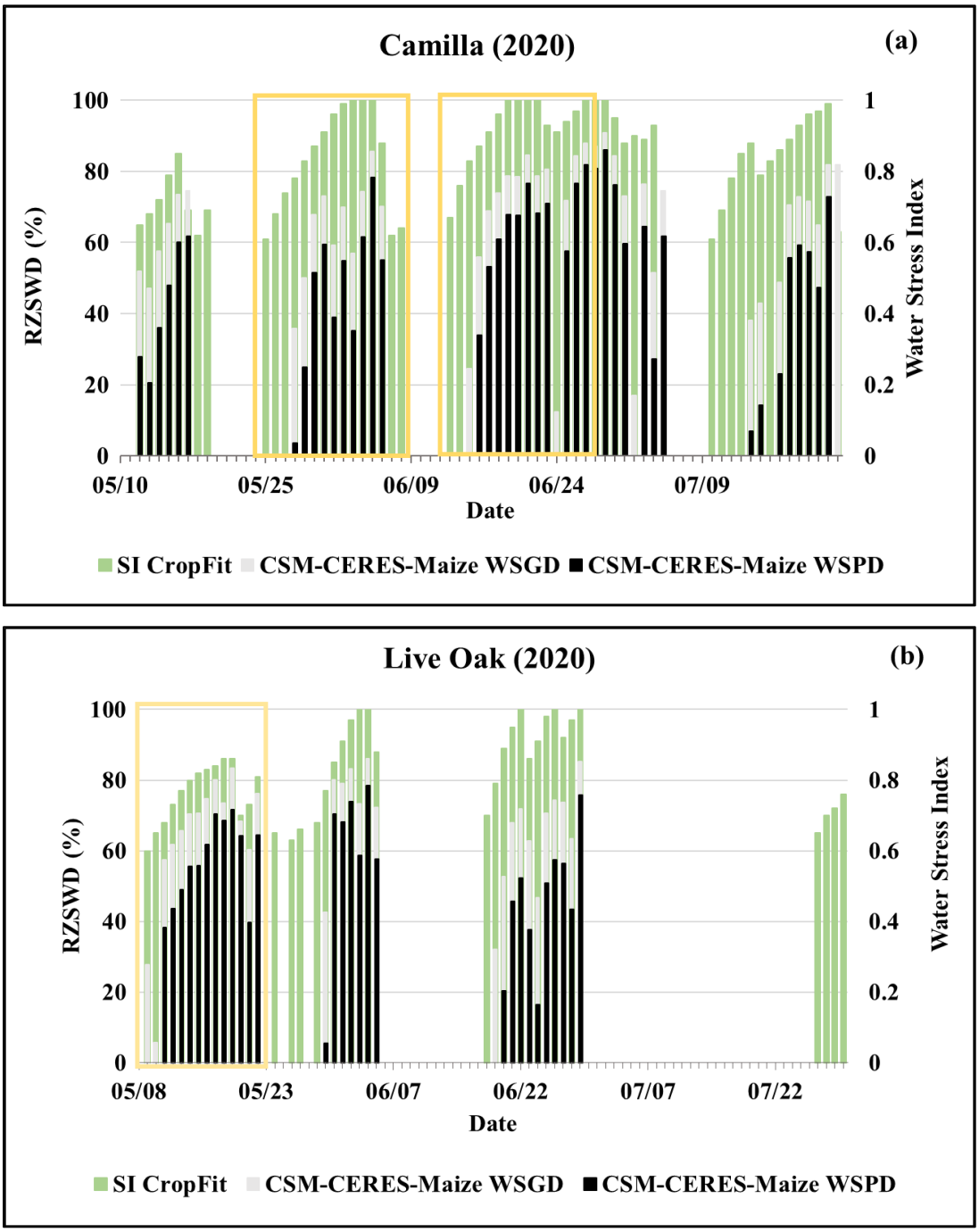

Figure 2.11 Examples of days when SmartIrrigation CropFit (SI CropFit) root zone soil water deficit (RZSWD) ≥60% (green bars) overlain by days when water stress index related to photosynthesis (WSPD) >0 (black bars) and water stress index related to growth (WSGD) >0 (gray bars) by CSM-CERES-Maize from virtual maize fields in Camilla, GA (2020) (a) and Live Oak, FL (2020) (b). The yellow rectangles indicate SI CropFit 15-day flash drought events.

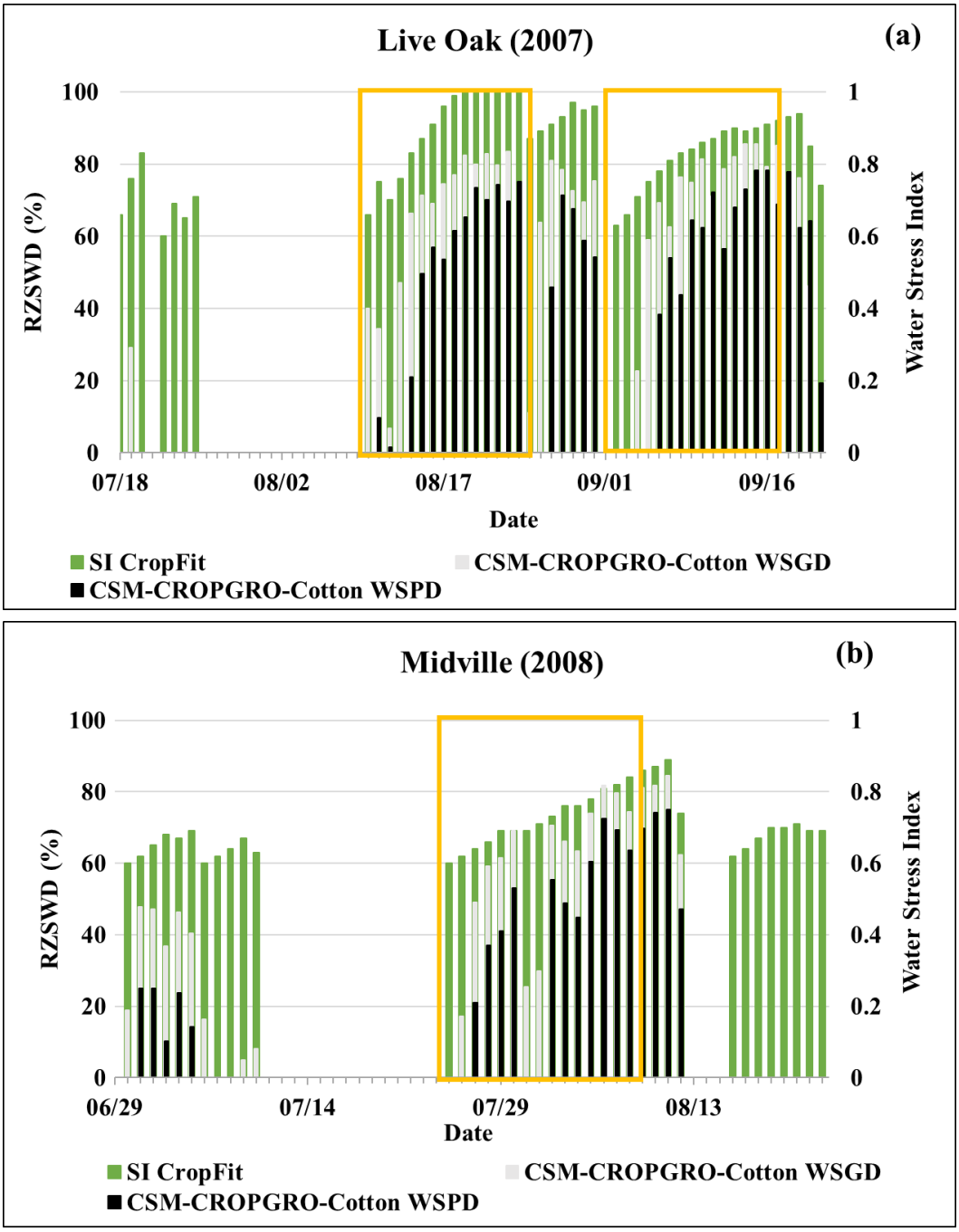

Figure 2.12 Examples of days when SmartIrrigation CropFit (SI CropFit) root zone soil water deficit (RZSWD) ≥60% (green bars) overlain by days when water stress index related to photosynthesis (WSPD) >0 (black bars) and water stress index related to growth (WSGD) >0 (gray bars) by CSM-CROPGRO-Cotton from virtual cotton fields in Live Oak, FL (2007) (a) and Midville, GA (2008) (b). The yellow rectangles indicate SI CropFit 15-day flash drought events.

statistically. Figures 2.11 and 2.12 provide a visual comparison of the response of SI CropFit RZSWD to that of DSSAT-CSM WSPD and WSGD temporally at example virtual maize and cotton fields, respectively. The bars in the two graphs indicate days when SI CropFit RZSWD ≥60% (green bars), days when WSPD >0 (black bars), and days when WSGD >0 (gray bars). The yellow rectangles indicate SI CropFit 15-day flash drought events. In general, the DSSAT-CSM indices predicted fewer crop water stress days than SI CropFit days with RZSWD ≥60% in most of the virtual fields for both crops, with WSGD better matching SI CropFit. This is because WSGD indicates crop water stress earlier than WSPD, as leaf expansion is reduced earlier than photosynthesis (Hoogenboom et al., 2023). However, the three crop water stress metrics exhibited similar patterns even though one estimates plant available soil water and infers crop water stress, while the other two estimate crop water stress directly. These patterns indicate that WSGD may potentially be used to establish an RZSWD threshold for identifying flash drought periods. For example, RZSWD ≥70% would better match the periods of WSPD and WSGD >0. However, additional research is needed to quantify the level of crop water stress represented by the 0-1 range of WSPD (Woli et al., 2012).

The statistical relationship between the number of SI CropFit RZSWD ≥60% flash drought days per month and the number of days DSSAT-CSM WSPD >0 and WSGD >0 was evaluated using the coefficient of determination (R^2) resulting from linear regression. The comparisons were done for three months for each crop that bracketed the crop's reproductive phase (May, June, July for maize; July, August, September for cotton). As expected, the comparison was more robust for WSGD, and those results are presented in Table 2.3.

For maize, the linear regression analyses resulted in R^2 ranging from 0.26 to 0.91. The best agreement between the methods occurred in the northern Georgia virtual fields, where most R^2

Table 2.3 Statistical comparison between root zone soil water deficit-RZSWD ≥60 as calculated by SmartIrrigation CropFit (SI CropFit) and the water stress index related to growth (WSGD) predicted by the CSM-CERES-Maize model and CSM-CROPGRO-Cotton model from 2003-2022 using the linear regression method.

Virtual Fields	Coefficient of Determination (R^2)					
	May	June	July		August	September
	Maize	Maize	Maize	Cotton	Cotton	Cotton
			Georgia			
Blairsville	ND[1]	0.85	0.85	-	-	-
Calhoun	ND[1]	0.82	0.86	-	-	-
Eatonton	0.73	0.88	0.85	-	-	-
Griffin	0.56	0.90	0.71	-	-	-
Watkinsville	0.56	0.91	0.83	-	-	-
Camilla	0.79	0.79	0.77	0.88	0.85	0.62
Midville	0.72	0.79	0.79	0.59	0.68	0.66
Plains	0.85	0.88	0.89	0.67	0.87	0.62
Tifton	0.87	0.91	0.89	0.88	0.87	0.87
			Florida			
Citra	0.90	0.59	0.38	0.56	0.80	ND[1]
Live Oak	0.54	0.71	0.26	0.61	0.89	0.45
Marianna	0.82	0.79	0.75	0.71	0.74	0.41
Quincy	0.59	0.69	0.91	0.79	0.74	0.49

[1] ND = No flash drought events or DSSAT-CSM crop water stress simulated.

values were >0.8, while the worst agreement occurred for the Coastal Plain virtual fields in Florida (Table 2.3). Two virtual fields in Georgia (Blairsville, Calhoun) are in the mountainous region, and three virtual fields (Eatonton, Griffin, and Watkinsville) are in the Piedmont physiographic region of the state (Figure 2.4) and thus at higher elevations, resulting in cooler spring and early summer temperatures. At these sites, water stress was observed in maize mainly during June and July by both DSSAT-CSM and SI CropFit (Table 2.3). For the other eight sites, which are further south and located in the Coastal Plain with elevation generally below 100 m, water stress was observed by both DSSAT-CSM and SI CropFit primarily during May and June, especially at four sites in the Florida Coastal Plain. In the Coastal Plain, May receives much less precipitation than other months of the growing season. These periods correspond to when the reproductive period occurs at these locations and match observations by other researchers. For example, Christian

(2019) found that flash drought in the southeastern U.S. is generally observed at the beginning to middle of the maize-growing season, which reaches its peak during May. In June and July 2011, the standardized evaporative stress ratio (SESR) showed that most of the southeastern U.S. was experiencing drought (Edris et al., 2023). From late June to late July of 2016, there was a flash drought in south-central Georgia that lasted around 35 days (Christian et al., 2019).

For cotton, periods of flash drought/crop water stress were observed primarily in July and August for the four Florida virtual fields and the three virtual fields in Georgia. In contrast, these periods occurred more frequently in August and September for the Midville virtual field in Georgia. In the Coastal Plain, July and August generally receive the most annual precipitation, but the precipitation events are not evenly distributed and often come as intense localized thunderstorms. It is not uncommon to have a 15-day period without precipitation during these two months. September tends to be a dry month with most precipitation events associated with tropical cyclones. The linear regression analyses resulted in R^2 values that ranged from 0.41 to 0.88 but were generally lower than for maize. For Midville, R^2 trended lower in September than in August. For the other seven virtual fields, there were no clear trends associated with location or month, other than there was higher variability in R^2 than was observed with maize.

Overall, it appears that the SI CropFit RZSWD and the DSSAT-CSM WSGD methods independently identified mostly the same periods during which maize and cotton experienced water stress because of flash drought events. This indicates that the SI CropFit RZSWD method is a robust approach for identifying flash drought events.

The flash drought interactive map tool

The Flash Drought Interactive Map Tool (https://sicropfit.austn.co/mapView) that was described previously allows users to explore and visualize flash drought frequency maps of the

study regions under scenarios with different combinations of crop (cotton or maize), flash drought periods (10 or 15 days), RZSWD (≥60%, ≥70%, and ≥80%), and either the entire growing season or the reproductive phase of the crop (Figure 2.13). In addition to viewing the map, users can click on a selected county, and the tool extracts the range of values associated with that county. In the map shown in Figure 2.13, the mean number of 15-day RZSWD ≥60% flash drought events that occurred during the maize reproductive phase for the period of record (2003-2022) in Tift County, Georgia, ranges from 1.0-1.5. By clicking on "Reports" in the menu on the left side of the screen (Figure 2.13), users can also view and download a file with the detailed results for each virtual field. The Flash Drought Interactive Map Tool provides users, especially growers, with the ability

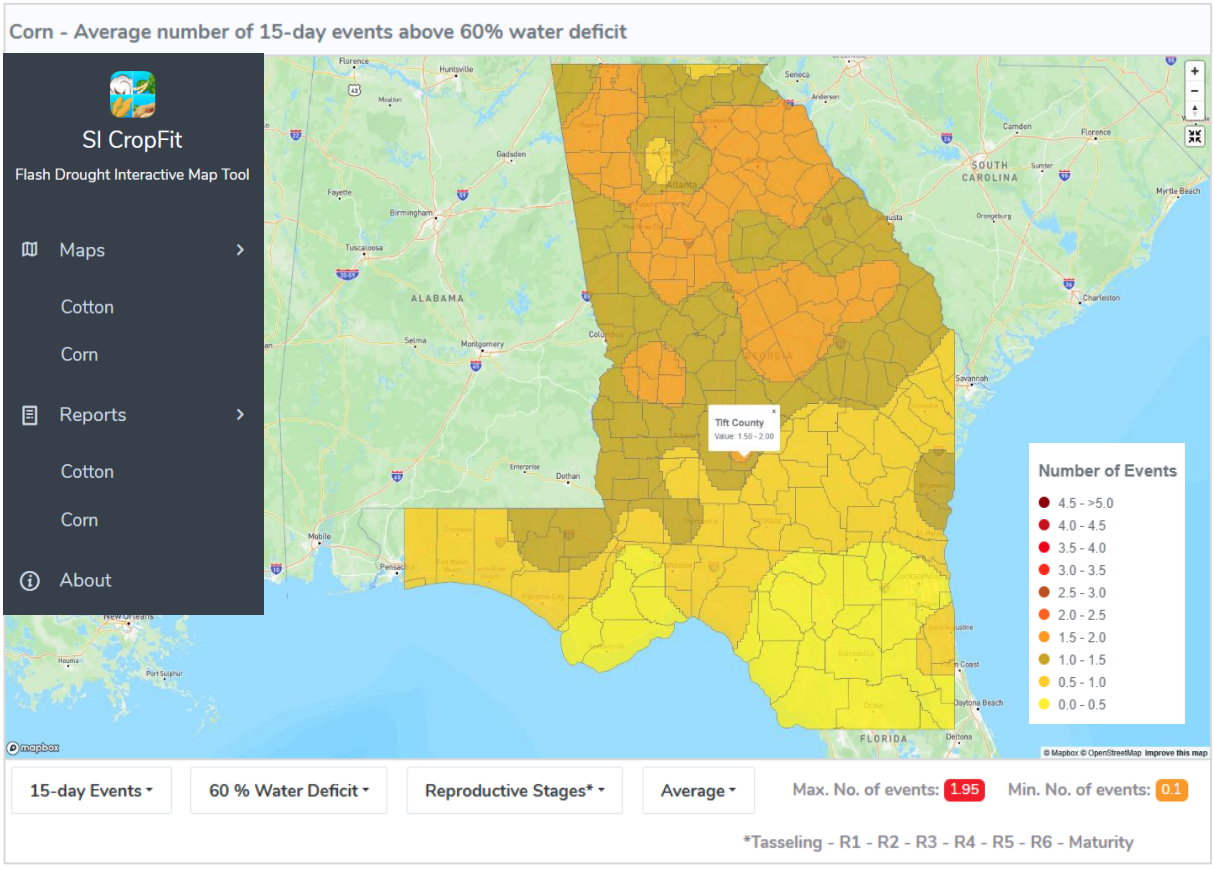

Figure 2.13 Screenshot of the Flash Drought Interactive Map Tool showing the mean number of 15-day root zone soil water deficit-RZSWD ≥60% flash drought events that occurred during the maize reproductive phase for the period of record (2003-2022). In this example, the user has clicked on Tift County, Georgia, where the values range from 1.0-1.5 flash drought events.

to quantify the risk associated with growing rainfed crops in the areas contained within the map boundaries. In Tifton County, for example, it is likely that a 15-day RZSWD ≥60% flash drought event will occur every year during the maize reproductive phase.

In the interest of including higher resolution maps in this paper, some frequency contour maps were also created in ArcGIS (ESRI, Redlands, California, USA), again using the inverse distance weighting (IDW) method. Figure 2.14 shows the resulting maps for maize for RZSWD ≥60% and ≥80%, while Figure 2.15 shows the corresponding maps for cotton. For maize, the total number of flash drought events for RZSWD ≥60% ranged from 6 to 47 (Figure 2.14a) and for RZSWD ≥80% from 3 to 24 (Figure 2.14b). The most flash drought events occurred in a band from south-central to northeast Georgia, while the fewest events occurred in north-central Florida. This pattern is not explained by precipitation alone, as the mean maize growing season precipitation in the mountain and Piedmont region of Georgia was 537 mm. In the Coastal Plain regions of Georgia and Florida, it was 495 mm and 632 mm, respectively (Figure 2.5). However, in the mountain and Piedmont regions of Georgia, mean cumulative ET_C approached mean cumulative precipitation during the maize reproductive phase, thus increasing the likelihood of soil water deficit conditions (Figure 2.5a).

Maps of the mean annual number of RZSWD ≥60% (0.3 to 2.35 per growing season) and RZSWD ≥80% (0.15-1.2 per growing season) flash drought events for maize during the period of record are shown in Figures 2.14c and 2.14d, respectively. These maps are likely most useful to growers as they better convey the likelihood of experiencing a flash drought event during the maize growing season. The results indicate that a flash drought event is likely to be experienced during each growing season in Georgia. Any virtual field with a mean ≥1 was likely to experience a flash drought event during the reproductive phase, which can significantly reduce yield.

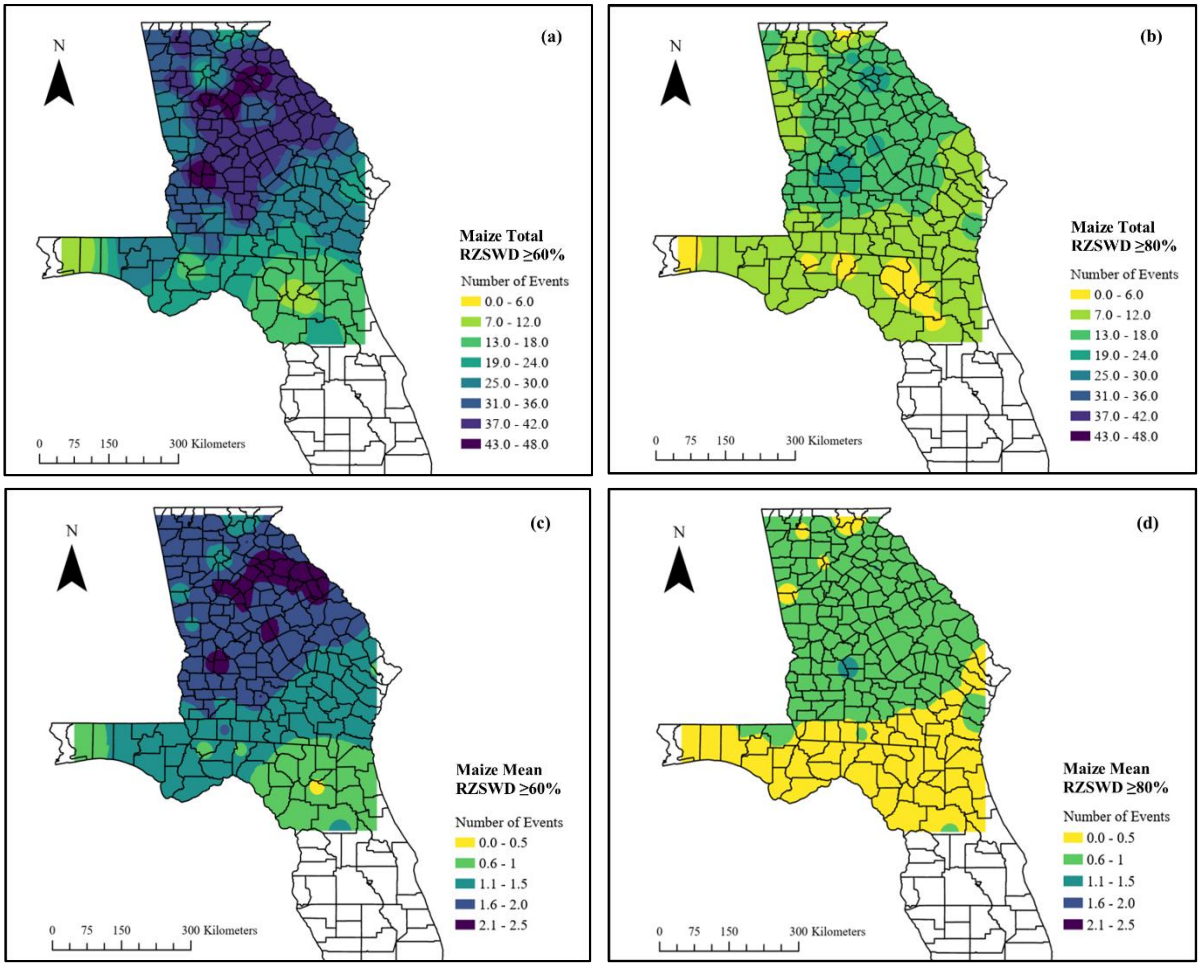

Figure 2.14 Frequency of occurrence of 15-day flash drought events for rainfed maize in Georgia and Florida from 2003-2022 when root zone soil water deficit- RZSWD ≥60% in (a) total number of events and (c) mean annual number of events; and RZSWD ≥80% in (b) total number of events and (d) mean annual number of events.

Figures 2.15a and 2.15b show the frequency of growing season flash drought events in the cotton-grown areas of Florida and Georgia for RZSWD ≥60% and RZSWD ≥80%, respectively, while Figures 2.15c and 2.15d show the corresponding mean annual number of flash drought events during the growing season. The most flash drought events occurred in a band along the northern edge of the Coastal Plain in Georgia, which matches what was observed for maize. The fewest events occurred along the southernmost cotton-grown region of Florida. As described earlier, the total and mean number of flash drought events for cotton was lower than that of maize in both Georgia and Florida. In the Coastal Plain region of Florida, the mean cotton growing season

precipitation was 829 mm, while in Georgia, it was 581 mm (Figure 2.6). The mean annual number of flash drought events at RZSWD ≥60% (0.05 to 1.95 per growing season) (Figure 2.15c) generally decreased from north to south. RZSWD ≥80% was below 1 for the entire cotton growing region (Figure 2.15d).

The maps contain areas of concentric circular patterns, often referred to as the "bull's eye" effect. This is an artifact of interpolation techniques. The IDW method used to create maps assigns greater weight to points that are closer together and less weight to points that are farther apart and

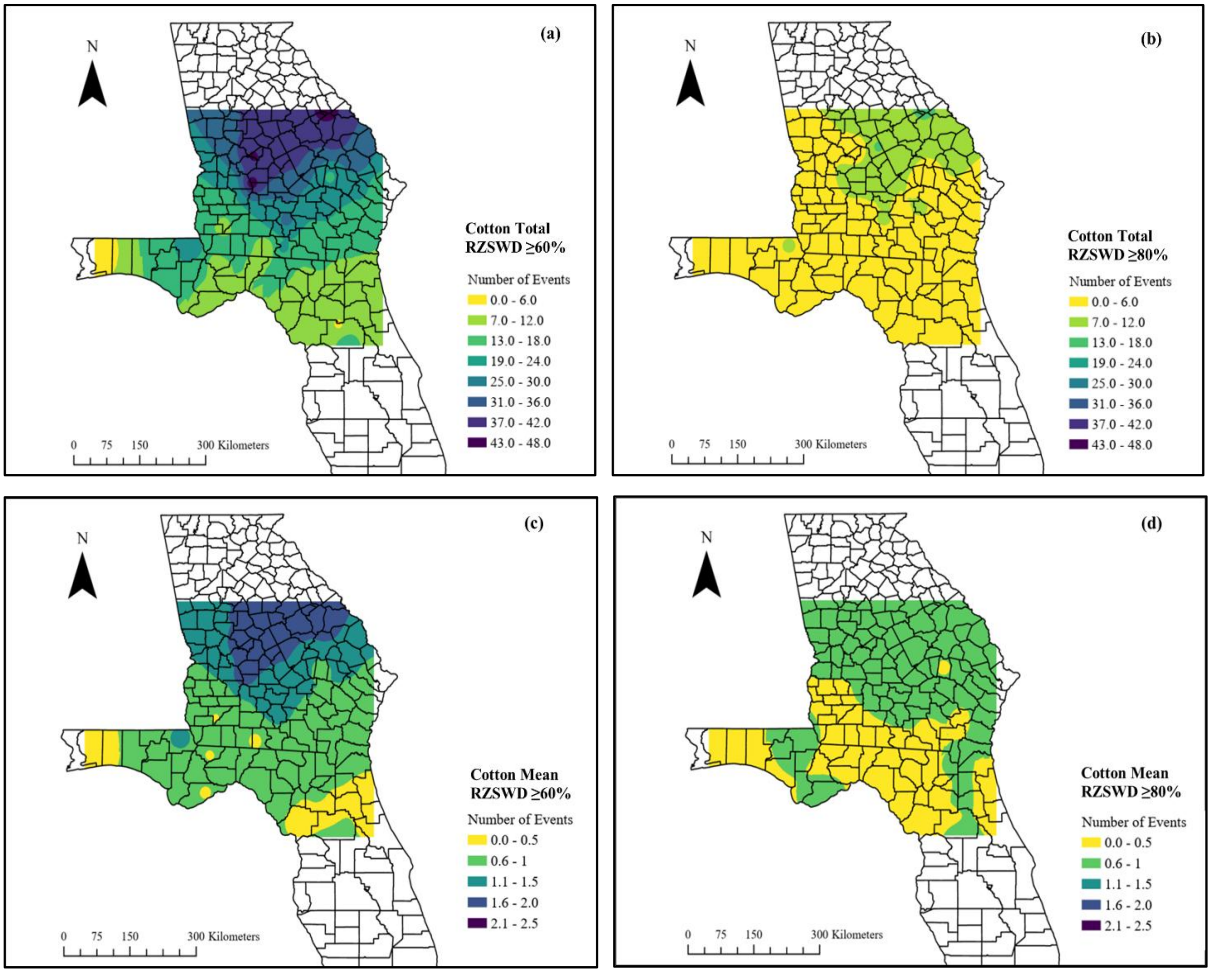

Figure 2.15 Frequency of occurrence of 15-day flash drought events for rainfed cotton in Georgia and Florida from 2003-2022 when root zone soil water deficit- RZSWD ≥60% in (a) total number of events and (c) mean annual number of events; and RZSWD ≥80% in (b) total number of events and (d) mean annual number of events.

is affected by the number of neighboring values. In this study, some virtual field locations were isolated from neighboring fields, leading to the bull's eye effect.

Comparisons to other studies

Several studies have been conducted to quantify the frequency of flash droughts in the recent past. For example, Hobbins et al. (2016) compared the 14-day Evaporative Demand Drought Index (EDDI-14) to other commonly used drought indices. They found that the EDDI demonstrated better early warning of flash drought when compared to the USDM. Ford et al. (2023) applied the EDDI method as well as several other methods to identify flash drought across the continental U.S. between 2002-2021. They found that the EDDI method exhibited a relatively low flash drought frequency over the southeastern U.S., while other methods all had a relatively high frequency in the same region. For example, the EDDI-14 method estimated the total flash drought events in the southeastern U.S. over the 20-year study period to be 23 (approximately 1.15 events per year per 4 km grid cell) while the ΔEDDIz method (the mean change in EDDI-14 for a particular grid cell and calendar day) identified 45 events (about 2.25 events per year per grid cell). Using a soil moisture percentile drop method, Lesinger and Tian (2022) identified 60 flash drought events between 1981-2018 in the southeastern U.S. with a typical duration of 3-4 weeks. Kaniewski (2021) estimated that flash drought occurrences rose in several southern states, including Mississippi, Alabama, Georgia, South Carolina, and the Florida panhandle, ranging from roughly six to fourteen per 4 km grid cell from 2000-2019. Although these methods differ from the method used in this study, it is notable that the total number of estimated flash drought events, as well as the estimated annual number of events, are within the same range.

Conclusions

Between 2003-2022, Georgia experienced more flash droughts than Florida. Approximately twice as many mean annual RZSWD ≥80% events occurred at Georgia virtual fields than in Florida virtual fields. In Georgia, rainfed maize experienced flash drought at RZSWD ≥60% on average at least once every growing season, and at least 50% of the maize flash drought events occurred during the crop's reproductive phase. In Florida, this figure was as low as 12%.

Although the overall number of cotton flash drought events in both states was lower than for maize, 75% of cotton flash drought events in Georgia and 50% in Florida occurred during the reproductive phase. One explanation for this is that September and October, when cotton is still in its reproductive phase, normally receive comparatively less precipitation than earlier in the growing season. So, when there are longer periods between precipitation events, flash drought occurs more rapidly.

What differentiates the SI CropFit method from other flash drought studies is that it was applied to individual crops. This resulted in a better understanding of how flash drought affects individual commodities grown in the southeastern U.S. as flash drought events were assessed both for the entire growing season and for the reproductive phase of maize and cotton. Because SI CropFit is a functioning and publicly available irrigation scheduling tool, individual growers can apply it to their rainfed fields to document when they experience flash drought events. Although the method was evaluated only for cotton and maize, the same soil water balance method is used for the peanut and soybean SI CropFit models. Consequently, the method can be used to assess flash drought in four rainfed crops – cotton, maize, peanut, and soybean.

More broadly, agencies that are responsible for administering state and federal disaster assistance programs for growers can use SI CropFit to quantify the occurrence of flash drought

and coupled with crop simulation models, can estimate the impact of the flash drought events on yield (Chapter 3). Furthermore, policymakers and other stakeholders can more effectively allocate resources for drought mitigation and increase the regional resilience of agricultural systems by using spatial mapping of flash drought frequency.

CHAPTER 3

QUANTIFYING THE EFFECT OF FLASH DROUGHTS ON RAINFED MAIZE AND COTTON YIELD IN THE SOUTHEASTERN UNITED STATES[2]

[2]Jannat, J., G. Hoogenboom, L. Baxter, C. J. Bryant, J. L. Snider, X. Lu, A. Orfanou, and G. Vellidis. To be submitted to *Agronomy Journal.*

Abstract

Flash drought is the rapid onset or intensification of short-term agricultural drought. This research aimed to quantify the effect of flash drought on maize (*Zea mays*) and cotton (*Gossypium hirsutum*) grown under rainfed conditions in the southeastern United States (U.S.). In the study reported here, the Decision Support System for Agrotechnology Transfer (DSSAT) Cropping System Model (CSM)-CERES-Maize and CSM-CROPGRO-Cotton crop growth models were used to simulate yield reductions resulting from 15-day flash drought events that occurred during the pre-reproductive and reproductive phase of rainfed cotton and maize grown in Florida and Georgia. Maize was simulated for 13 virtual fields (four in Florida and nine in Georgia), ranging from the mountains to the Coastal Plain. Cotton was simulated for eight virtual fields – four in each state, and all in the Coastal Plain. The DSSAT-CSM modeling showed maize yield reductions ranging from 40-50% in the selected virtual fields in Georgia and Florida, respectively, for a 15-day flash drought event occurring during the first half of June, which is a critical reproductive time for maize in the region. These reductions are a function of sandy soil with low water holding capacity and high air temperatures, typically associated with summer flash drought events. The impact of flash drought on cotton was not as severe, with maximum yield reductions of approximately 25% for events occurring from mid-July to mid-August.

Introduction

Overview of flash drought

Drought is often defined as the prolonged lack of precipitation and can have serious effects on rainfed crop production (Manuel et al., 2008; Price et al., 2017; Kuwayama et al., 2018). Nguyen et al. (2023) showed that between 1979-2019, crop yields varied between 27–30% because of several prolonged drought events in the southeastern United States (U.S.). Flash drought is the

rapid onset and intensification of relatively short-term agricultural drought, which can also adversely affect rainfed crop yields (Otkin et al., 2018, 2022; Li et al., 2020; Chen et al., 2020; Woloszyn et al., 2021). Based on the physical drivers, flash droughts can be classified as heat wave-driven or precipitation deficit-driven (Mo and Lettenmaier, 2015, Wang and Yung, 2018). When these conditions extend to 10 days or more, soil moisture in the root zone of sandy soils is rapidly depleted, resulting in yield losses (Mozny et al., 2012; Otkin et al., 2018; NOAA, 2022).

Compared to the continental U.S., the southeastern region of the country typically experiences more flash drought episodes (Lesinger and Tian, 2022). One of the factors leading to the higher incidence of flash drought is that the southeastern Coastal Plain, the region's dominant crop production area, is characterized by sandy soils with low water holding capacity. During summer, precipitation events are associated with localized thunderstorms, sometimes resulting in some areas receiving precipitation regularly while nearby areas may not receive precipitation for two or three weeks. This pattern can result in very localized flash drought events (Fortin, 2019; NIDIS, 2024).

In Chapter 2, the frequency and duration of flash drought events were quantified for rainfed crops in the southeastern U.S. SmartIrrigation (SI) CropFit, a smartphone-based irrigation scheduling tool that uses the evapotranspiration-based FAO-56 method and maintains a daily soil water balance, was used to quantify the occurrence of flash drought events for rainfed maize (*Zea mays*) and upland cotton (*Gossypium hirsutum L.*) at 61 virtual field locations in Florida and Georgia over a 20-year period (2003-2022). Based on the literature, a flash drought event was defined as a period when plant-available soil water in the root zone was less than 40% of field capacity for 15 consecutive days during the growing season. The study found that rainfed maize in Georgia experienced flash drought on average at least once per growing season, and at least

50% of the maize flash drought events occurred during the crop's reproductive phase. In Florida, this figure was as low as 12%. Although the overall number of cotton flash drought events in both states was lower than for maize, 75% of cotton flash drought events in Georgia and 50% in Florida occurred during the crops' reproductive phase.

Effects of drought on crop yield

Water stress affects the different physiological characteristics of crops, which leads to yield reduction. It leads to lower photosynthetic rates, which in turn leads to decreases in cell division and cell enlargement, root differentiation, foliage dimensions, shoot length, and plant yield (Kumawat et al., 2018). The severity of these effects depends on the duration and intensity of the water stress period (Kumawat et al., 2018).

Water stress affects the physiological characteristics of crops, which leads to yield reduction. It leads to lower photosynthetic rates and decreases the frequency of cell division and cell enlargement, root differentiation, foliage dimensions, shoot length, and plant yield (Kumawat et al., 2018). The severity of these effects depends on the duration and intensity of the water stress period (Kumawat et al., 2018).

Maize (*Zea mays*) is a multipurpose crop grown under different agroclimatic conditions around the world. By area, it is the most grown crop in the U.S., with 385.6 million tonnes produced in 2023 (USDA-ERS, 2024). Water stress during the crop's reproductive phase, and especially during silk and pollen formation (flowering), can lead to daily yield losses of up to 8% (Aslam et al., 2015; Sah et al., 2020; Kim and Lee, 2023). Liu et al. (2022), Oury et al., 2016a, and Oury et al., 2016b also observed yield losses for maize under water stress during the flowering stage that were attributed to ovary abortion, decrease in grain number, completing the basal kernel filling process faster without increasing the kernel filling rate, and reduced kernel weight.

Upland cotton (*Gossypium hirsutum*) is widely grown in the southeastern U.S., with production reaching 2.7 million tonnes during the 2023 marketing year. This was approximately 10.6% of the total global production (USDA, 2023). Cotton is more resilient to crop water stress than maize (Ullah et al., 2017). However, the impacts of drought stress on cotton's physiological processes and yield are significant. The length of a drought, as well as other environmental stressors, all affect the severity of these impacts. A significant decrease in boll and seed yield can occur from flower abortion, which is caused by water stress during flowering and affects the growth and structure of fruiting bodies (Snowden et al., 2014; Iqbal et al., 2017; Zonta et al., 2017; Khan et al., 2018). Water stress during the flowering and boll-forming stages also affects fiber quality by altering fiber sucrose metabolism (Gao et al., 2020). Long-term water stress can also impair photosynthetic electron transport, which can damage cells and result in a persistent reduction in the photosynthesis of cotton (Sekmen et al., 2014; Parkash et al., 2024). In a study to evaluate the mechanism of photosynthetic inhibition under drought stress conditions in cotton in Georgia, Meeks et al. (2019) found that in early-season drought, net photosynthesis decreased between 20% and 60%. Hejnak et al. (2015) found that the total dry weight decreased by 8% under drought conditions. Gao et al. (2020) measured seed cotton yield reductions of up to 11-17% depending on the cultivars, under ambient temperature (31.0/26.4°C) and soil relative water content level at 60%.

Mathematical simulation of the effects of water stress on maize and cotton

The Decision Support System for Agrotechnology Transfer (DSSAT) is a universally used decision support tool that includes dynamic crop growth simulation models for over 45 crops (Hoogenboom et al., 2019). DSSAT Cropping System Model (CSM)-CERES-Maize, which is one of the most popular and widely used crop models within DSSAT (Yakoub et al., 2017), provides

a framework to conduct research for understanding the effect of various management practices and changes in environmental conditions on the growth and yield of maize by evaluating the relative response of different scenarios-such as for irrigation management (Kaur and Arora, 2018; Malik and Dechmi, 2019); climate change (Ngwira et al., 2014; Farhangfar et al., 2015), etc. The CSM-CERES-Maize model's module structure makes it possible to simulate crop water stress and its possible effects on crop development, production, and growth (Amiri et al., 2022). The CSM-CERES-Maize has been used to simulate maize production under various water stress scenarios. For example, Elliott et al. (2018) conducted a study to observe the compatibility of crop growth models to predict state-level maize yields, in which the CSM-CERES-Maize model showed relatively better performance during dry periods but over- and under-predicted maize yield in some states of the U.S. The yield reduction of summer maize caused by drought stress that occurred in the Huaibei Plain of China (Geng et al., 2017) and in Western Guanzhong Plain, China (Shen et al., 2020), was simulated with the CSM-CERES-Maize. The model has resulted in relatively accurate simulations of maize growth and yields under different irrigation levels, including rainfed conditions in Zambia (Chisanga et al., 2021) and the U.S. (Kisekka et al., 2016; Amiri et al., 2022). The days to flowering and maturity, as well as the yield and aboveground biomass of maize, were all accurately simulated by CSM-CERES-Maize under rainfed conditions in western Kansas, U.S. (Araya et al., 2017). Onyekwelu and Sharda (2024) used the model to assess the effects of climate change on rainfed maize production in the U.S. Great Plains. Simulations indicated a productivity loss of up to 45%. CSM-CERES-Maize was also utilized to measure the level of water stress in the southeastern U.S. and to predict the effects of drought on maize final yields (McNider et al., 2011). Sharda et al. (2017) used the CSM-CERES-Maize model to predict the impact of climate change and soil variability on rainfed maize yield over 30 years in Alabama.

The CSM-CROPGRO-Cotton model has been used in the southeastern U.S. to study irrigation water use, climate variability, and ENSO impact on cotton yield (Garcia et al., 2010; Paz et al., 2012). The model has also been used to simulate cotton production under various water stress scenarios. Modala et al. (2015) experimented with the evaluation of the model to predict cotton growth and yield in comparison with the observed data from 2008-2010 and 2012 under different irrigation strategies in the Texas Rolling Plains. Although the evapotranspiration (ET) simulation in the model was not satisfactory under deficit irrigation (0% and 33% ET replacements) during dry seasons, the model showed significant potential to predict cotton growth and yield in arid conditions under different irrigation management scenarios. In another study conducted in the Texas High Plains, CSM-CROPGRO-Cotton was used to evaluate the impacts of deficit irrigation on water use efficiency and seed cotton output in dry, normal, and wet years over the past 41 years (Himanshu et al., 2021). Li et al. (2020) showed that the model accurately predicted cotton growth and yield under water deficit strategies, offering a decision support system for sustainable agriculture in Southern Xinjiang, China. Another similar study was conducted in Changji City, China (Lin et al., 2024), where the model was applied to optimize irrigation scheduling by observing the effects of deficit irrigation treatments on cotton yield applied during different growth stages of cotton. Yield reduction of cotton was observed under water stress conditions with limited irrigation compared to well-watered conditions using the model in Faridkot, India (Kumar et al., 2023).

In the flash drought study described earlier in Chapter 2 of this dissertation used the CSM-CERES-Maize and CSM-CROPGRO-Cotton models were used to confirm flash drought events identified by SI CropFit. They used the water deficit stress index for photosynthesis and the water deficit stress index for growth, which are available in both models, to demonstrate that the flash

drought events identified by SI CropFit coincided with periods of crop water stress identified by the two crop water stress indices. The simulations were conducted on 13 of the 61 fields used in the flash drought study.

Goals and objectives

The overall goal of the work presented here was to use a crop growth model to assess the impact of flash drought on rainfed crops in the southeastern U.S. Specific objectives were to 1) use the CSM-CERES-Maize and the CSM-CROPGRO-Cotton models to simulate the yield response of rainfed maize and cotton to the occurrence of flash drought, and 2) assess the effects of flash drought on yield during different phenological stages of the crop.

Materials and methods

Application of DSSAT-CSM

The CSM-CERES-Maize and CSM-CROPGRO-Cotton models (v.4.8.2) (Hoogenboom et al., 2023) were used to simulate the yield response of rainfed maize and cotton to the occurrence of flash drought during different phenological stages at the 13 virtual fields (four in Florida and nine in Georgia) used by in Chapter 2 of this dissertation (Table 3.1; Figure 3.1). The 13 virtual fields were all located at the University of Georgia or the University of Florida research and education centers (REC) to ensure the availability of detailed soil and meteorological information that was needed for running DSSAT-CSM. The virtual fields represented a hypothetical cotton or maize field 0.1 ha in size (32 × 32 m) and centered on the geographic coordinates of the Florida Automated Weather Network (FAWN) (https://fawn.ifas.ufl.edu) or University of Georgia Weather Network (UGAWN) (http://weather.uga.edu) weather station at each REC. The REC / virtual field locations were selected to be representative of the major cotton and maize growing areas of Florida and Georgia and geographically distributed to capture regional variability in topography, soils and

climate (Table 3.1, Figure 3.1). In Georgia, only the four virtual fields in the Coastal Plain were used for cotton, as this is the primary cotton growing area of the state.

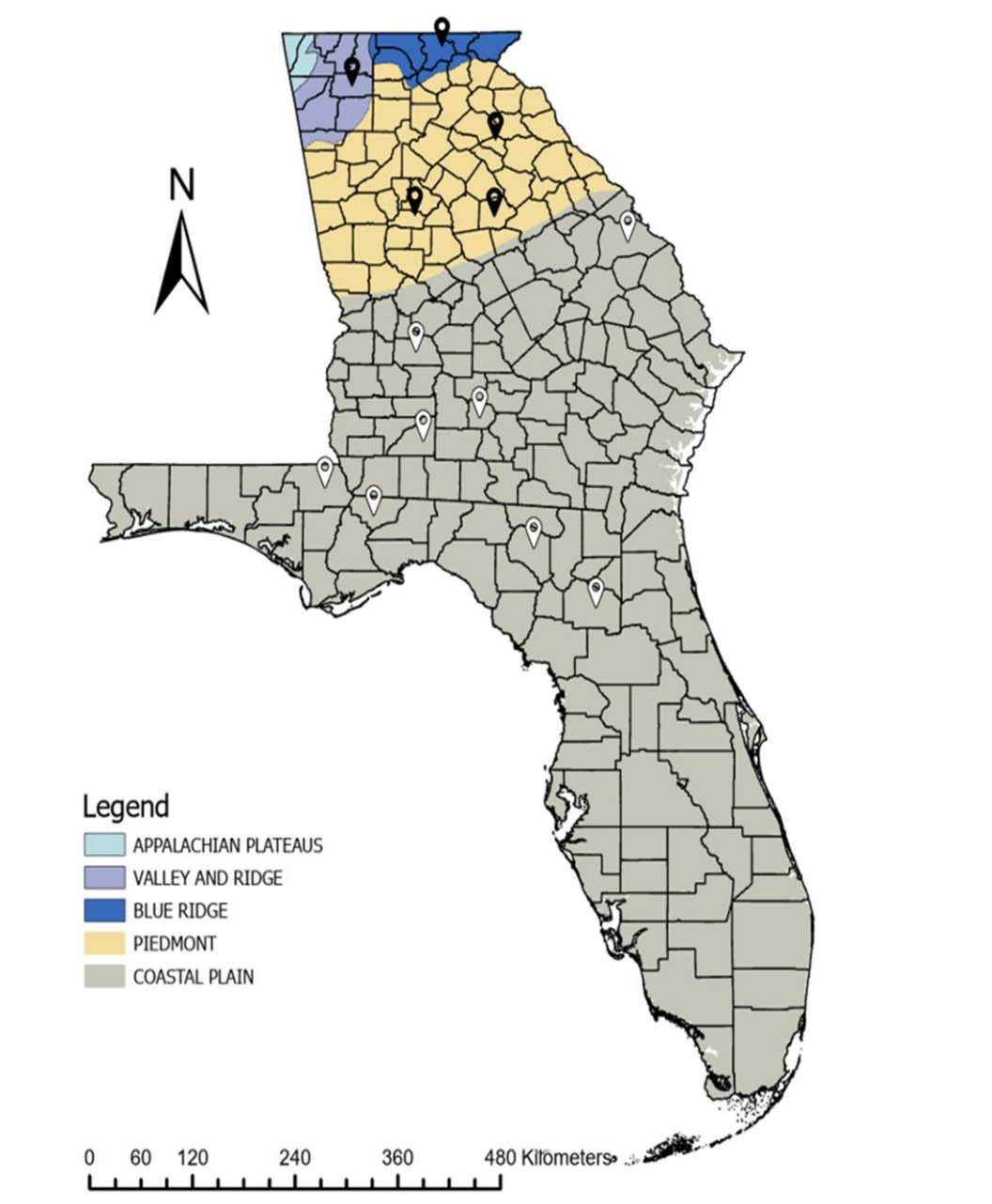

Figure 3.1 Maps showing the location of the 13 virtual fields (nine virtual fields in Georgia and four virtual fields in Florida) used in the study. Black pins indicate virtual fields used only for maize. Virtual fields used for maize and cotton are indicated with white pins. In Georgia, cotton is grown primarily in the Coastal Plain.

Table 3.1 Names, physiographic classification, soil type, period of record for meteorological data, and geographic coordinates of the 13 virtual fields (nine virtual fields in Georgia and four virtual fields in Florida) used in this study. The dashed line distinguishes Mountain/Piedmont sites from Coastal Plain sites in Georgia.

Site Name	Physiographic Classification		Soil Type	Period of Record	Coordinates
	Region	Subregion			
Georgia					
Blairsville	Blue Ridge	Blue Ridge	Clayey	1993–2023	34°50'20.3"N, 83°55'41.1"W
Calhoun	Ridge and Valley	Great Valley	Fine loam	1993–2023	34°33'27.4"N, 84°48'56.8"W
Eatonton	Lower Piedmont	Midland	Loam	1993–2023	33°23'49.0"N, 83°29'17.6"W
Griffin	Lower Piedmont	Midland	Clayey	1992–2023	33°15'46.5"N, 84°17'01.8"W
Watkinsville	Lower Piedmont	Midland	Sandy loam	1993–2023	33°52'09.5"N, 83°26'59.8"W
Camilla	Coastal Plain	Dougherty Plain	Loamy sand	1998-2023	31°16'48.3"N, 84°17'29.8"W
Midville	Coastal Plain	Vidalia Upland	Loamy sand	1992–2023	32°52'32.2"N, 82°12'57.9"W
Plains	Coastal Plain	Fall Line Red Hills	Sandy loam	1993–2023	32°02'48.3"N, 84°22'15.7"W
Tifton	Coastal Plain	Tifton Upland	Loamy sand	1992–2023	31°28'44.05"N, 83°31'55.00"W
Florida					
Citra	Coastal Plain	Marion Hills	Sand / loamy sand	2001–2023	29°24'36.4"N, 82°10'23.5"W
Live Oak	Coastal Plain	Northern Plains	Fine Sand/Loamy sand	2004–2023	30°18'18.0"N, 82°53'55.5"W
Marianna	Coastal Plain	Dougherty Plain	Loamy sand	2003–2023	30°51'00.0"N, 85°09'54.6"W
Quincy	Coastal Plain	Tifton Upland	Loamy fine sand	2003–2023	30°32'44.9"N, 84°35'56.3"W

For crop simulation in DSSAT-CSM, soil data, meteorological data, management practices (planting date, planting depth, planting population, fertilizer application, etc.), and cultivar-specific genetic coefficients are needed. Both the maize and cotton models simulate several variables, including water stress indices, nutrient content, leaf area, leaf mass, above-ground biomass, and yield under various management approaches and climate variations once it has been calibrated.

Model simulation

Data from a 3-year maize study conducted between 2016-18 at the University of Georgia's NESPAL field in Tifton, GA (Orfanou, 2020) were used to develop genetic coefficients for the 'Pioneer P1794VYHR' maize cultivar (Pioneer, Johnston, IA, USA) and were also used to calibrate the CSM-CERES-Maize model (Table 3.2). The already-calibrated 'Deltapine 555 BG/RR (DP555BR)' cultivar that is available in the CSM-CROPGRO-Cotton model was used for cotton simulations. The genetic coefficients used for cotton simulations are shown in Table 3.3.

Table 3.2 Genetic coefficients for the 'Pioneer P1794VYHR' maize cultivar used in the CSM-CERES-Maize model (Orfanou, 2020).

Parameters	Description	Value
P1	Thermal time from seedling emergence to the end of the juvenile stage (based 8 ◦C)	206.3
P2	Photoperiod sensitivity coefficient	0.75
P5	Thermal time from silking to physiological maturity (based 8 ◦C)	989.3
G2	Maximum possible number of kernels per plant.	990
G3	Kernel filling rate (mg/day)	8.8
PHINT	Degree days to appear leaf tip	38.9

Table 3.3 Genetic coefficients for the 'Deltapine 555 BG/RR' (DP555BR)' cotton cultivar used in the CSM-CROPGRO-Cotton model.

Parameters	Description	Value
CSDL	Critical short-day length below which reproductive development progresses rapidly with no day length effect (h)	23.0
EM-FL	Time from plant emergence to flower appearance (photothermal days)	38.0
FL-SH	Time between first flower and first pod (R3) (photothermal days)	11.0
FL-SD	Time between first flower and first seed (R5) (photothermal days)	16.0
SD-PM	Time between first seed (R5) and physiological maturity (R7) (photothermal days)	43.0
FL-LF	Time between first flower (R1) and end of leaf expansion (photothermal days)	65.0
SLAVR	Specific leaf area of cultivar under standard growth conditions (cm2/g)	170
SIZLF	Maximum size of full leaf (three leaflets) (cm^2)	300
SFDUR	Seed filling duration for pod cohort at standard growth conditions (photothermal days)	35
SDPDV	Average seed per pod under standard growing conditions (#/pod)	27
PODUR	Time required for cultivar to reach final pod load under optimal conditions (photothermal days)	12

Soil and meteorological data for the virtual fields

Soil profiles for the Blairsville, Calhoun, Camilla, Griffin, Watkinsville, and Marianna virtual fields were already included in DSSAT-CSM from previous studies and were used for simulations. Detailed soil data (particle size analysis, soil pH, cation exchange capacity (CEC), bulk density, etc.) for the remaining seven virtual fields were secured from a variety of sources, including Perkins (1987) and the NRCS Web Soil Survey, to create new soil profiles for each virtual field in the SBuild utility in DSSAT-CSM. The coordinates and area of the virtual fields

were used to extract soil data from the NRCS Web Soil Survey. Soil water content in the soil layer at the drained upper limit and lower limit of plant extractable soil water, saturated water content, bulk density, saturated hydraulic conductivity, and other soil parameters were generated by SBuild from the soil profile data.

Daily meteorological data, including maximum and minimum air temperature, solar radiation, and precipitation, were imported into the WeatherMan weather module, analyzed, and exported in the appropriate format for use in DSSAT-CSM. Meteorological data were retrieved from FAWN for the weather stations associated with the four Florida virtual fields and from the UGAWN for weather stations associated with the nine Georgia virtual fields. The meteorological period of record for each location is reported in Table 3.1. Mean monthly precipitation for the growing season months for each of the sites is shown in Figure 3.2.

Planting dates

Although maize planting dates vary across Florida and Georgia from year to year and by location, an average planting date of April 15 was selected for Florida and April 1 for Georgia based on discussions with Extension specialists in both states (Hand et al., 2024, and Wright et al., 2003). The planting date for rainfed maize in Florida is later than that of irrigated maize, so the reproductive phase coincides with the beginning of the summer rainy season in June (Wright et al., 2020). Planting dates for rainfed and irrigated maize do not vary in Georgia (Tubbs et al., 2024).

The optimal time to plant rainfed cotton in Florida and Georgia is a function of soil temperature, moisture content, and other factors and varies from early April to early June. After consulting with Extension personnel in both Florida and Georgia and related Extension

publications (Tubbs et al., 2024; Wright et al., 2020), an average planting date of May 15 was chosen for both states.

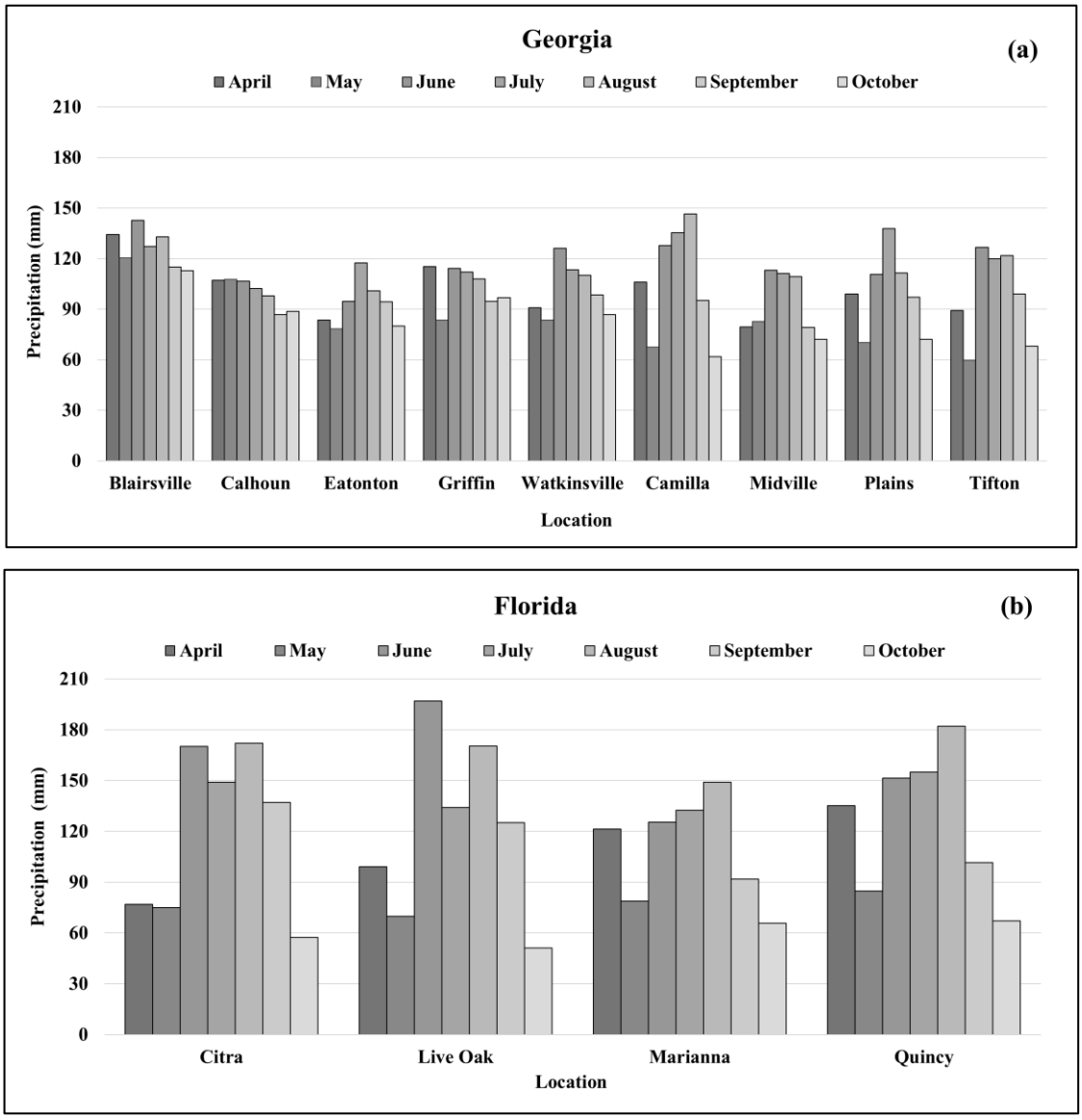

Figure 3.2 Mean monthly total precipitation at the (a) nine virtual fields in Georgia and (b) four virtual fields in Florida during the cotton (April-August) and maize (May-October) growing seasons. The period of record used to calculate means ranged from 20-32 years based on the weather station at each location.

Seasonal analysis to assess the effect of flash drought on maize and cotton yield

DSSAT-CSM's seasonal analysis tool was used to assess the impact of flash drought on yield. Simulations were run at the 13 selected virtual fields for maize and the eight virtual fields for cotton for a period ranging from 20 to 32 years, depending on the length of the meteorological data record of the weather station at the site. Using the recommendations of the University of Georgia's Corn Production Guide (Tubbs et al., 2024) and the University of Florida's Field Corn Production Guide (Wright et al., 2020), rainfed maize planting density was set to 5 plants/m^2, the planting depth to 5 cm, and the row spacing to 91 cm. For cotton, the planting density, planting depth, and row spacing were set to 14 plants m^{-2}, 2.5 cm, and 91 cm, respectively, from guidelines provided by Wright et al. (2003) and the University of Georgia's Cotton Production Guide (Hand et al., 2024). The nitrogen balance routine was turned off, which allowed the model to provide nitrogen as needed so that it was not a yield-limiting factor. The Priestley-Taylor (1972) method was used to calculate potential ET, and the Ritchie-Ceres method (Ritchie, 1972) to estimate soil water evaporation.

Flash drought was simulated by withholding precipitation for 15-day intervals using the DSSAT-CSM Environment Modification tool during the pre-reproductive and reproductive phase of maize, which are the most susceptible to water stress. The duration of the flash drought period followed the findings in Chapter 2 of this dissertation. Similarly, the timing of the cotton and maize reproductive phase was determined in Chapter 2 using the accumulated heat units-driven cotton and maize phenology model within SI CropFit (Table 3.4).

For maize, the reproductive phase occurred in May and June for all 13 virtual fields. The intervals for which precipitation was withheld spanned this period and were T_{M1} (1-15 May), T_{M2} (16-31 May), T_{M3} (1-15 June), and T_{M4} (16-30 June) (Table 3.4). For the eight cotton virtual fields,

Table 3.4 The specific phenological stage associated with each withholding precipitation period for 15-day intervals for maize and cotton.

Crop	Flash Drought Periods	Growth stage
Maize	T_{M1} (1-15 May)	V_6-V_9
	T_{M2} (16-31 May)	V_9
	T_{M3} (1-15 June)	V_9, Tasseling, R_1
	T_{M4} (16-30 June)	R_1-R_4
Cotton	T_{C1} (1-15 July)	First Square to First Flower
	T_{C2} (16-31 July)	First Flower to First Open Boll (i)
	T_{C3} (1-15 August)	First Flower to First Open Boll (ii)
	T_{C4} (16-31 August)	First Flower to First Open Boll (ii)

the reproductive phase occurred in July and August. The intervals for which precipitation was withheld were T_{C1} (01-15 July), T_{C2} (16-31 July), T_{C3} (01-15 August), and T_{C4} (16-31 August) (Table 3.4). The models were run for the period of record using each flash drought interval.

The CSM-CERES-Maize model and CSM-CROPGRO-Cotton model were run iteratively each year at each virtual field for the entire period for which meteorological data were available, using the recorded meteorological data to simulate rainfed yield. The models were then rerun for the period of record, suppressing precipitation for one of the flash drought periods shown in Table 3.4 to simulate the yield effect of flash drought. In other words, each year was simulated with one flash drought period. This was repeated until all four flash drought periods were simulated. The differences in yield resulting from the simulated flash drought period (suppressed precipitation) and the actual precipitation records were used to calculate the percentage yield reduction (Eq. 3.1).

$$Yield\ reduction\ (\%) = 100 \times [(Y_a - Y_f) / Y_a] \quad \text{Eq. 3.1}$$

where,

Y_a = yield resulting from the actual precipitation records and

Y_f is the yield resulting from the simulated flash drought period.

ANOVA was used to statistically examine the impacts of suppressing precipitation for the $T_{M1} – T_{M4}$ and $T_{C1} – T_{C4}$ time period treatments on maize and cotton yield, respectively. A p-value <0.05 was used to indicate a significant difference among the treatments. Tukey's HSD test was used to show significant differences between treatments.

Results and discussion

Maize and cotton percent yield reductions

Figures 3.3a and 3.3b show the mean percent yield reductions for the period of record for maize at each of the virtual fields resulting from suppressing precipitation during the four ($T_{M1} – T_{M4}$) flash drought periods. Simulated yield reductions exceeded 40% in Georgia and 50% in Florida, and there were statistically significant differences between the simulated yield reductions for each of the flash drought periods at each virtual field. For example, flash drought during T_{M3} (01-15 June) resulted in significantly higher yield reductions for all the virtual fields except for Blairsville and Calhoun, which are in the mountainous region of Georgia (Figure 3.3). At those two sites, the largest reductions occurred during T_{M4} (16-30 June) and were smaller than for the other sites. For all locations, the smallest reductions occurred during T_{M1} (01-15 May), which may be considered the pre-reproductive phase (Table 3.4). In Florida, where all the virtual fields had sandy soils, the T_{M3} (01-15 June) yield reductions were all greater than 50%. These results reflect how catastrophic just two weeks without precipitation can be for rainfed maize production in areas with sandy soil when this occurs during the reproductive phase.

The highest mean yield reduction in Georgia during T_{M3} (01-15 June) was 46.8% in Camilla, while the lowest mean yield reduction was 28.7% in Watkinsville. Overall, higher yield reductions were found for the Georgia Coastal Plain sites than those in the mountainous and Piedmont regions of the state. This is primarily caused by the differences in soil type (Table 3.1).

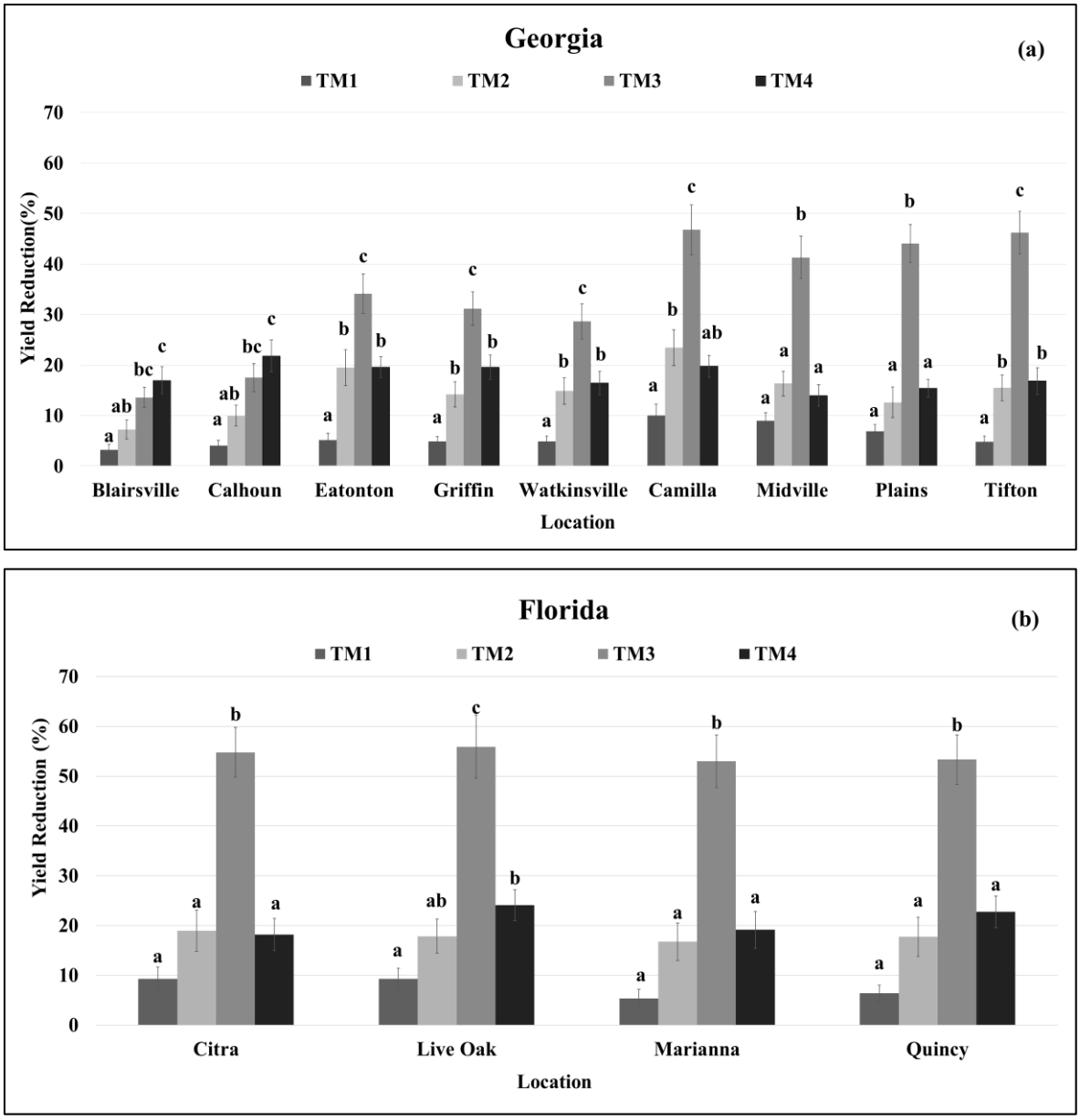

Figure 3.3 Mean percent yield reducns for maize compared to rainfed for the period of record resulting from suppressing precipitation during four flash drought periods defined as T_{M1} (1-15 May), T_{M2} (16-31 May), T_{M3} (1-15 June), and T_{M4} (16-30 June) for (a) Georgia (nine virtual fields) and (b) Florida (four virtual fields). Standard errors of the mean are shown by error bars. Bars with different letters have means that are statistically significantly different at $p < 0.05$.

The soils of the virtual fields located in the mountainous and Piedmont regions of Georgia have much higher water holding capacity than those in the Coastal Plain. However, air temperature and precipitation patterns were also important factors. The mean growing season precipitation for

20 years (2003-2022) was 522 mm for the mountainous/Piedmont sites and 475 mm for the Coastal Plain sites. In Florida, the highest mean yield reduction during T_{M3} (01-15 June) was 58.9% in Live Oak, while the lowest mean yield reduction was 53.0% in Marianna, which indicates a larger flash drought impact on yield.

Figures 3.4a and 3.4b show the mean percent yield reduction for the period of record for cotton resulting from suppressing precipitation during the four (T_{C1} – T_{C4}) flash drought periods. Simulated maximum yield reductions were approximately 25% in both Georgia and Florida, while minimum yield reductions were 10% in Georgia and 11% in Florida. Unlike maize, the largest yield reductions at each site were not consistently in the same flash drought period but were either in the T_{C2} (15-31 July) or T_{C3} (01-15 August) period at all virtual fields. These two periods coincide with the first flower to first open boll phenological stages of cotton (Table 3.4). Compared to maize, the potential for significant yield loss in cotton is distributed over a longer period because the flowering and boll-set period in cotton extends over several weeks. The impact of a two-week flash drought is therefore less severe than for maize. Differences in yield reductions between the T_{C1} – T_{C4} periods were not statistically significant at Live Oak and Marianna, FL. Overall, simulated yield reductions resulting from drought were smaller than those in maize, indicating that cotton is more resilient to crop water stress during its reproductive phase.

Maize and cotton yields under the occurrence of flash drought

The strength of using crop growth simulation models such as DSSAT-CSM is that they allow comparisons of the relative changes in yields under different production scenarios. Figure

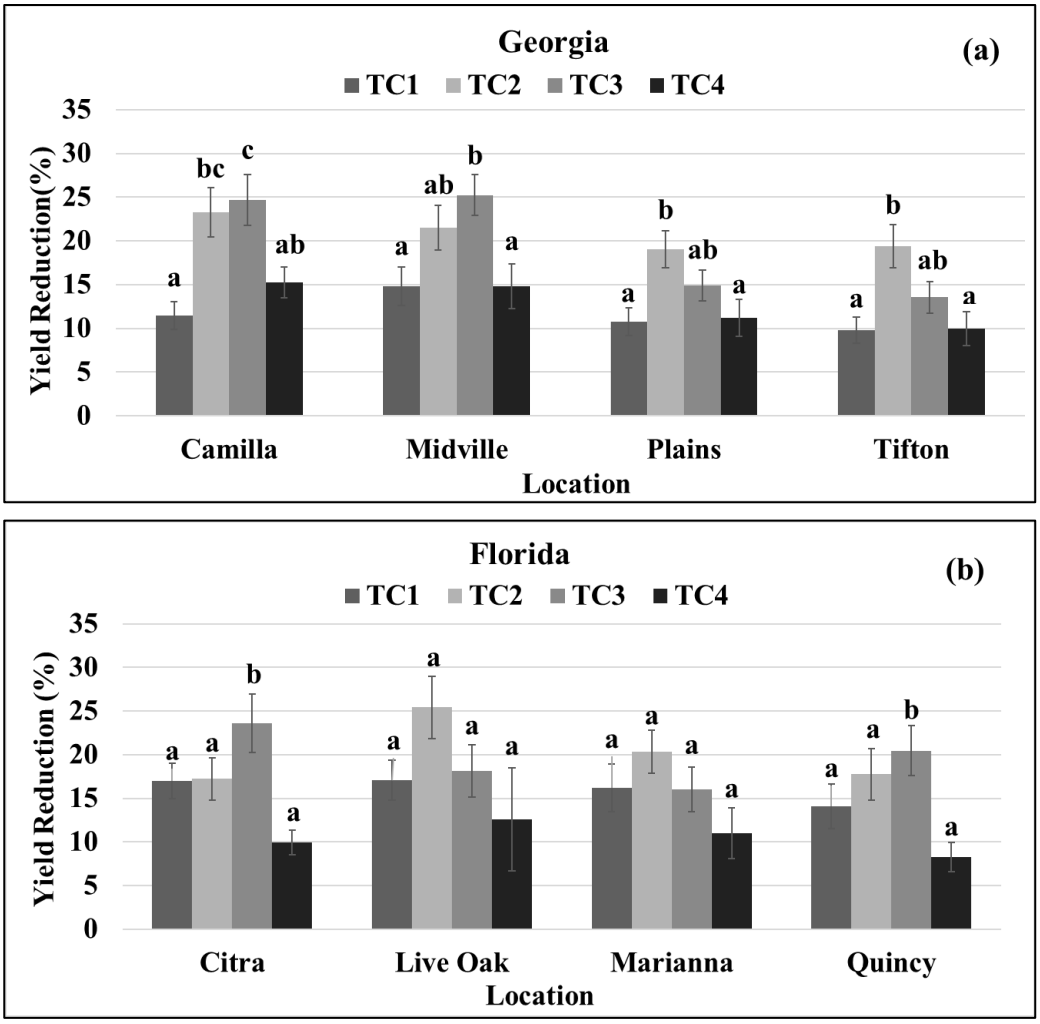

Figure 3.4 Mean percent yield reductions for cotton compared to rainfed for the period of record resulting from suppressing precipitation during four flash drought periods defined as T_{C1} (01-15 July), T_{C2} (16-31 July), T_{C3} (01-15 August), and T_{C4} (16-31 August) for (a) Georgia (four virtual fields) and (b) Florida (four virtual fields). Standard errors of the mean are shown by error bars. Bars with different letters have means that are statistically significantly different at $p < 0.05$.

3.5 shows simulated maize yields under rainfed, and four flash drought scenarios represented by T_{M1} (1-15 May), T_{M2} (16-31 May), T_{M3} (1-15 June), and T_{M4} (16-30 June) for two virtual fields – one in the Coastal Plain of Georgia (Tifton) and the other in the Coastal Plain of Florida (Marianna). The value of the graphs is in comparing the differences between the yields of the five scenarios. These two virtual fields were selected for comparison because although the percent yield reduction from flash drought was similar, the simulated yields were very different.

In the graphs, the box represents the distribution of 50% of the simulated yield, the whiskers represent the distribution of the other 50% of the simulated yield, the horizontal line represents the median, the X represents the mean, and the circles represent outliers. Figure 3.5a

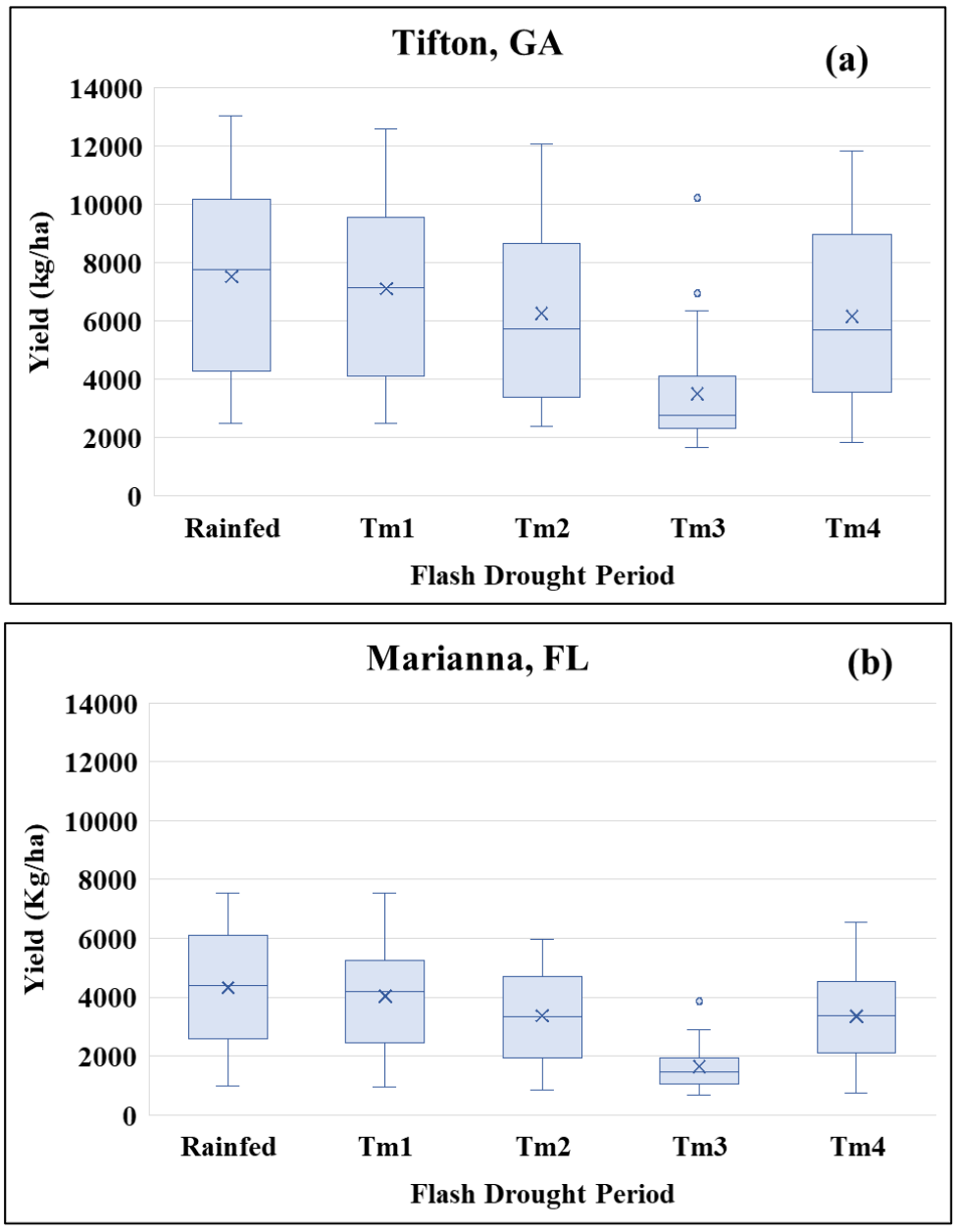

Figure 3.5 Maize yield simulated under rainfed conditions and resulting from suppressing precipitation during four flash drought periods defined as T_{M1} (1-15 May), T_{M2} (16-31 May), T_{M3} (1-15 June), and T_{M4} (16-30 June) for (a) Tifton, GA from 1992-2022 and (b) Marianna, FL from 2003-2022. In each graph, the box represents the distribution of 50% of the data, the whiskers represent the distribution of the other 50% of the data, the horizontal line in each box represents the median, and the X represents the mean.

shows the results for the Tifton, GA virtual field for the period of record (1992-2022), while Figure 3.5b shows the results for Marinna, FL (2003-2022). As described earlier, the simulated yield was the lowest for both locations under the T_{M3} scenario. In Tifton, the mean rainfed yield was 7279 kg ha^{-1}, while the mean T_{M3} yield was 3394 kg ha^{-1}, a difference of 3885 kg ha^{-1}. In Marianna, the mean rainfed and T_{M3} yields were 3898 kg ha^{-1} and 1484 kg ha^{-1}, respectively, while the difference between the two was 2414 kg ha^{-1}. Mean rainfed yields in Marianna over the period of record were approximately half of those in Tifton and most likely a function of the sandier soils with low water holding capacity of the Florida location, as growing season precipitation in Mariana is higher than that for Tifton (Figure 3.2). It is also interesting to note that T_{M1} yield was similar to the rainfed yield at both locations, again confirming that flash drought in the pre-reproductive phase does not have significant yield impacts.

Figure 3.6 shows the simulated cotton yields under rainfed, and four flash drought scenarios represented by T_{C1} (01-15 July), T_{C2} (16-31 July), T_{C3} (01-15 August), and T_{C4} (16-31 August) for the same two virtual fields. As with maize, there is a substantial difference in mean rainfed yields between the two virtual fields (Tifton = 3467 kg ha^{-1}, Figure 3.6a; Marianna = 1636 kg ha^{-1}, Figure 3.6b). At both locations, the largest flash drought-related yield loss occurred during $T_{C2,}$ but unlike maize, the yield losses resulting from flash drought were smaller.

Comparison to other studies

The impact of flash drought on maize and cotton yields described above agrees with both experimental and simulated results from other published studies. For example, Zhang et al. (2019) reported that drought risk predicted by CSM-CERES-Maize was the highest during the jointing and heading stage (reproductive phase), which was the most important and rapid growth period for maize. Amiri et al. (2022) found that rainfed maize yields were 38% lower than those that were

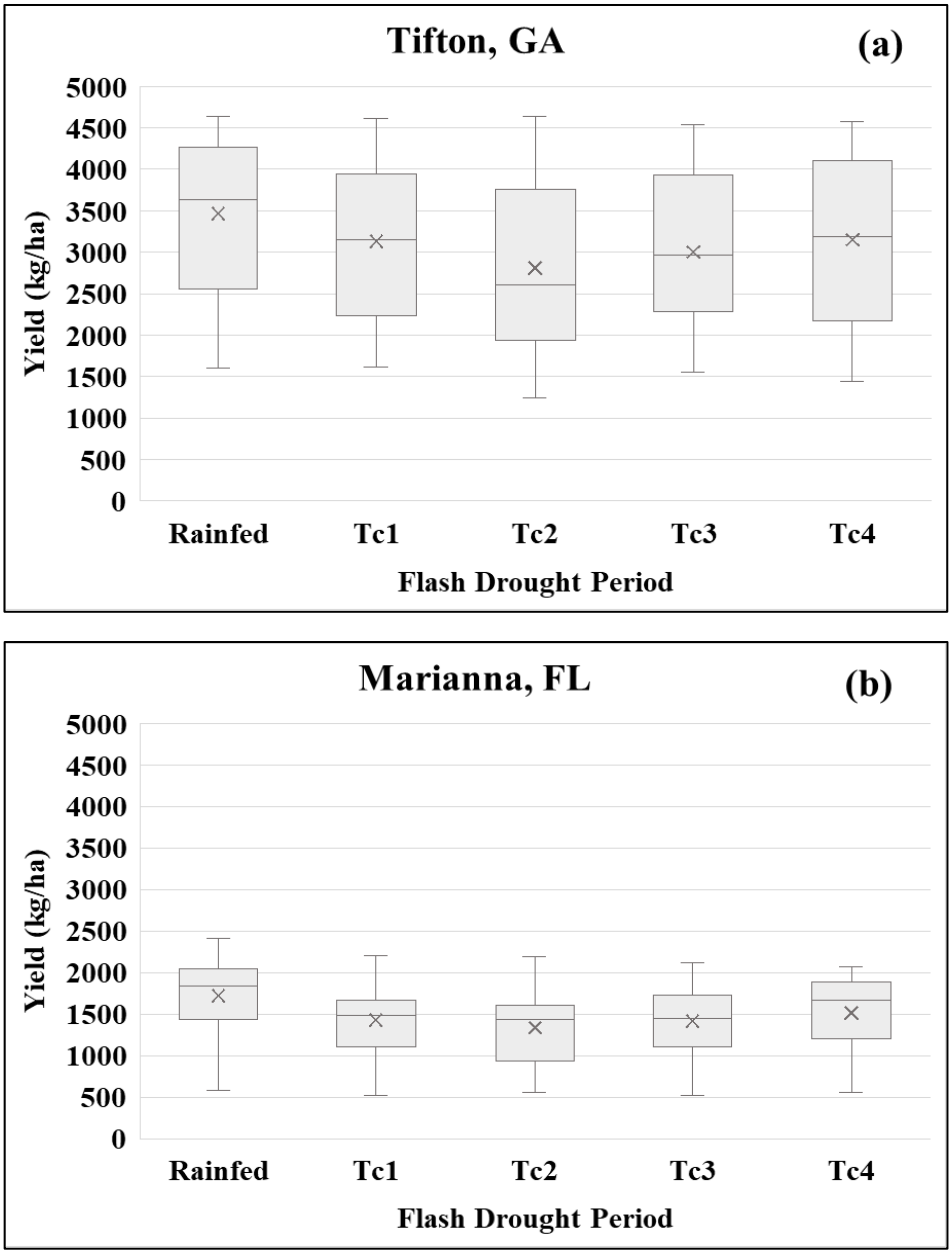

Figure 3.6 Cotton yield simulated under rainfed conditions and resulting from suppressing precipitation during four flash drought periods defined as T_{C1} (01-15 July), T_{C2} (16-31 July), T_{C3} (01-15 August), and T_{C4} (16-31 August) for (a) Tifton, GA from 1992-2022 and (b) Marianna, FL from 2003-2022. In each graph, the box represents the distribution of 50% of the data, the whiskers represent the distribution of the other 50% of the data, the horizontal line in each box represents the median, and the X represents the mean.

fully irrigated. In a study that evaluated which reproductive phase was most sensitive to drought using CSM-CERES-Maize, Shen et al. (2020) found simulated yield reductions of 60.7%, 40.6%, and 87% when drought occurred during the heading and filling, jointing and filling, and jointing and heading stages, respectively. Mi et al. (2018) showed that the reduction in maize yield under drought was higher during the reproductive phase (41.6%-46.6%) than during the vegetative phase (18.6–26.2%).

Using CSM-CROPGRO-Cotton, Bozorov et al. (2018) and Himanshu et al. (2023) found that the flowering stage of cotton was more vulnerable to drought than other growth stages, which matches the findings of this study. In a cotton field study conducted by Luo et al. (2016), moisture stress during the early blooming to full flowering stage reduced seed yield by 42%. Moisture stress between full flowering and full bolling reduced seed yield by 31%.

Conclusions

Flash drought events of 15 days or longer that occur during the reproductive phase can result in significant yield reductions to rainfed crops. DSSAT-CSM modeling showed maize yield reductions exceeding 40% for Coastal Plain virtual fields in Georgia and exceeding 50% in Coastal Plain virtual fields in Florida for a flash drought event occurring during the first half of June. These reductions are a function of sandy soils with low water holding capacity and high air temperatures, typically associated with summer flash drought events. The impact of flash drought on cotton was not as severe, with maximum yield reductions of approximately 25% for events occurring from mid-July to mid-August.

Overall, maize grown under rainfed conditions in the southeastern Coastal Plain is much more susceptible to flash drought than cotton. Growers already know this, and their knowledge can be seen in practice when maize is planted in the irrigated area of a field and cotton or peanuts

are planted in the non-irrigated areas. Nevertheless, this is one of the first studies to quantify the effects of flash drought on yield across different physiographic regions of the southeastern U.S.

CHAPTER 4

DEVELOPING A CROP COEFFICIENT CURVE FOR BERMUDAGRASS USING THE DSSAT CSM-CROPGRO-PERENNIAL-FORAGE MODEL[3]

[3]Jannat, J., S. Maktabi, L. Baxter, G. Hoogenboom, C. J. Bryant, J. L. Snider, and G. Vellidis. To be submitted to *Agronomy Journal.*

Abstract

Among warm-season perennial grasses, forage bermudagrass (*Cynodon dactylonis*) is widely used for hay production and grazing in the southeastern United States (U.S.) The study reported here is one component of a larger project whose goal was to quantify the impact of flash drought on rainfed crops, including forages, in the southeastern U.S. In this study, the CSM-CROPGRO-Perennial-Forage model was applied to predict crop water use and develop a crop coefficient (K_C) curve for rainfed forage bermudagrass in southern Georgia to incorporate the K_C curve into the SmartIrrigation (SI) CropFit for flash drought prediction. The study was conducted for three years (2022-2024) on two large rainfed bermudagrass plots ("Alicia" and "Tifton 85" cultivars on each plot) located on the University of Georgia's Tifton campus. Four hay cuttings were conducted during the growing season of each of the three study years, and leaf area index, herbage mass, and total forage were measured each time. Soil volumetric water content was measured continuously. The data were used to parameterize and evaluate the performance of the CSM-CROPGRO-Perennial-Forage model. The model was used to estimate daily crop evapotranspiration (ET_C) for both cultivars. Daily simulated K_C values were calculated by dividing daily crop evapotranspiration ET_C by reference evapotranspiration (ET_O) calculated using the FAO-56 method. The simulations were compared to daily crop evapotranspiration from the soil moisture sensor and crop coefficient values developed empirically from the soil moisture data. Although the model's performance metrics were lower than those published in applications of the model to irrigated studies, the trends of the simulated variables matched those of the observed variables. Because of large daily and monthly variations in empirical and simulated curves, to develop a generic curve, all the simulated DSSAT-derived daily K_C values for the 3-year period were plotted on one graph, and a polynomial curve fit to the data. This resulted in a classic K_C

curve for a perennial crop with lower crop water use during the winter months and water use approaching reference ET during the peak of the summer season. It can be integrated into SI CropFit as it represents the crop water use patterns of rainfed forage bermudagrass in southern Georgia.

Introduction

Bermudagrass production in Georgia

Bermudagrass is a warm-season perennial grass that is produced as a forage crop across the globe. It is both grazed and cut for hay and is an important nutrient source for livestock (Huang et al., 2011; Rouquette et al., 2011; Daniel et al., 2016). In Georgia, it is grown on approximately 1.2 million ha (Baxter et al., 2023). “Alicia”, “Coastal”, “Tifton 44”, “Russell”, and “Tifton 85” are bermudagrass cultivars commonly used in the Coastal Plain physiographic region of the southeastern United States (U.S.) Because “Tifton 85” produces higher hay yields and has greater digestibility than most other cultivars (Lee et al., 2017), it is a popular selection among growers.

For this study, two cultivars- “Alicia” and “Tifton 85” were used. “Alicia” is easily established and produces high hay yields, but its forage is generally lower quality than “Tifton 85” (Hancock et al., 2013; Lee et al., 2017). “Alicia” is also prone to thin stands and leaf spot (Hancock et al., 2013). "Tifton 85" is characterized by its taller, more upright growth trait, larger and rapidly spreading stems, and broader, darker-colored leaves (Hancock et al., 2013). It has fewer, larger rhizomes, which serve as underground energy storage stems, contributing to better drought tolerance (Newman, 2007; Hancock et al., 2013).

Effects of water stress on bermudagrass

Bermudagrass is tolerant of drought due to its large and deep rooting rhizome system (Husmoen et al.,2012; Zhou et al., 2014; Gopinath et al., 2022; Baxter et al., 2022) and rapid

stomata closure at the early stages of drought stress (Zhou et al., 2013). However, adequate soil moisture is vital for bermudagrass growth. Without adequate soil moisture, plant uptake of soil water and nutrients is reduced, adversely affecting photosynthesis and respiration (Khan et al., 2018; Seleiman et al., 2021; Bijalwan et al., 2022), leaf water potential (Goche et al., 2020; Hemati et al., 2022), and stomatal conductance (Kumar et al., 2023). Stomatal closure results in a decrease in the crop's photosynthetic rate (Huang et al., 2014), ultimately affecting crop yield. On the other hand, Steinke et al. (2011) found that some turf cultivars lost 50% of their green ground cover in 20 days without rain or irrigation, while other cultivars survived a full 60-day dry period without experiencing cover loss. Jesperson et al. (2019) found that drought stress reduced membrane stability and respiration rates in some turf cultivars, which slowed the growth of the grasses.

The southeastern U.S. offers ideal conditions for forage production because of its abundant rainfall and warm environment (Stewart et al., 2014). As a result, research conducted on forage irrigation in the Southeast has received very little attention, especially for bermudagrass (Baxter et al., 2021). Nevertheless, irrigation generally results in consistently higher growth rates and yields of cultivars used as forages (Hendrick et al., 2020). Stone et al. (2012) found that bermudagrass mean yields increased by 612 kg ha^{-1} per cutting during the four-week interval of harvest with 100% irrigation treatments and by 1600 kg ha^{-1} per cutting during the eight-week interval of harvest with 100% irrigation treatments compared to non-irrigated treatment in a study conducted in the Coastal Plain region of South Carolina. Despite these findings, it is mostly hay fields that are non-irrigated. For example, in Georgia, approximately 15374 ha of hay fields out of 2,26,511 ha are irrigated (USDA-NASS, 2022).

Impact of flash drought

In contrast to prolonged drought, flash drought is the rapid onset and intensification of relatively short-term agricultural drought (Otkin et al., 2018, 2022; Li et al., 2020; Chen et al., 2021; Woloszyn et al., 2021). Like prolonged drought, it occurs because of lower-than-normal precipitation rates and abnormally high temperatures, winds, and solar radiation (Otkin et al., 2018; Woloszyn et al., 2021). The resulting crop water stress has an impact on several physiological features of crops, including a reduction in photosynthetic rates and the frequency of cell division and expansion, root differentiation, shoot length, leaf dimensions, and plant yield (Kumawat et al., 2018). Gross primary production based on photosynthetically active radiation and sun-induced fluorescence of pasture or grassland started declining in late May during the 2012 flash drought in the Midwest U.S. (Jin et al., 2019). Furthermore, in Georgia, Florida, and Louisiana, flash drought from 2000 to 2023 caused forage growth to halt and pastures and hay fields to dry out, according to USDA crop progress and crop condition reports, National Climate Assessment Reports, and State Climate Summaries (Deepa and Vijayan, 2025).

The rapid onset of flash drought reduces response time for planning and affects mitigation (Pendergrass et al., 2020). For example, forage supplies rapidly deteriorated during a 2016 flash drought in the northern Great Plains of the U.S., making it difficult for ranchers to care for their herds (Haigh et al., 2019). Flash drought is a common occurrence in the southeastern U.S., which typically experiences more flash drought episodes than the rest of the continental U.S. (Lesinger and Tian, 2022). A significant and well documented flash drought event that resulted in severe damage to rainfed forages and other crops in the southeastern U.S. occurred in September 2019 (Voiland, 2019; Ford et al., 2023; Gibbons et al., 2023).

Crop evapotranspiration measurement and crop-specific growth curve development

Daily crop water use, which is also referred to as crop evapotranspiration or ET_C, is a complex process influenced by several meteorological variables, including relative humidity, solar radiation, wind speed, and air temperature (Allen et al., 2005). Crop parameters such as species and phenological stage also play key roles in determining ET_C values. The United Nations Food and Agriculture Organization (FAO)'s Irrigation and Drainage Paper No. 56, commonly referred to as FAO-56 (Allen et al., 1998), provides guidelines for estimating crop water requirements. The FAO-56 method uses Eq. 4.1 to estimate daily ET_C.

$$ET_C = Kc \times ET_O \qquad \text{Eq. 4.1}$$

where,

ET_C = daily crop evapotranspiration (ET), also referred to as daily crop water use (mm day^{-1}),

K_C = a daily crop coefficient extracted from a crop-specific K_C curve, and

ET_O = Penman-Monteith reference ET (mm day^{-1}).

The FAO has published K_C curves for many of the world's crops, including forages such as bermudagrass used for hay. Those curves are typically generic and are not refined for specific ecoregions. Moreover, the initial data used to develop the curves may have originated in an ecoregion with very different environmental conditions from where the curve is applied. For example, the FAO curve (Figure 4.1) for forage bermudagrass cut for hay was developed with data collected in arid areas of California, USA. In Figure 4.1, the K_{CMid} coefficient is an average estimate of Kc before and after hay cuttings (Allen et al., 1998).

Crop coefficient curves can be developed using a variety of methods. Some methods focus on measuring daily changes in soil moisture, while others focus on direct measurements of ET. Weighing lysimeters determines ET_C by assessing daily changes in soil and crop mass and are

considered the standard for K_C curve development (Ghiat et al., 2021). However, this approach requires substantial investment in the construction and operation of the lysimeters. Observing changes in soil moisture within the root zone with soil moisture sensors and from those data estimating ET_C is another approach that has been recently applied (Vellidis et al., 2016; Maktabi et al., 2022; Bedwell et al., 2025). The eddy covariance approach uses the vertical flux of water vapor to measure ET directly but is also expensive and difficult to implement (Ghiat et al., 2021).

Crop coefficient curves for forage and turf grass have been developed using weighing lysimeters and soil moisture sensors. Weighing lysimeters were used in a study conducted in São Paulo State, Brazil, to develop ET_C values and a K_C curve for forage bermudagrass (*Cynodon* spp.) (Sanches et al., 2019). The bermudagrass was grown as a single crop for a year and overseeded with ryegrass and black oats in the autumn and winter. ET_C was calculated using weighing lysimeters, and K_C values were estimated from those data using ET_O calculated with the Penman-Monteith equation. A Kc curve was developed from the daily K_C values using Eq. 4.1. In another study using weighing lysimeters, K_C curves were developed for hybrid turfgrass bermudagrass

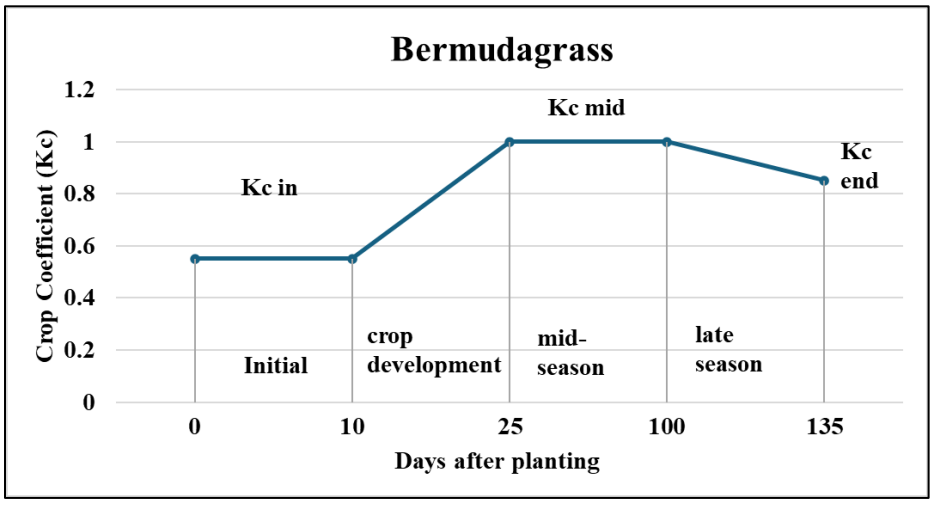

Figure 4.1 Crop coefficient (K_C) curve of Bermudagrass (hay) developed for use with the FAO Penman-Monteith reference evapotranspiration (ET_O) by applying K_C values observed under the non-stressed and well-managed condition in the California Desert, USA.

(*Cynodon dactylon* (L.) Pers. × *Cynodon transvaalensis* Burtt-Davy) and tall fescue (*Festuca arundinacea* Schreb.) in North Carolina, U.S. (Pinnix and Miller, 2019). In this study, tall fescue had higher K_C values than bermudagrass. In a study conducted in Florida, U.S., K_C curves for four warm-season turfgrass species- "Tifway" bermudagrass (*Cynodon dactylon* (L.) Pers. *x Cynodon transvaalensis* Burtt-Davy), "Empire" zoysiagrass (*Zoysia japonica* Steud.), "Floratam" St. Augustinegrass (*Stenotaphrum secundatum* (Walter) Kuntze), and "Argentine" bahiagrass (*Paspalum notatum* Flugge) were developed by measuring ET_C using weighing lysimeters and calculating ET_O with the American Society of Civil Engineers (ASCE)-Environmental & Water Resources Institute (EWRI) standardized method. Crop coefficients were derived using Eq. 4.1 (Wherley et al., 2015). Using the FAO-56 dual crop coefficient technique for ET_O and a weighing lysimeter to estimate ET_C, Mark (2016) developed seasonal K_C curves for ten turfgrasses in Colorado, U.S. All the above-mentioned studies were conducted under optimal soil moisture conditions.

Maktabi (2022) developed K_C curves for two cultivars of rainfed forage bermudagrass, rainfed tall fescue, and both rainfed and irrigated bahiagrass with data collected from capacitance-type soil moisture sensors installed in several locations in central and southern Georgia, U.S., from 2021-2022. In this study, daily changes in root zone volumetric water content (VWC) were used to estimate daily ET_C, and ET_O was calculated using the FAO-56 method (Allen et al., 1998). The K_C curves from this study for the "Alicia" and "Tifton 85" bermudagrass cultivars are shown in Figure 4.2.

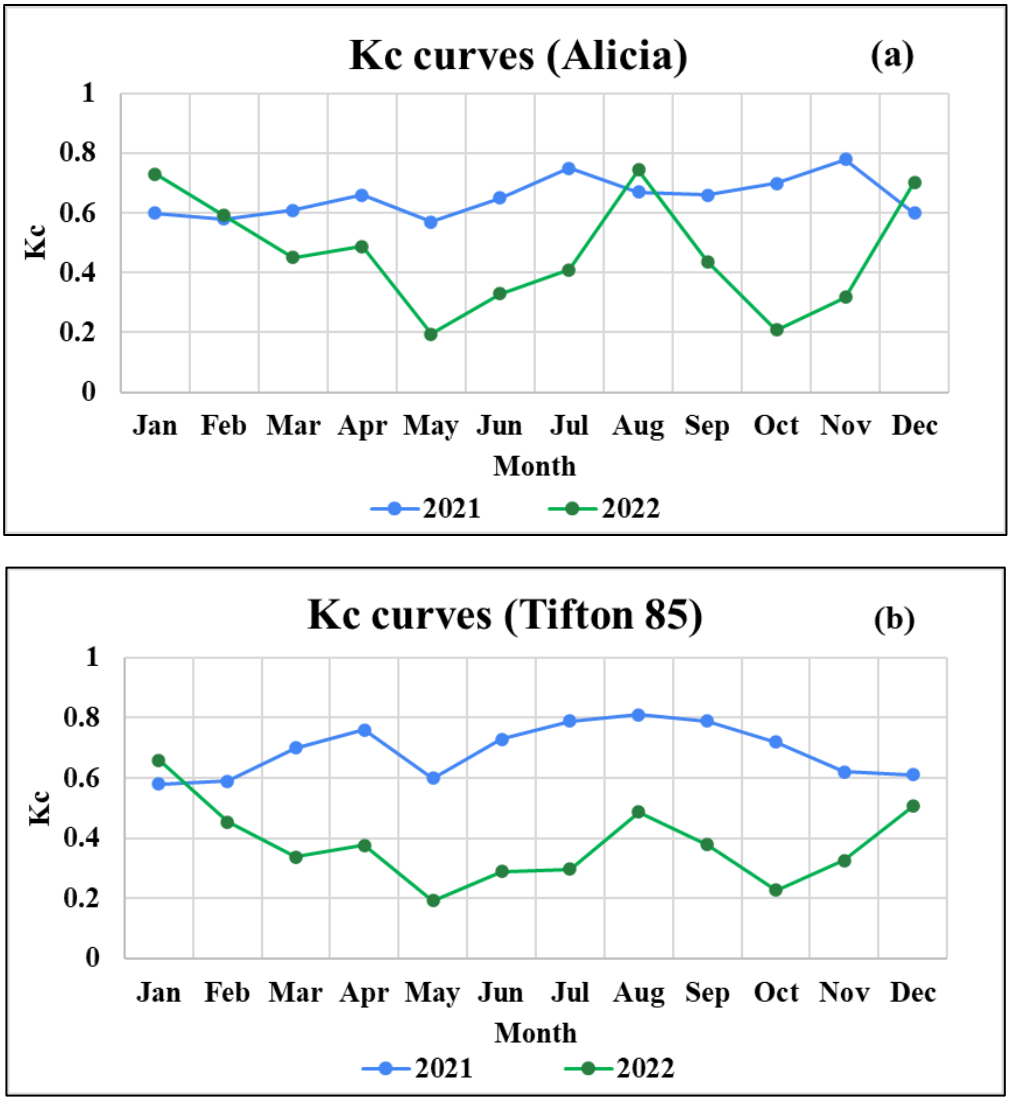

Figure 4.2 Monthly mean crop coefficient (K_C) curves of (a) "Alicia" and (b) "Tifton 85" during the 2021 and 2022 growing seasons in Tifton, GA (Maktabi, 2022).

Mathematical simulation of the crop evapotranspiration and development of the Kc curve of bermudagrass

Using lysimeters or measuring soil moisture from which to estimate daily crop water use are reliable experimental methods, but require significant resources and time. Another approach to understanding the ET dynamics of agricultural crops is to use comprehensive crop growth

simulation models. These types of models typically estimate daily ET_C, which in turn can be used in conjunction with Eq. 4.1 to develop K_C curves. The great advantage of using crop growth models is that if long meteorological data records are available, simulations can be run for many years from which annual K_C curves can be estimated and used to develop a mean K_C curve that is representative of a region.

The Decision Support System for Agrotechnology Transfer (DSSAT) is a widely used suite of dynamic crop growth simulation models for over 42 crops (Hoogenboom et al., 2019). DSSAT-CSM provides a framework for conducting research to understand the effect of various management practices and changes in environmental conditions on the growth and yield of crops by evaluating the relative response of different scenarios. DSSAT-CSM includes the CSM-CROPGRO-Perennial-Forage model (Rymph et al., 2004), which provides species adaptations and data files for three perennial forages, including "Tifton 85" bermudagrass (Pequeno et al., 2017).

Several studies have used DSSAT-CSM to measure ET_C under different scenarios for crops such as maize (Marek et al., 2017; Menefee et al., 2021), cotton (Dejonge & Thorp et al., 2017; Thorp et al., 2020), and sweet corn (Hailegnaw et al., 2024). However, little has been published on using crop growth models to estimate the ET_C of forage grasses. Castaño-Sánchez et al. (2020) used the CSM-CROPGRO-Perennial-Forage model to forecast ET_C and yield of alfalfa under an elevated CO_2 environment.

Goals and objectives

The significant and well documented flash drought event that occurred in September 2019 and resulted in severe damage to rainfed forages and other crops in the southeastern U.S. (Voiland, 2019; Ford et al., 2023; Gibbons et al., 2023 was not effectively captured by the U.S. Drought Monitor (USDM) and other tools used to document damage to crops. As a result, growers were

not able to access state and federal disaster assistance programs. The study described here is a component of a larger project whose overall goal was to quantify the frequency of flash drought events and estimate their impact on the yield of rainfed crops in the southeastern U.S. (Chapters 2 and 3). In those studies, the SmartIrrigation CropFit (SI CropFit) mobile application for irrigation scheduling (https://smartirrigationapps.org/) was used to identify flash drought events during the maize and cotton growing seasons in Georgia and Florida. SI CropFit uses the FAO-56 method to estimate ET_C for cotton, maize, peanut, soybean, and sweetcorn.

The study conducted by Maktabi (2022) during 2021-2022 and subsequently repeated by the authors in 2023 and 2024, was designed to develop the K_C curves for three forage grasses (bahiagrass, bermudagrass, and tall fescue) needed to incorporate these crops into SI CropFit and ultimately be used to assess the effect of flash drought on these forage grasses in Florida and Georgia. The K_C curves for the 2022 growing season showed sharp drops in K_C values during the spring and autumn, which was attributed to low crop water use associated with extended periods without precipitation (Figure 4.2). With only four years of field data, the 2022 K_C curves bias the 4-year mean K_C values downwards, making them inappropriate for direct use in SI CropFit.

The overall goal of this study was to use the CSM-CROPGRO-Perennial-Forage model to validate the K_C curves developed by Maktabi (2022) and the current project team for bermudagrass, a high-value and extensively used forage grass of the southeastern Coastal Plain. The specific objectives of the study were to: (1) evaluate the four ET estimation methods available in the CSM-CROPGRO-Perennial-Forage model for use in developing a bermudagrass K_C curve and (2) develop a bermudagrass K_C curve to be incorporated into SI CropFit.

Materials and methods

Study site

The data used to develop the bermudagrass K_C curve by Maktabi (2022) and the data used in this study were collected from the University of Georgia Plant Sciences Farm (31.489282, -83.521486) located on the university's Tifton campus. The area's physiographic classification is the Tifton Upland subregion of the southeastern Coastal Plain. Soil generally ranges from sandy to loamy sand. The climate is categorized as humid-subtropical with hot, humid summers and mild winters, having mean annual maximum and minimum air temperatures of 25.2°C, 18.9°C, and 12.7°C, respectively, with annual precipitation of 1,207 mm and 109 mean rainy days (University of Georgia Weather Network). Two large plots, each 162 m^2 (18 × 9 m), were used for the study (Figure 4.3). The soil in the plots is classified as a Tifton loamy sand. One plot was planted with the "Alicia" bermudagrass cultivar and the other with the "Tifton 85" cultivar. Both cultivars are widely used in the Coastal Plain region. Bermudagrass was established in the two plots in 2015. Sprigs were hand-spread at a rate of 2690 kg ha^{-1} and incorporated 5 cm into the soil with a shallow disc. Immediately following planting, 25.4 mm of water was applied to the plots. After that, the plots were managed under rainfed conditions. Fertilizer (N 16 kg ha-1, P_2O_5 4 kg ha^{-1} and K_2O 8 kg ha^{-1}) was applied 4 to 5 times per growing season at 45 kg ha^{-1} after each harvest of the grass (mean annual total of 224 kg ha^{-1}). The plots were burnt off every spring to control weeds, pests, plant diseases, and the thatch layer to increase forage yield.

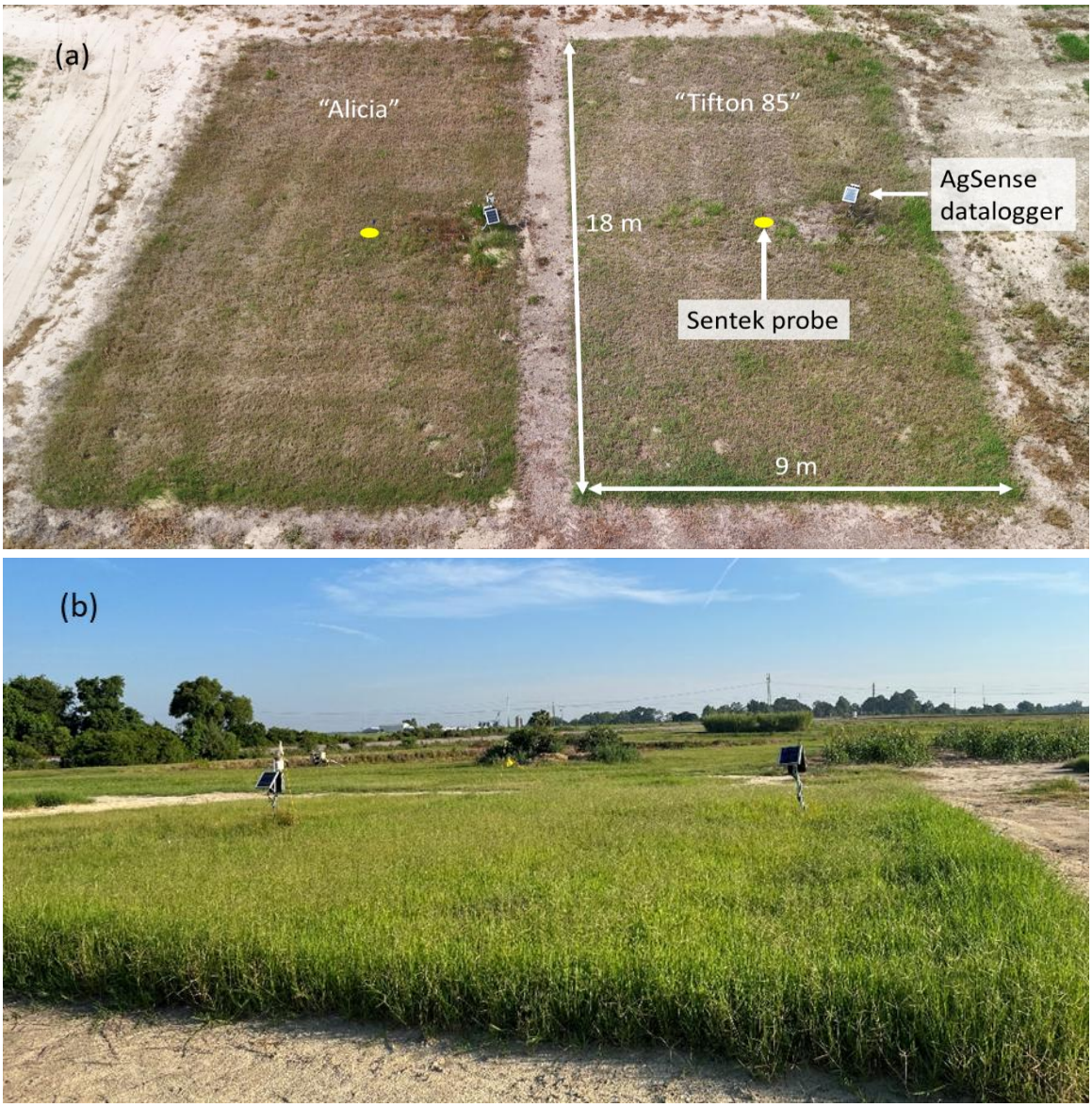

Figure 4.3 Aerial view of bermudagrass plots at the University of Georgia Tifton campus Plant Sciences Farm from mid-April 2025 (a) and ground view of the "Tifton 85" field at peak growth from June 2022 (b). Peak growth indicates harvesting time, which occurs 4-5 times per season.

Data collection

Three intact 90 cm soil cores were collected from the 1.5 m-wide bare strip between the two plots (Figure 4.3). The cores were segmented into 15 cm increments and analyzed for physical and chemical properties. The USDA Natural Resources and Conservation Services (NRCS) Web

Soil Survey was used to determine soil properties from 90-180 cm. Bulk density was measured by airdrying the samples, recording the mass of the increments, and dividing by the increment volume. After airdrying, a subsample of each increment was sent to a commercial laboratory (Waters Agricultural Laboratories, Inc. in Camilla, GA) for soil properties and nutrient analysis. Standard procedures were followed to determine soil texture, pH, soil organic matter, cation exchange capacity (CEC), and nutrient composition, including nitrogen (N), phosphorus (P), sulfur (S), potassium (K), calcium (Ca), magnesium (Mg), iron (Fe), manganese (Mn), zinc (Zn), boron (B), and copper (Cu). Soil physical and chemical property values from the three 15-cm segments at each depth were averaged and used to represent the soil in both plots in the DSSAT-CSM simulations (Table 4.1).

In the early spring of 2021, each plot was instrumented with two 60 cm Sentek Drill and Drop soil moisture probes (Sentek Sensor Technologies, Stepney SA, Australia). The probes were installed approximately in the center of each plot (Figure 4.3). Soil moisture as volumetric water content (VWC) and soil temperature were measured at six depths in 10 cm increments, beginning at 10 cm below the soil surface. The probes were connected to AgSense data loggers (AgSense Solutions, South Dakota, U.S.) that transmitted data to a cloud interface at 30-minute intervals.

Table 4.1 Selected soil physical and chemical properties derived from the three soil cores collected for the two plots. Values represent the mean ± standard error of three replications.

Depth (cm)	**Clay (%)**	**Silt (%)**	**Sand (%)**	**Organic Carbon (%)**	**Total nitrogen (%)**	**Cation exchange capacity (Cmol/kg)**	**pH**
0-15	6.8±0.72	2.7±1.44	90.5±1.73	1.02±0.13	0.16±0.01	2.9±0.23	4±0.03
15-30	8.8±1.09	2.0±0.82	89.2±1.62	1.02±0.13	0.15±0.01	3.9±0.19	4±0.03
30-45	16.2±1.19	2.0±0.82	81.8±1.27	1.02±0.13	0.13±0.01	3.9±0.21	4.1±0.18
45-60	17.5±1.43	2.5±0.53	80.0±1.25	1.02±0.13	0.18±0.01	4.2±0.17	4.5±0.26
60-75	16.0±1.79	5.2±0.18	78.8±1.80	1.02±0.13	0.14±0.01	4.4±0.23	4.8±0.34
75-90	21.1±2.13	2.6±0.61	76.3±1.61	1.02±0.13	0.14±0.01	4.4±0.35	5.1±0.21
90-180	21.1±2.13	2.6±0.61	76.3±1.61	1.02±0.13	0.14±0.01	4.4±0.35	5.1±0.21

The data loggers were installed near the east edge of the plots. VWC data were collected continuously from the two plots except for a period of 5 months in 2023 and three months in 2024 when one of the probes failed in the “Tifton 85” plot.

Samples to estimate total forage and herbage mass were collected four times per year in 2022, 2023, and 2024 before the grass was cut for hay in the two plots on the schedule shown in Table 4.2. Total biomass samples were collected by cutting all the grass within a 0.092 m^2 (1 ft^2) PVC quadrat with shears or scissors to ground level at four randomly selected locations in each plot. Samples for herbage mass were collected using the same technique, but the grass was cut at 7.6 cm above the ground surface. The leaf area index (LAI) was measured in two ways – an indirect field method and a direct laboratory method, as both methods are commonly used to measure LAI for bermudagrass (Kiniry et al., 2007; Alderman et al., 2011; Borges et al., 2017). In the field method, the light interception of the crop was measured with a ceptometer (LP-80, METER, Pullman, WA) in the plot before cutting and then converted to LAI with fixed light extinction coefficients for bermudagrass. In the laboratory method, plant samples were separated as leaf and stem. LAI was measured using a bench-top leaf area meter (LI-3100, LI-COR Biosciences, Lincoln, NE). The dried mass was calculated by placing the samples in paper bags and drying them in a forced-air oven at 65°C for at least 48 hours. The dried samples were weighed, and mass was reported in units of kg ha^{-1}. Mean values of the four measurements of LAI, herbage mass, and total forage from each plot were used in subsequent analyses.

Table 4.2 Leaf area index (LAI), herbage mass, and total forage of "Alicia" and "Tifton 85" during 2022-2024 growing seasons were collected four times per growing season. Values represent the mean ± standard error of four replications.

Harvest Date	**LAI (m^2m^{-2})**				**Herbage Mass (kg ha^{-1})**		**Total forage (kg ha^{-1})**	
	Alicia (Lab)	**Alicia (Field)**	**Tifton 85 (Lab)**	**Tifton 85 (Field)**	**Alicia**	**Tifton 85**	**Alicia**	**Tifton 85**
2022								
23 Jun	0.76±0.14	0.87±0.28	0.93±0.17	1.08±0.13	2028±221	2637±425	3008±214	3897±365
01 Aug	1.21±0.23	1.42±0.12	1.38±0.31	1.55±0.22	2002±131	3094±463	3755±275	4734±409
06 Sep	1.62±0.35	1.71±0.28	1.73±0.15	1.81±0.23	2136±312	2032±365	3341±189	3485±303
12 Oct	0.73±0.18	0.90±0.13	1.02±0.21	0.81±0.19	1297±243	1889±480	2244±103	3019±224
Total					**7463**	**9652**	**12348**	**15135**
2023								
24 May	1.23±0.27	1.38±0.38	1.54±0.15	1.87±0.21	1426±245	1689±313	2690±58	2609±101
07 Jul	1.59±0.32	1.72±0.28	1.67±0.11	1.94±0.32	2104±142	1533±88	3815±98	2926±112
28 Aug	1.85±0.18	2.04±0.24	1.98±0.21	2.05±0.27	2787±229	1646±214	4191±211	3524±189
18Oct	1.28±0.39	1.12±0.32	1.05±0.23	1.17±0.15	1670±172	2890±289	3349±145	3977±229
Total					**7987**	**7758**	**14045**	**13036**
2024								
25 May	1.29±0.23	1.39±0.18	1.43±0.28	1.55±0.25	2122±212	2735±145	3725±142	4570±223
08 Jul	1.01±0.18	1.22±0.25	1.13±0.13	1.25±0.21	2352±334	2680±344	4064±228	4273±438
21 Aug	0.73±0.10	0.86±0.06	0.86±0.12	0.99±0.15	1210±146	1233±188	2816±121	2333±249
15th Oct	0.79±0.14	0.65±0.11	0.52±0.07	0.39±0.09	1044±221	672±202	1953±322	1264±177
Total					**6728**	**7320**	**12558**	**12440**

Field ET measurement and crop growth curve (Kc) development

"Alicia" and "Tifton 85" K_C curves for 2021 and 2022 were developed by Maktabi (2022) using VWC data. The same approach was used by the authors for the VWC data collected in 2023 and 2024. VWC measurements from each of the six depths of each probe at 05:30 every morning were averaged to calculate the mean probe VWC. The two mean probe VWC values from each plot were averaged to develop a mean VWC. Daily changes in mean field VWC (ΔVWC) were estimated between field capacity and when the slope of ΔVWC approached zero by subtracting today's mean field VWC from yesterday's mean field VWC. The resulting ΔVWC values were filtered to remove outliers and assumed to be equivalent to daily crop evapotranspiration as measured by the soil moisture sensors ($ET_{C\text{-}SMS}$). Meteorological data to calculate ET_O using the FAO-56 method (Allen et al., 1998) were retrieved from the University of Georgia Weather Network (UGAWN) (http://weather.uga.edu) for the Tifton weather station located approximately 500 m from the plots. Daily $K_{C\text{-}SMS}$ was calculated using Eq. 4.1. Monthly mean $K_{C\text{-}SMS}$ values were determined by averaging daily $K_{C\text{-}SMS}$ values and used to develop "Alicia" and "Tifton 85" K_C curves.

Using the CSM-CROPGRO-Perennial-Forage model to simulate bermudagrass ET_C

In this study, the CSM-CROPGRO-Perennial-Forage (CROPGRO-PFM) (v.4.8.2) was used to estimate daily ET_C for bermudagrass in the plots described above. For crop simulation in DSSAT-CSM, soil data, meteorological data, management practices, and cultivar-specific genetic coefficients are needed. The model simulates several variables, including ET_C, nutrient content, leaf area, leaf mass, total forage, and yield under various management approaches and climate variations once it has been calibrated.

Model simulation

As the field data set collected in this study was not extensive enough to develop new genetic coefficients for the two bermudagrasses and be used for calibrating and evaluating the performance of the model, the genetic coefficients for the "Tifton 85" bermudagrass cultivar already available in the model (Table 4.3) from a study conducted in Brazil (Pequeno et al., 2017) were used to simulate both the "Tifton 85" and "Alicia" cultivars. Field measurements of LAI, herbage mass at maturity (kg ha^{-1}), and total forage (kg ha^{-1}) from 2022 to 2024 were used as observations for evaluating the performance of the model. To simulate perennial grass growth and harvest, the model required field observations of harvest dates, measured stubble mass (the mass of stubble

Table 4.3 Genetic coefficients for the 'TIFTON 85 BERMUD' bermudagrass cultivar used in the CSM-CROPGRO-Perennial forage model (Pequeno et al., 2017).

Parameters	Description	Value
EM-FL	Time from plant emergence to flower appearance (photothermal days)	45.0
FL-SD	Time between first flower and first seed (R5) (photothermal days)	12.0
SD-PM	Time between first seed (R5) and physiological maturity (R7) (photothermal days)	45.0
LFMAX	Maximum leaf photosynthesis rate at 30 C, 350 vpm CO_2, and high light (mg CO_2/m^2-s)	1.05
SLAVR	Specific leaf area of cultivar under standard growth conditions (cm^2/g)	170
SIZLF	Maximum size of full leaf (three leaflets) (cm^2)	2.0
WTPSD	Maximum weight per seed (g)	0.02
SFDUR	Seed filling duration for the pod cohort at standard growth conditions (photothermal days)	15.0
SDPDV	Average seed per pod under standard growing conditions (#/pod)	2.05

remaining in the plot after harvest and abbreviated as MOW), and the leaf fraction in the stubble (RSPLF). This information was added to a model input file named MOW. Though all the initial conditions and management practices were the same for both varieties, the cultivar-specific data included in the MOW file resulted in different simulation outcomes for "Alicia" and "Tifton 85".

Bermudagrass ET_C estimates

The DSSAT-CSM soil-plant-atmosphere module uses soil, plant, and atmosphere data to simulate potential ET, soil evaporation, root water uptake, light interception by the canopy, and plant transpiration. ET estimation includes a soil water balance calculation (Ritchie, 1998; Ritchie & Otter, 1985). Data input requirements include daily meteorological values, soil water content by layer in the initial condition, detailed soil properties, LAI, and root length density for each layer (Jones et al., 2003). VWC data from the installed Sentek soil moisture probes were used to represent the initial soil moisture condition before planting in DSSAT-CSM.

Meteorological data were retrieved from the UGAWN Tifton weather station and included maximum and minimum air temperature (˚C), solar radiation (MJ m^{-2} day^{-1}), precipitation (mm day^{-1}), relative humidity (%), and wind speed (m s^{-1}). Total monthly precipitation, daily solar radiation, and daily mean air temperature from 2022 to 2024 for the site are shown in Figure 4.4. Meteorological data were imported, analyzed, and exported in the appropriate format using the DSSAT-CSM WeatherMan weather module. Soil physical and chemical properties (soil texture, soil pH, cation exchange capacity, organic carbon, total nitrogen, etc.) derived from the soil cores collected for the two plots (Table 4.1) were used to create the DSSAT-CSM soil file with SBuild.

Root length density, drainage lower and upper limits, saturated water content, saturated hydraulic conductivity, and other parameters were generated by DSSAT-CSM based on the soil profile data provided. Based on a negative exponential function of LAI, potential ET is divided

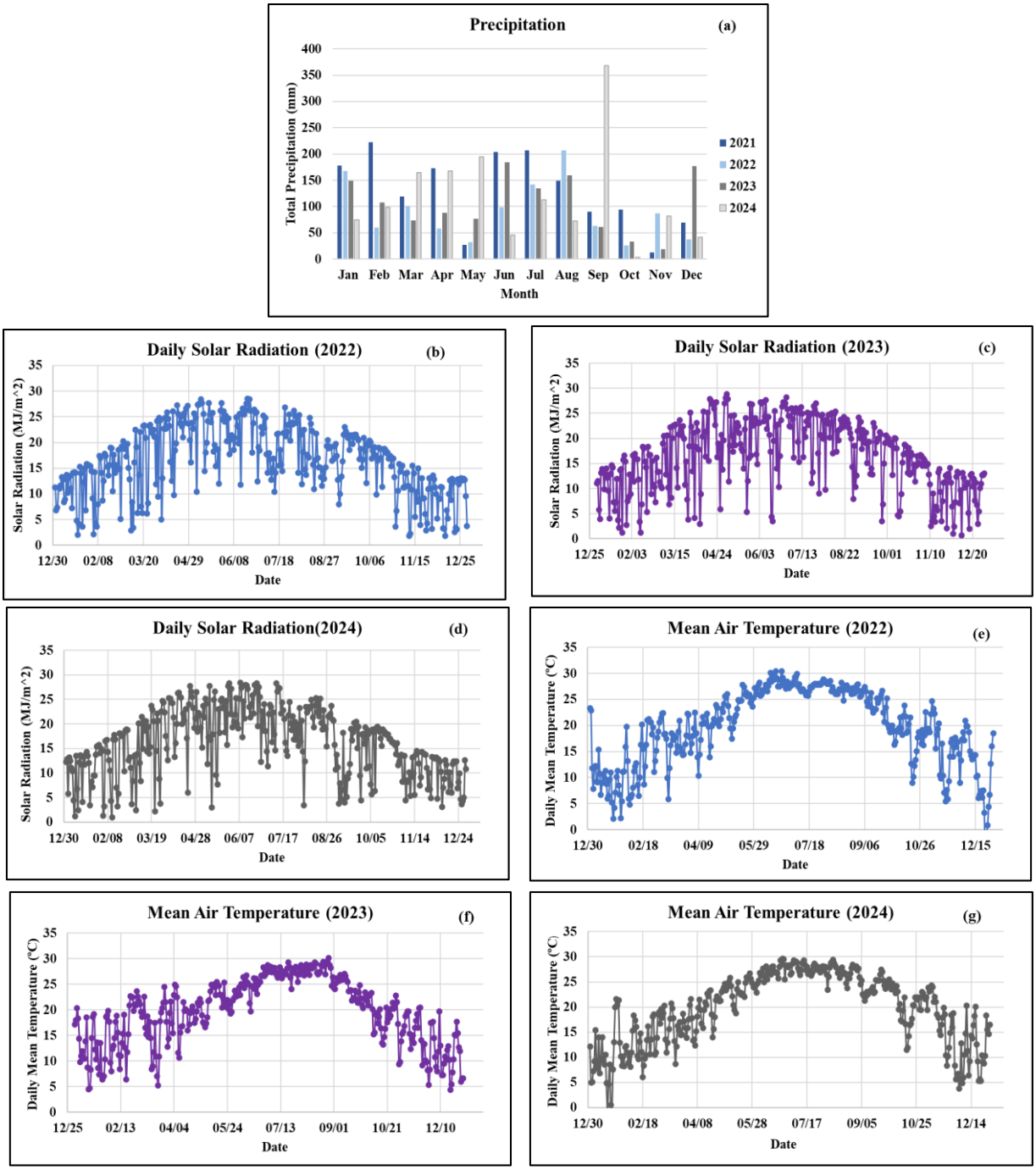

Figure 4.4 Monthly total precipitation from 2021-2024 (a), daily solar radiation of 2022 (b), 2023 (c), 2024 (d), and daily mean air temperature of 2022 (e), 2023 (f), and 2024 (g) of Tifton weather station.

into two parts: potential plant transpiration and potential soil evaporation, which is determined by the percentage of solar energy that reaches the soil surface. Actual soil evaporation follows a two-stage process (Ritchie, 1972). Evaporation proceeds at its potential rate until a cumulative soil

evaporation quantity since wetness is attained, following the initial wetting of the soil surface by irrigation or precipitation. Subsequently, a daily soil-limiting amount of soil evaporation is calculated. Potential root water absorption is calculated by computing a maximum water flow to roots in each layer and adding these values to determine whether the soil or atmosphere restricts plant transpiration (Ritchie and Otter, 1985; Ritchie, 1998; Jones and Ritchie, 1991). Both the soil water content and the root length density in each layer are considered in these computations. Potential root water uptake in each layer is calculated using an approximation of the radial flow equation, which makes assumptions regarding the maximum water potential difference between the roots and the soil, root diameter, and the impact of soil texture on hydraulic conductivity.

Actual management practices were selected for the simulations. The model requires a planting date to begin simulations. As described earlier, the bermudagrass in the two plots was planted in 2015 and well-established. To ensure that the model was simulating an established crop from 2022 onwards, a planting date of 01 March 2021 was used. Because field data from 2021 were not available, data from 2023 were used to create the 2021 MOW and RSPLF files, as the 2023 growing season weather patterns closely resembled those of the 2021 growing season. To simulate rainfed management, the model was configured to operate without irrigation beginning January 1, 2021. The CENTURY model (Parton et al., 1988, 1994) was used to simulate soil organic matter (SOM) because it is more adaptable to the long-term dynamics of SOM in agricultural systems, such as the decomposition of plant litter deposited during the season and the root, rhizome, and stolon mass that senesces in the soil during the long-term growth of perennial crops. The Ritchie-Ceres method (Ritchie, 1972) was used for soil water evaporation.

In SI CropFit, ET_O is calculated using the FAO-56 method. In DSSAT, ET_O is referred to as Potential ET (PET) and can be estimated with several different methods, including FAO-56. In

this study, four PET methods were evaluated to determine which PET method best matched the method used in SI CropFit. The four PET methods used were: the FAO-56 method (PET_{FAO}), the Priestley-Taylor method (PET_{PT}), and the American Society of Civil Engineers (ASCE) standardized method for grass (PET_{ASCE} grass) and the ASCE standardized method for alfalfa (PET_{ASCE} alfalfa) (Allen et al., 2005). PET_{FAO} is calculated using the Penman-Monteith equation found in FAO Irrigation and Drainage Paper No. 56 (Allen et al., 1998; Thorp et al., 2020). PET_{PT} is a simplified version of the Penman-Monteith ET_O equation that requires only daily solar irradiance and maximum and minimum air temperatures and is widely used (Priestley and Taylor, 1972). The PET_{ASCE} methods utilize a modified Penman-Monteith equation (DeJonge and Thorp, 2017).

These four methods were used to calculate PET, and the results were compared to ET_O calculated using the FAO-56 method ($ET_{O\text{-}FAO}$) with meteorological data from the UGAWN Tifton weather station. The UGAWN also provides reference ET calculated using the Priestley-Taylor method ($ET_{O\text{-}PT}$), and since these data were available, they were also compared to the PET results. ET_C was estimated with DSSAT using each of the PET methods ($ET_{C\text{-}FAO}$, $ET_{C\text{-}PT}$, $ET_{C\text{-}ASCE}$ grass, $ET_{C\text{-}ASCE}$ alfalfa) and compared to $ET_{C\text{-}SMS}$ calculated from the soil moisture sensor data.

Statistical analysis

To evaluate the model's performance, several statistical indicators were calculated, including the coefficient of determination (R^2), the index of agreement (d-index), also known as Willmott's D (Willmott, 1981), and the root-mean-square error (RMSE). The d-index and R^2 range from 0 to 1, with higher values indicating a stronger agreement between simulated and observed data. R^2 measures the proportion of the variance in the observed data that is explained by the model. The d-index quantifies the degree of correspondence and accuracy of the model, where 1.0

denotes a perfect fit, and 0.0 indicates no agreement (Adhikari et al., 2016). When comparing model performance across variables with different units, the RMSE estimates the mean difference between simulated and measured values with the same unit. A higher d-index and a lower RMSE indicate improved model accuracy and agreement with observed data.

Results and discussion

Field data

As a warm-season perennial, bermudagrass is usually dormant from late fall to early spring in subtropical climates (Lee et al., 2017). During this period, there is little to no growth in total forage. Each year, the total forage began to increase as the plants emerged from dormancy in the spring, followed by a decline during the fall. In southern Georgia, the growing season is typically May – October although it can be extended by warmer than normal temperatures. Herbage and biomass samples were collected during the growing season only. Growing season precipitation, solar radiation, and temperature are the primary environmental parameters that determine rainfed bermudagrass hay production. The number of hay cuttings during the growing season is a function of these variables, and in rainfed production, precipitation is generally the determinant parameter. During the three years that data were collected (2022-2024), there were four hay cuttings per year (Table 4.2), but the timing of the cuttings varied and was determined by growth associated with environmental conditions.

In southern Georgia, most growing season precipitation is received between June and August. Precipitation in 2022 and 2023 (Figure 4.4a) followed this pattern with June-August precipitation totals of 448 mm and 478 mm, respectively. In contrast, the June-August precipitation in 2024 was much lower (231 mm). There were large differences in early growing season (March–May) precipitation patterns as well. March – May 2024 was much wetter (527 mm) than the same

periods in 2022 (192 mm) and 2023 (238 mm). The large amount of precipitation received in September 2024 was associated with Hurricane Helene (187 mm). Mean growing season solar radiation was slightly lower in 2024 (18.96 MJ m^{-2}) than in 2022 (19.66 MJ m^{-2}) and 2023 (19.89 MJ m^{-2}) (Figures 4.4b-4.4d). In contrast, was mean air temperature was lower in 2022 (24.82° C) and 2023 (24.25° C) than in 2024 (25.03° C) (Figures 4.4e-4.4g).

Of the three environmental parameters, precipitation patterns appear to have affected plant growth the most, with higher herbage mass collected in 2022 and 2023 than in 2024 for both cultivars (Table 4.2). This is also evident in the K_C curves developed by Maktabi (2022) (Figure 4.2) where the K_C for both "Alicia" and "Tifton 85" trended lower in March, April and May of 2022 when spring precipitation (192 mm) was about 60% of that received in 2021 (318 mm). With near or above normal precipitation in June, July, and August, K_C rebounded. The effect of precipitation and other variables on plant growth is discussed in more detail further below.

There are few published studies of bermudagrass production under rainfed conditions with which to compare the field data collected in this study. In a study conducted in Tifton, Hendricks et al. (2020) observed a range of 7,877-8,993 kg ha^{-1} in herbage mass of rainfed "Tifton 85" between 2017-2018. The Hendricks et al. (2020) yields are generally higher than the yields reported in this study, but the ranges overlap, and the differences can be accounted for by the prevailing environmental conditions. In another study, the mean yield of "Coastal" and "Tifton 85" was 5,738 kg ha^{-1} harvested on a 21-day interval and 8,282 kg ha^{-1} at single season harvest under rainfed conditions in Stephenville, Texas (Muir et al., 2010). Annual yields of rainfed "Tifton 85" ranged from 17900-18700 kg ha-^{1} in Piracicaba, Sao Paulo state, Brazil, depending on harvesting frequency (Pequeno et al., 2015). Lee et al. (2017) found that Bermudagrass may yield between 11,200-15,690 kg ha^{-1} under ideal environmental conditions.

Field-measured LAI tended to be higher than LAI measured in the lab (He et al., 2007). This is most likely because the field method measures light interception, which for bermudagrass, is affected by the total forage, including stems. In the lab measurements, leaves are separated from stems, and only the area of the leaves is included in the LAI calculation. For both cultivars, LAI reached a peak in late summer, after which it began to decline. Depending on the varieties, bermudagrass canopy architecture varies with larger stems, broader leaves, denser sod, intervaginal tillers etc. (Hancock et al., 2013) which tend to increase canopy or leaf light interception (Volterrani et al., 2017). As a result, "Tifton 85" tended to have larger LAI values than "Alicia", which was expected as the LAI patterns match the herbage mass patterns and "Tifton 85" has broader leaves and larger stems compared to other varieties (Hancock et al., 2013). In a fertilizer application study, the LAI of "Tifton 85" was observed to be around 1.9-2.8 m^2 m^{-2} with 60 Kg N ha^{-1} application under rainfed conditions in the field measurement in Sao Paulo state, Brazil, which is higher than the LAI observed in this study (Borges et al., 2017). The range LAI of "Coastal" bermudagrass was around 0.5-2.51 m^2 m^{-2} (with few exceptions) following lab measurement under rainfed conditions in Temple and Mays field, TX (Kiniry et al., 2007).

PET comparison

An important step in DSSAT-CSM simulation is the accurate representation of PET, which establishes the maximum amount of water that can be lost from the cropping system through transpiration and evaporation. Table 4.4 presents the annual cumulative sum of simulated daily PET_{FAO}, PET_{PT}, PET_{ASCE} grass, and PET_{ASCE} alfalfa compared to reference ET calculated from meteorological data ($ET_{O\text{-}FAO}$ and $ET_{O\text{-}PT}$) from 2022 to 2024. The PET_{ASCE} alfalfa method resulted in the highest PET annual sums (Table 4.4), which was expected as the method, by definition, has a higher potential for ET as alfalfa is a taller crop with more biomass than shorter grasses (Dejonge

and Thorp, 2017). PET annual sums were generally higher than $ET_{O\text{-}FAO}$ and $ET_{O\text{-}PT,}$ except for $PET_{PT,}$ which closely matched $ET_{O\text{-}FAO}$ for each of the three years. These observations have been reported in other studies (e.g., Kimball et al., 2019). The mean difference between PET_{FAO} and $ET_{O\text{-}FAO}$ annual sums was 13.3%. This may have been caused by differences in daily ET_O calculations for days with above-mean wind speeds (≥ 4.0 m s^{-1}) (Garcia, Raes, Allen, & Herbas, 2004; Hoogenboom et al., 2003; Menefee et al., 2021). Wind speed is not included in the Priestly-Taylor method, and this may have led to smaller annual differences between PET_{PT} and $ET_{O\text{-}PT}$ annual sums (8.7%).

The annual cumulative sum of crop water use (ET_C) of "Alicia" and "Tifton 85" measured in the field study ($ET_{C\text{-}SMS}$) and predicted by DSSAT-CSM ($ET_{C\text{-}FAO}$, $ET_{C\text{-}PT}$, $ET_{C\text{-}ASCE}$ grass and $ET_{C\text{-}ASCE}$ alfalfa) are shown in Table 4.4. Only DSSAT-CSM ET_C values from the same days as $ET_{C\text{-}SMS}$ were available, were used for comparisons. DSSAT-CSM crop water use was higher than estimates made from soil moisture sensor measurements, with $ET_{C\text{-}SMS}$ ranging between 37-58% of $ET_{C\text{-}FAO}$, $ET_{C\text{-}PT}$. The differences between field measurements and DSSAT-CSM were larger in 2022 and 2024 when there were extended dry periods, which may have resulted in soil water availability simulation errors (Kimball et al., 2019; Menefee et al., 2021). During the 2022 growing season, $ET_{C\text{-}FAO}$ was more than twice as high as $ET_{C\text{-}SMS}$ for "Tifton 85". Although $ET_{C\text{-}SMS}$ estimates for "Alicia" and "Tifton 85" varied, the crop water use of the two cultivars predicted by DSSAT-CSM did not differ significantly, primarily because the genetic coefficients used in the model for the two cultivars were the same. Total growing season precipitation was higher than both measured and simulated ET_C for all three years, although, as described earlier, there were extended periods without precipitation in 2022 and 2024. Consequently, the highest crop water use was both observed and simulated in 2023.

Table 4.4 Annual cumulative sum of potential evapotranspiration (PET) and daily crop evapotranspiration (ET_C) measured in the field study and predicted by DSSAT-CSM under four PET methods from 2022-2024.

Reference ET	**Annual Cumulative Sum of ET (mm)**					
	2022	**2023**	**2024**			
$ET_{O\text{-}FAO}$[1]	1246	1219	1189			
$ET_{O\text{-}PT}$[1]	1131	1120	1101			
PET_{FAO}[2]	1421	1383	1337			
PET_{PT}[2]	1242	1218	1192			
PET_{ASCE} grass[2]	1852	1794	1728			
PET_{ASCE} alfalfa[2]	2064	1998	1908			
Crop ET	**Alicia**			**Tifton 85**		
	2022	2023	2024	2022	2023	2024
$ET_{C\text{-}SMS}$[3]	271	305	228	236	141	250
$ET_{C\text{-}FAO}$[2]	427	417	348	486	224	367
$ET_{C\text{-}PT}$[2]	408	426	342	471	213	356
$ET_{C\text{-}ASCE}$ grass[2]	404	410	312	468	212	335
$ET_{C\text{-}ASCE}$ alfalfa[2]	413	402	318	482	218	343

[1] Calculated from UGAWN weather station data.
[2] Estimated with DSSAT-CSM
[3] Estimated from soil moisture measurements.
[4] Reference Evapotranspiration using 1998 method ($ET_{O\text{-}FAO}$)
[5] Reference Evapotranspiration using Priestley-Taylor method ($ET_{O\text{-}PT}$)
[6] Potential Evapotranspiration using FAO-56 method (PET_{FAO})
[7] Potential Evapotranspiration using Priestley-Taylor method (PET_{PT})
[8] Potential Evapotranspiration using the American Society of Civil Engineers (ASCE) Standardized method PET_{ASCE} for grass
[9] Potential Evapotranspiration using the American Society of Civil Engineers (ASCE) Standardized method PET_{ASCE} for alfalfa
[10] Daily crop evapotranspiration from soil moisture sensor ($ET_{C\text{-}SMS}$)
[11] Daily crop evapotranspiration using FAO-56 method ($ET_{C\text{-}FAO}$)
[12] Daily crop evapotranspiration using Priestley-Taylor method ($ET_{C\text{-}PT}$)
[13] Daily crop evapotranspiration using the American Society of Civil Engineers (ASCE) Standardized method $ET_{C\text{-}ASCE}$ for grass
[14] Daily crop evapotranspiration using the American Society of Civil Engineers (ASCE) Standardized method $ET_{C\text{-}ASCE}$ for alfalfa

To determine which PET method to use for developing a DSSAT-based K_C curve for bermudagrass, the four PET methods were compared statistically to $ET_{O\text{-}FAO}$ (the method used in SI CropFit) using linear regression (R^2) and RMSE as performance metrics (Table 4.5). Similarly, $ET_{C\text{-}FAO}$, $ET_{C\text{-}PT}$, $ET_{C\text{-}ASCE}$ grass, and $ET_{C\text{-}ASCE}$ alfalfa, were compared statistically to $ET_{C\text{-}SMS}$ (Table 4.5). In general, all four methods showed strong linear relationships between calculated and simulated reference ET, with R^2 values near 1, but RMSE was better for PET_{FAO} and PET_{PT} than the two PET_{ASCE} methods. PET_{PT} RMSE values were slightly better than PET_{FAO} values (Table 4.5). In terms of crop water use, $ET_{C\text{-}FAO}$ and $ET_{C\text{-}PT}$ both resulted in better performance metrics than the ASCE methods. The metrics for 2022 were not as good as those for 2023 and 2024, and that may be because the simulation was initiated with planting in 2021, while the plots were planted in 2015. The model currently does not allow simulations to be initiated with an established crop. The harvest data required by the model were not available for years before 2022. The mean daily $ET_{C\text{-}SMS}$ of "Alicia" during May- October, 2022-2024, ranged from 1.49 to 2.37 mm d^{-1} while the corresponding range of $ET_{C\text{-}FAO}$ was 2.32 to 3.28 mm d^{-1}. Similar results were observed in other studies. In a study conducted using weighing lysimeters in São Paulo State, Brazil, the mean daily forage bermudagrass ET_C was 3.57 mm d^{-1} (Sanches et al., 2019). Between May and October, turfgrass bermudagrass mean daily ET_C measured with weighing lysimeters ranged from 1.78-5.59 mm d^{-1} under rainfed conditions in Raleigh, NC (Pinnix and Miller, 2019). Because of the relatively small differences in performance metrics resulting from using PET_{FAO} and PET_{PT} when compared to calculated and field measured values, PET_{FAO} was selected for further simulations to maintain consistency with the ET_O method used in SI CropFit.

Table 4.5 Statistical analysis of potential evapotranspiration (PET) and daily crop evapotranspiration (ET_C) measured in field study and predicted by CSM-CROPGRO-Perennial-Forage under four PET methods from 2022-2024

PET method	**Statistical Analysis**	**Year**		
		2022	**2023**	**2024**
PET_{FAO}	R^2	0.98	0.95	0.98
	RMSE (mm d^{-1})	0.45	0.48	0.35
PET_{PT}	R^2	0.98	0.97	0.98
	RMSE (mm d^{-1})	0.38	0.38	0.35
PET_{ASCE} grass	R^2	0.97	0.94	0.96
	RMSE (mm d^{-1})	1.86	1.82	1.63
PET_{ASCE} alfalfa	R^2	0.90	0.82	0.88
	RMSE (mm d^{-1})	2.53	2.42	2.14

Crop ET		**Alicia**			**Tifton 85**		
		2022	2023	2024	2022	2023	2024
$ET_{C\text{-}FAO}$	R^2	0.39	0.52	0.44	0.26	0.33	0.54
	RMSE (mm d^{-1})	1.55	1.38	1.59	1.89	1.58	1.54
$ET_{C\text{-}PT}$	R^2	0.39	0.54	0.43	0.29	0.35	0.55
	RMSE (mm d^{-1})	1.63	1.48	1.69	1.99	1.69	1.66
$ET_{C\text{-}ASCE}$ grass	R^2	0.36	0.43	0.37	0.24	0.31	0.55
	RMSE (mm d^{-1})	1.42	1.39	1.47	1.78	1.46	1.43
$ET_{C\text{-}ASCE}$ alfalfa	R^2	0.37	0.45	0.36	0.24	0.30	0.53
	RMSE (mm d^{-1})	1.49	1.42	1.55	1.88	1.59	1.52

[1] Potential Evapotranspiration using FAO-56 method (PET_{FAO})
[2] Potential Evapotranspiration using Priestley-Taylor method (PET_{PT})
[3] Potential Evapotranspiration using the American Society of Civil Engineers (ASCE) Standardized method PET_{ASCE} for grass
[4] Potential Evapotranspiration using the American Society of Civil Engineers (ASCE) Standardized method $PET_{ASCE,}$ for alfalfa
[5] Daily crop evapotranspiration using FAO-56 method ($ET_{C\text{-}FAO}$)
[6] Daily crop evapotranspiration using Priestley-Taylor method ($ET_{C\text{-}PT}$)
[7] Daily crop evapotranspiration using the American Society of Civil Engineers (ASCE) Standardized method $ET_{C\text{-}ASCE}$ for grass
[8] Daily crop evapotranspiration using the American Society of Civil Engineers (ASCE) Standardized method $ET_{C\text{-}ASCE}$ for alfalfa

Plant growth simulation

Table 4.6 presents the statistical indicators used to compare model predictions for LAI (m^2 m^{-2}), herbage mass (kg ha^{-1}), and total forage (kg ha^{-1}) to data collected in the field. The simulated results were compared to the four annual field observations for 2022-2024. Model predictions of LAI were compared to the field (indirect) method, as those values were higher and thought to be more representative of actual field conditions. Overall, R^2 values were much better for "Alicia" than "Tifton 85", while d-index and RMSE values were similar for all three parameters. LAI d-index and RMSE values were very poor for both cultivars, primarily because DSSAT-CSM estimates of LAI were much higher than measured (Figures 5a and 6a). The RMSE for LAI was as much as three times higher than the mean measured values in Table 4.2, indicating a significant prediction error. This may be because neither the field technique nor the lab technique used for measuring LAI accurately measures this parameter in forage bermudagrass. Another reason may be that the genetic coefficients used in the model represent growing conditions different from those encountered in this study. The DSSAT-CSM User's Guide emphasizes the importance of calibrating crop-specific traits to ensure accurate LAI simulation and thus preventing significant overestimations (Hoogenboom et al., 2010). In contrast to LAI, the metrics showed better performance for simulated herbage mass and total forage. For these two parameters, the simulation

Table 4.6 Statistical analysis of simulated leaf area index (LAI), herbage mass, and total forage of "Alicia" and "Tifton 85" compared to measured data at the 12 sampling events (four events per year).

Cultivar	LAI			Herbage Mass			Total forage		
	R^2	**d-index**	**RMSE** (m^2m^{-2})	**R^2**	**d-index**	**RMSE** (kg ha^{-1})	**R^2**	**d-index**	**RMSE** (kg ha^{-1})
Alicia	0.59	0.15	3.33	0.54	0.46	1302	0.61	0.60	1256
Tifton 85	0.49	0.16	3.29	0.10	0.55	1248	0.38	0.69	1207

results were generally similar for the two cultivars except for the R^2 of herbage mass of "Tifton 85", which was low (0.11).

Figures 4.5 and 4.6 present the simulated and observed LAI, herbage mass, and total forage for the "Alicia" and "Tifton 85" bermudagrass cultivars during the 12 sampling events that took place from 2022 to 2024. DSSAT mostly overpredicted total forage and herbage mass for both varieties except in 2022 (Figures 4.5b- 4.5c, 4.6b- 4.6c). Similar results in 2022 may be related to the simulation beginning in 2021 with a newly planted plot, as described earlier. To test this hypothesis, the model was also initiated in 2022, and DSSAT-CSM greatly underpredicted the measured values.

For all three years (2022-2024), simulated annual total forage and herbage mass were higher than measured for "Alicia" and mostly higher for "Tifton 85" (Table 4.7). Both observed and simulated annual total forage of "Alicia" in 2022 was lower than in the 2023 and 2024 growing seasons (Table 4.7). The annual total forage of "Tifton 85" was the highest during the 2022 growing season in the field study, but the highest annual total forage was predicted by DSSAT-CSM during the 2023 growing season.

Despite the relatively poor performance of some metrics, the simulated results followed the same trends as the measured data, indicating that the model may be used for further analyses. It is important to note that the DSSAT-CSM model does not account for the effects of weeds, pests, and diseases on crop yield (Jones et al., 2003), all of which persisted at the study site despite weed and insect management practices. Additionally, the field data used for simulation may have been affected by water, nutrients, or other stresses, which may have resulted in the differences between measured and simulated results (Jones et al., 2003; Hoogenboom et al., 2010).

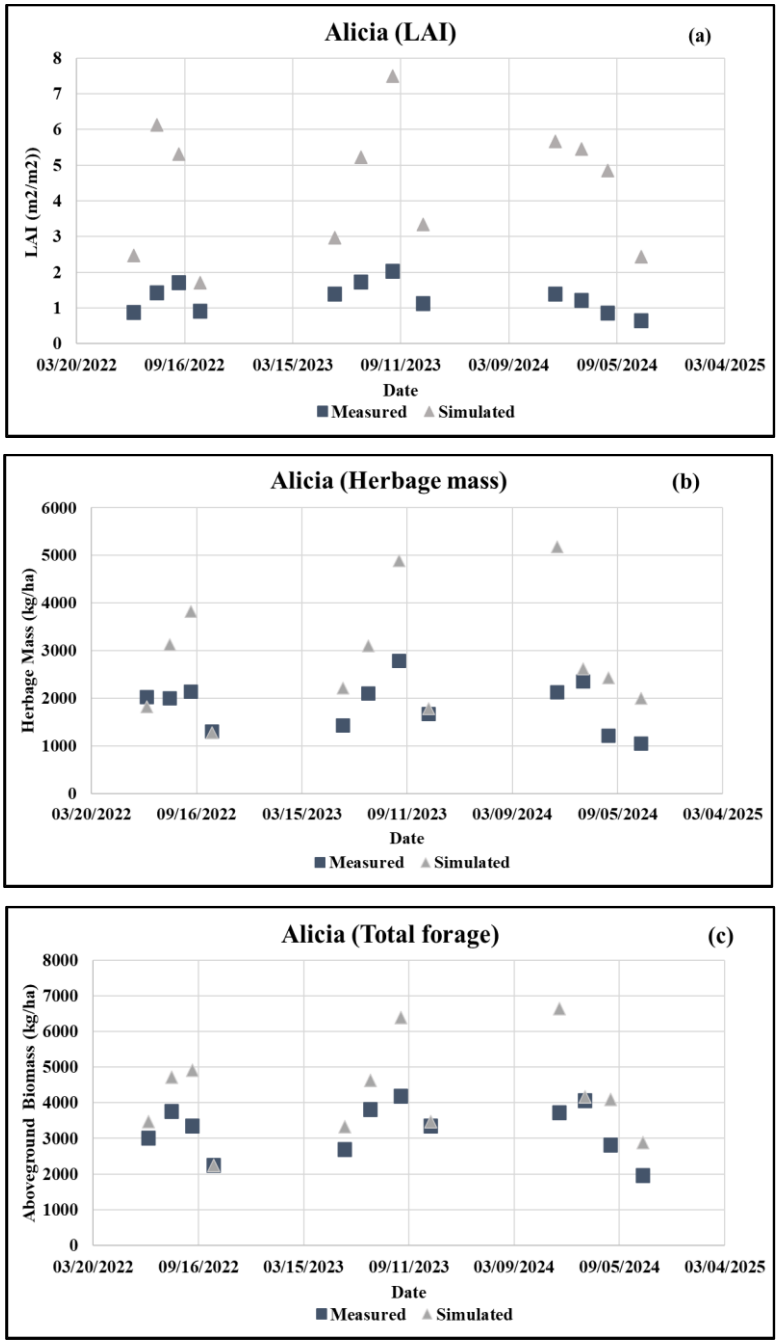

Figure 4.5 Measured and simulated (a) leaf area index (LAI) (m^2 m^{-2}), (b) herbage mass (kg ha^{-1}), and (c) total forage (kg ha^{-1}) of "Alicia" by applying the potential evapotranspiration using FAO-56 method (PET_{FAO}) method from 2022 to 2024.

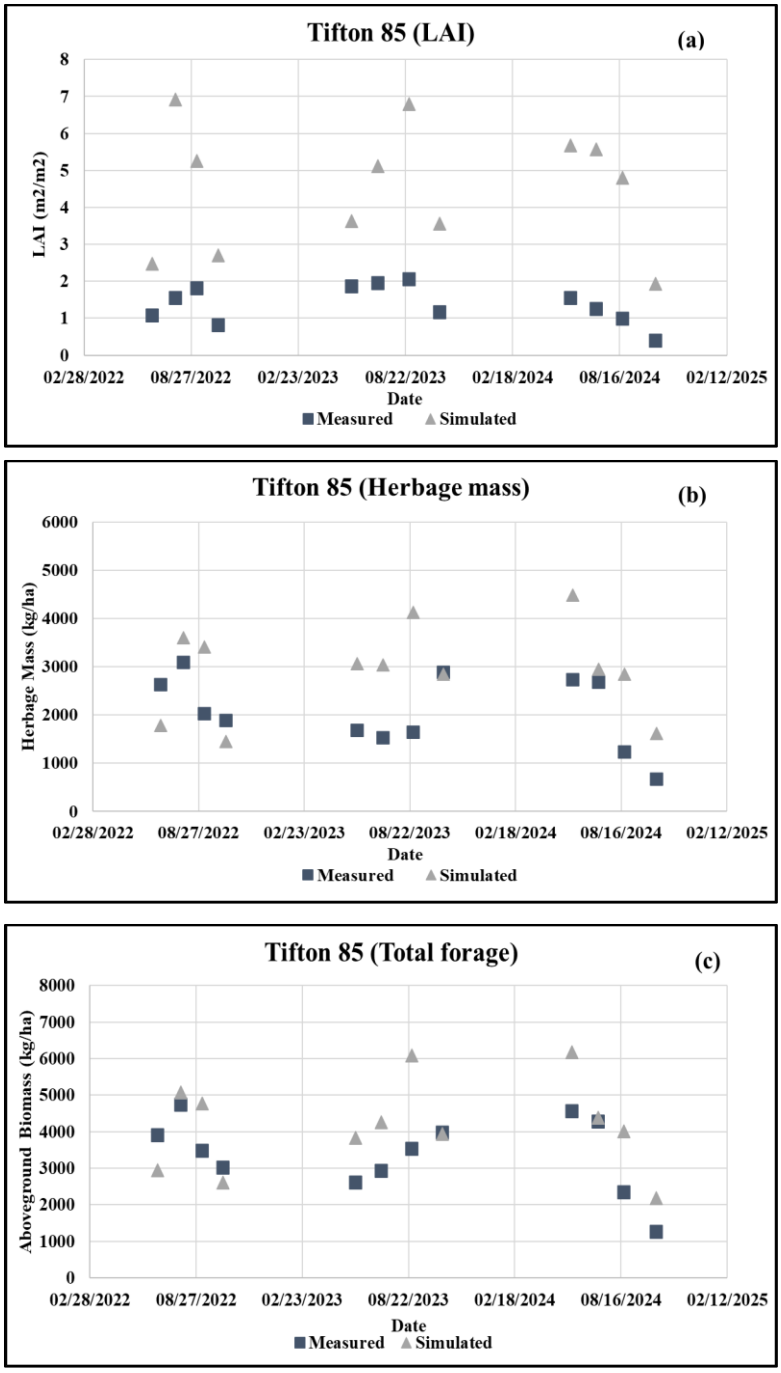

Figure 4.6 Measured and simulated (a) leaf area index (LAI) (m^2 m^{-2}), (b) herbage mass (kg ha^{-1}), and (c) total forage (kg ha^{-1}) of "Tifton 85" by applying the potential evapotranspiration using FAO-56 method (PET_{FAO}) from 2022 to 2024.

In general, studies that used data from their field trials to develop genetic coefficients for their unique conditions resulted in better performance metrics. For example, the Pequeno et al. (2017) study, from which the bermudagrass genetic coefficients and calibration values currently included in the CSM-CROPGRO-Perennial-Forage model were developed, resulted in a d-index=0.80 for simulated total forage when compared to measured values for "Tifton 85" bermudagrass. Similarly, a simulation of rainfed coastal bermudagrass by Woli et al. (2017) resulted in a d-index=0.99 for herbage mass. Simulation studies that applied the CSM-CROPGRO-Perennial-Forage model to other grass species using site-specific genetic coefficients also resulted in good performance metrics. For example, a study by Smith et al. (2023) resulted in d-index=0.85 for harvested herbage mass and a d-index=0.82 for total forage of bahiagrass from six different datasets undergoing different experiments, and Pedreira et al. (2011) resulted in a d-index=0.84 when simulating irrigated Bahiagrass. A simulation of irrigated alfalfa by Malik et al. (2018) resulted in herbage mass d-index=0.75 and LAI d-index=0.71.

Table 4.7 Annual total herbage mass and total forage of "Alicia" and "Tifton 85" during 2022-2024 growing seasons, both measured in the field and predicted by DSSAT-CSM under PET_{FAO} method.

Year	Annual total herbage mass (kg ha^{-1})		Annual total forage (kg ha^{-1})	
	Measured	Predicted	Measured	Predicted
		Alicia		
2022	7,463	10,658	12,348	15356
2023	7,987	11,958	14,045	17,810
2024	6,728	12,223	12,558	17,791
		Tifton 85		
2022	9,652	10,105	15,135	15,416
2023	7,758	13,073	13,036	18,122
2024	7,320	11,893	12,440	16,755

[1] Potential Evapotranspiration using FAO-56 method (PET_{FAO})

Forage bermudagrass K_C values and daily water use are not well documented in the literature, especially for rainfed production. A study conducted in southern Brazil found K_C ranged from 0.96 to 1.0 depending on the cutting frequency of "Tifton 85" bermudagrass under irrigated conditions (Paredes et al., 2018). Most of the existing literature on the daily water use of bermudagrasses focuses on turf. Measured K_C values for rainfed "Tifway" hybrid bermudagrass [*Cynodon dactylon* (L.) Pers. × *Cynodon transvaalensis* Burtt-Davy] ranged between 0.44 to 0.59 from May to October in a study conducted in Raleigh, NC. ET_O was calculated using the ASCE-EWRI Standardized reference evapotranspiration equation for grass canopies (Pinnix and Miller, 2019). Turfgrasses are mowed regularly and tend to have total forage than forage bermudagrasses. In contrast to rainfed conditions, K_C values of turf bermudagrass were higher under irrigated conditions, reflecting higher crop water use when soil water is available. During a three-year study in Florida, turf bermudagrass K_C varied from 0.17 in February to 0.99 in July (Wherley et al., 2015) under well-watered conditions. In another irrigated turfgrass study conducted in Tucson, AZ, the monthly fluctuation in bermudagrass K_C was correlated with the turf growth rate, ranging from 0.78 in June to 0.83 in September (Brown et al., 2001). There is even less published research on using crop simulation models like DSSAT-CSM to estimate daily crop water use in forages. The CSM-CROPGRO-Perennial-Forage model was applied to observe the crop ET of alfalfa response to CO_2 enrichment (Castaño-Sánchez et al., 2020).

Crop coefficient curves for bermudagrass

The simulated and empirically derived K_C curves for "Alicia" and "Tifton 85" for 2022-2024, as well as mean curves for that period, are shown in Figures 4.7 and 4.8, respectively. The simulated ($K_{C\text{-}DSSAT}$) curves resulted from applying Eq. 4.1 to the daily PET_{FAO} and $ET_{C\text{-}FAO}$ values estimated with DSSAT-CSM. Daily $K_{C\text{-}DSSAT}$ values were then used to calculate mean monthly

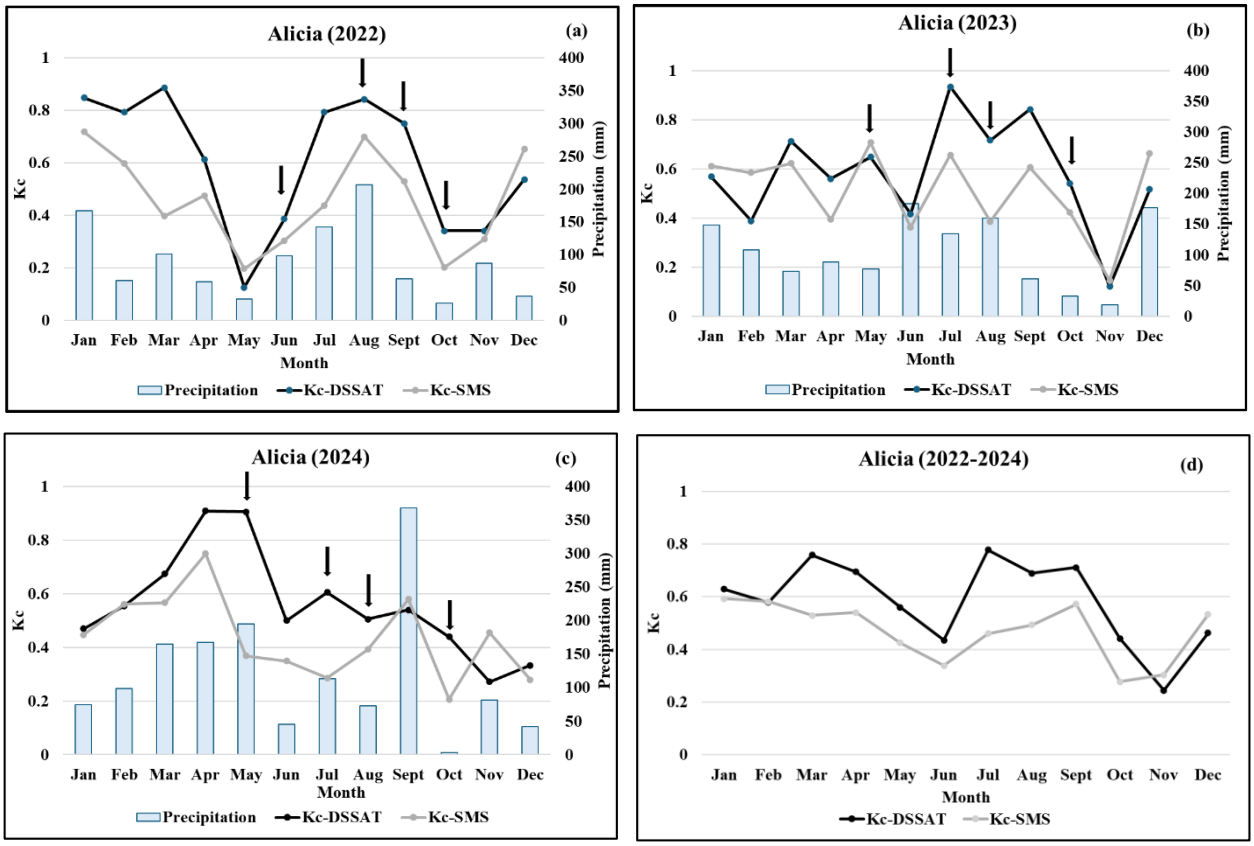

Figure 4.7 Crop coefficient (Kc) curves of "Alicia" developed based on monthly mean empirically derived crop coefficient ($K_{C\text{-}SMS}$) and simulated derived crop coefficient using FAO-56 ($K_{C\text{-}DSSAT}$) method during (a) 2022, (b) 2023, (c) 2024 and (d) mean of 2022-2024 growing seasons. The arrows indicate the harvesting date for each year. Total monthly precipitation is presented in blue bar.

$K_{C\text{-}DSSAT}$ values. Similarly, the empirically derived ($K_{C\text{-}SMS}$) curves resulted from applying Eq. 4.1 to the $ET_{C\text{-}SMS}$ values estimated with the ΔVWC method described earlier and the $ET_{O\text{-}FAO}$. Daily $K_{C\text{-}SMS}$ values were used to calculate mean monthly $K_{C\text{-}SMS}$ values.

In general, the annual $K_{C\text{-}DSSAT}$ and the $K_{C\text{-}SMS}$ curves have similar trends, but $K_{C\text{-}DSSAT}$ values were mostly higher than $K_{C\text{-}SMS}$ values. This was not surprising as daily $K_{C\text{-}DSSAT}$ values were approximately 27% higher than $K_{C\text{-}SMS}$ values over the 3-year period. The most significant differences were noted for "Alicia" in July and September of 2022, as well as in May and July of 2024, and for "Tifton 85" for several months of 2022. The lowest $K_{C\text{-}SMS}$ values were observed during the periods with significant differences in $K_{C\text{-}DSSAT}$ values.

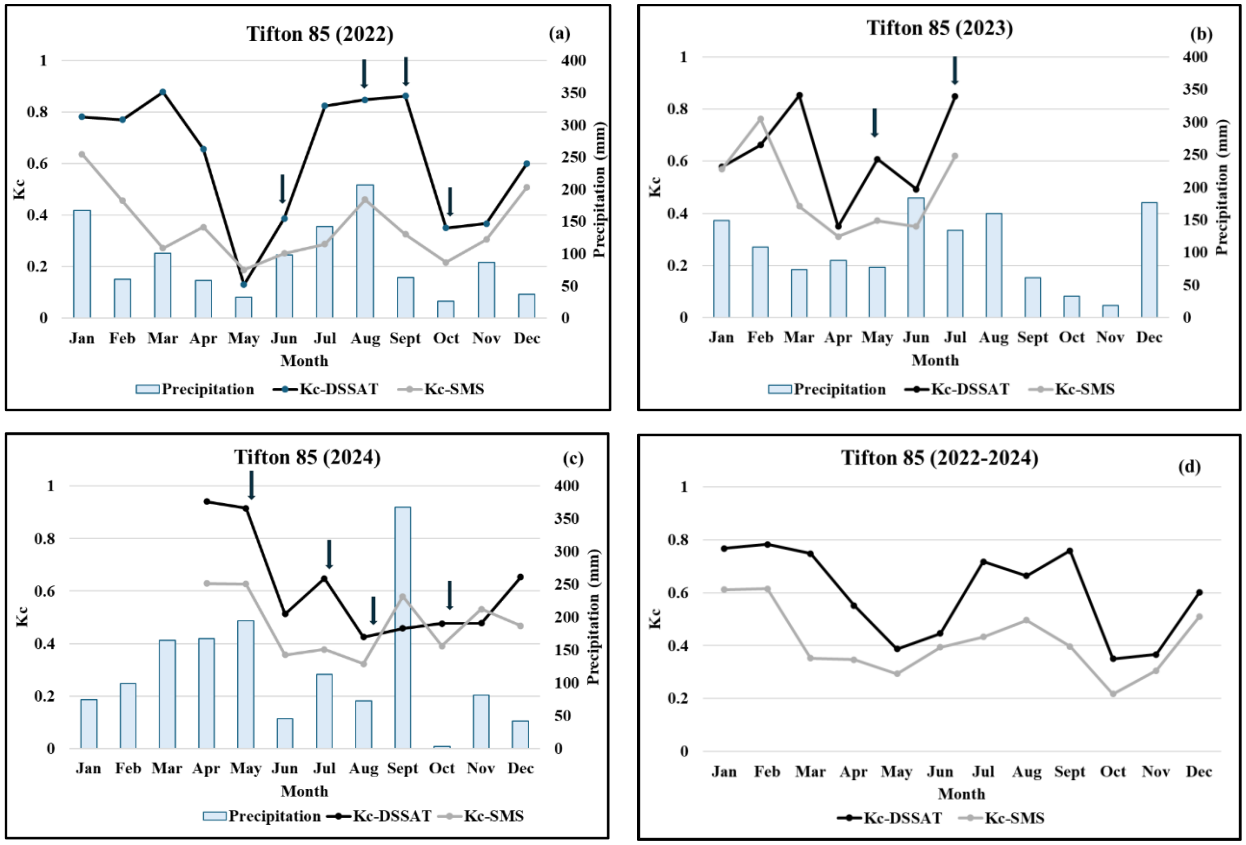

Figure 4.8 Crop coefficient (Kc) curves of "Tifton 85" developed based on monthly mean empirically derived crop coefficient ($K_{C\text{-}SMS}$) and simulated derived crop coefficient using FAO-56 ($K_{C\text{-}DSSAT}$) values during (a) 2022, (b) 2023, (c) 2024 and (d) mean of 2022-2024 growing seasons. The arrows indicate the harvesting date for each year. Total monthly precipitation is presented in blue bar.

It is interesting that both curves show relatively high K_C values in January of 2022 and 2023, when bermudagrass is typically dormant in southern Georgia. The air temperature at the end of 2021 and leading into 2022 and at the beginning of 2023 was unusually high for winter (Figures 4.4e and 4.4f). Mild winters in southern Georgia can keep bermudagrass active rather than completely dormant (Lee et al., 2017), with the associated crop water use. Higher precipitation was also observed in January of 2022 and 2023 compared to 2024 (Figure 4.7). The sharp decline in K_C values from March to May 2022 is likely associated with the much lower than normal precipitation during those months (Figure 4.7) and was captured for both cultivars and by both the empirically derived and simulated K_C values. A similar decline in K_C values was observed in the

late summer of 2024 when precipitation was unseasonably low (Figure 4.8c). The seasonal hay cuttings indicated by the black arrows in Figures 4.7 and 4.8 generally resulted in a decline in K_C values. The K_C curves developed using the K_C values for the entire 3-year period show good agreement between simulated and empirical K_C curves for "Alicia" (Figure 4.7d) and moderately good agreement for "Tifton 85" (Figure 4.8d).

To evaluate whether precipitation or other environmental factors such as solar radiation or air temperature were the primary drivers of these declines in K_C values, the precipitation, temperature, and solar radiation records for January (wet) and May 2022 (dry) were replaced with the corresponding records of January (dry) May 2024 (wet) and the 2022 year was simulated again separately for each record. In other words, the simulation was first run using the January and May 2024 precipitation records and the January and May 2022 solar radiation and temperature records. Then the January and May 2024 records were replaced with one of the other variables, while the other two used the 2022 records, etc., until all the combinations were evaluated. The results (Figure 4.9) indicate that precipitation was the primary driver of Kc trends during the growing season. The originally high K_C value of January 2022 and low K_C value of May 2022 were changed to a lower January K_C value and a higher May K_C value with the 2024 precipitation records but were not greatly affected by the 2024 solar radiation and temperature records.

The monthly variation in the K_C curves shown in Figures 4.7 and 4.8 is characteristic of the location and management practices applied to the two plots used in this study, and consequently, the curves cannot be considered generic K_C curves for use across a region. To develop a generic curve that can be applied regionally for bermudagrass cultivars, all the daily K_C values for the 3-year period from both cultivars were plotted on one graph, and a polynomial curve fit to the data. This approach was implemented in a study that developed a K_C curve for irrigated

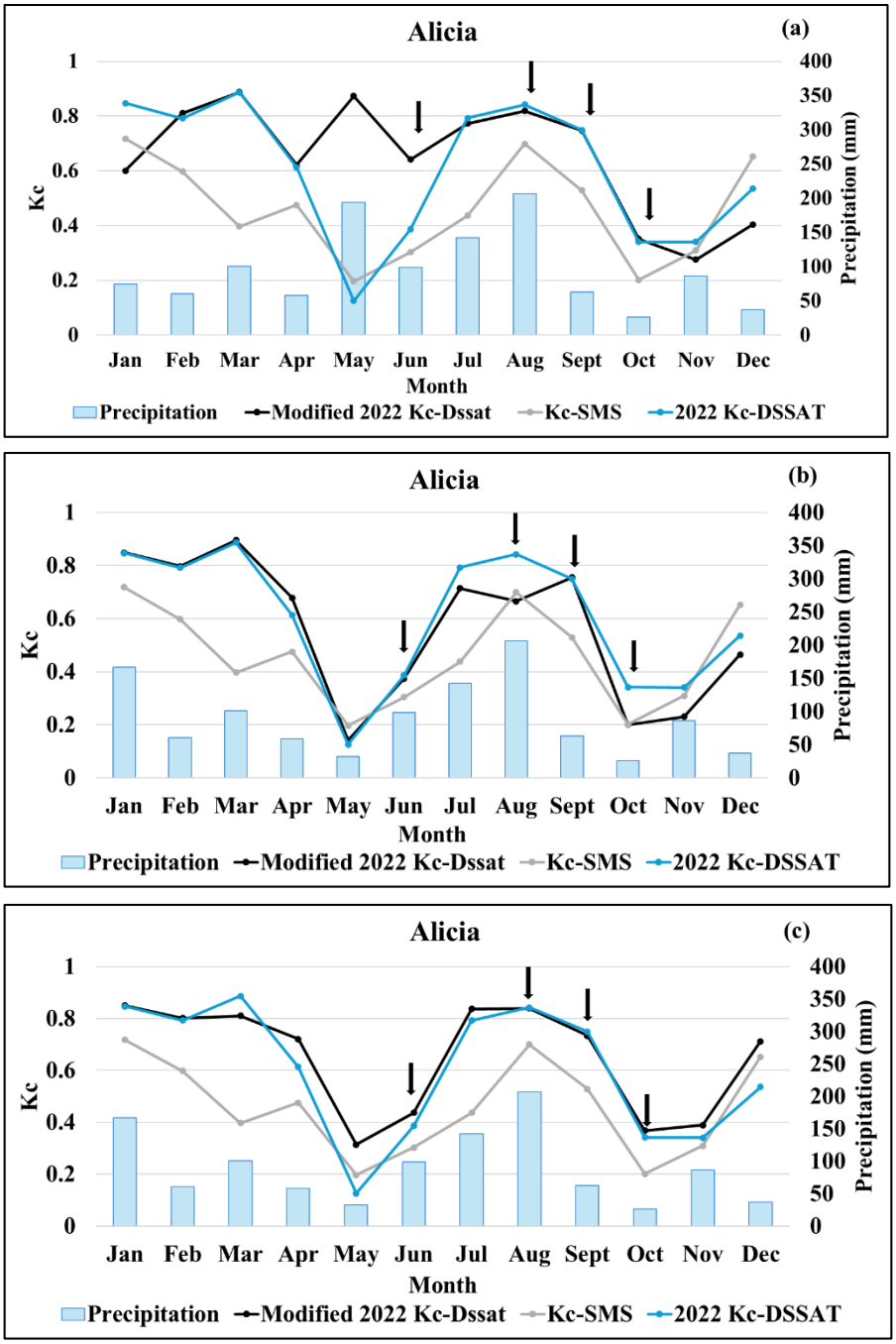

Figure 4.9 Crop coefficient (Kc) curves of "Alicia" of the 2022 growing season were modified by applying the environmental modification tool in DSSAT-CSM by replacing with daily precipitation (a), daily solar radiation (b), and daily maximum and minimum temperature (c) for January and May 2024. Modified Kc curves (black line) were compared to the DSSAT-derived ($K_{C\text{-}DSSAT}$) (blue line) and empirically derived ($K_{C\text{-}SMS}$) (grey line) curves. The arrows indicate the harvesting date for each year. Total monthly precipitation is presented in the blue bar.

sweet corn (Bedwell, 2025). The sweet corn K_C curve was used for irrigation scheduling and performed well when compared to other science-based scheduling methods. In addition, all K_C values below 0.2, as well as all K_C values below 0.4 during the growing season (March-October), were considered outliers caused by unusual, location-specific meteorological and management conditions and eliminated. DSSAT-CSM truncates maximum K_C values at 1. For comparison purposes, K_C values >1 were also truncated when developing the generic K_C curve for the empirically derived $K_{C\text{-}SMS}$ values.

Figure 4.10a presents the resulting graphs and curves for the empirically derived curve, and Figure 4.10b those for the DSSAT-derived curve, showing the general seasonal pattern over the year. The difference in the trends of the two polynomial curves is striking, with the empirically derived curve being relatively flat across the entire growing season and with maximum $K_{C\text{-}SMS}$ values of 0.65. This curve is representative of the actual growing conditions of the two plots used in this study. In contrast to the empirically derived curve, the $K_{C\text{-}DSSAT}$ curve (Figure 4.10b) resulted in a classic K_C curve for a perennial crop with lower crop water use during the winter months and peak water use during the summer growing season. The maximum $K_{C\text{-}DSSAT}$ value peaked at 0.9 during June and July, the peak growing season for bermudagrass in this region. The lowest $K_{C\text{-}DSSAT}$ values occurred in January ($K_{C\text{-}DSSAT}$ =0.5) and December ($K_{C\text{-}DSSAT}$ =0.4), the two months with the lowest solar radiation (Figures 4.4b- 4.4d) and generally low temperatures (Figures 4.4e- 4.4g). Theoretically, a $K_{C\text{-}DSSAT}$ on 31 December should be the same as a $K_{C\text{-}DSSAT}$ value on 01 January, but the simulation results were affected by the meteorological conditions of the three years used in the simulation. It is likely that the initial and final annual $K_{C\text{-}DSSAT}$ values would converge with longer simulation periods. In this study, harvest data were available for three years, which limited the simulation period.

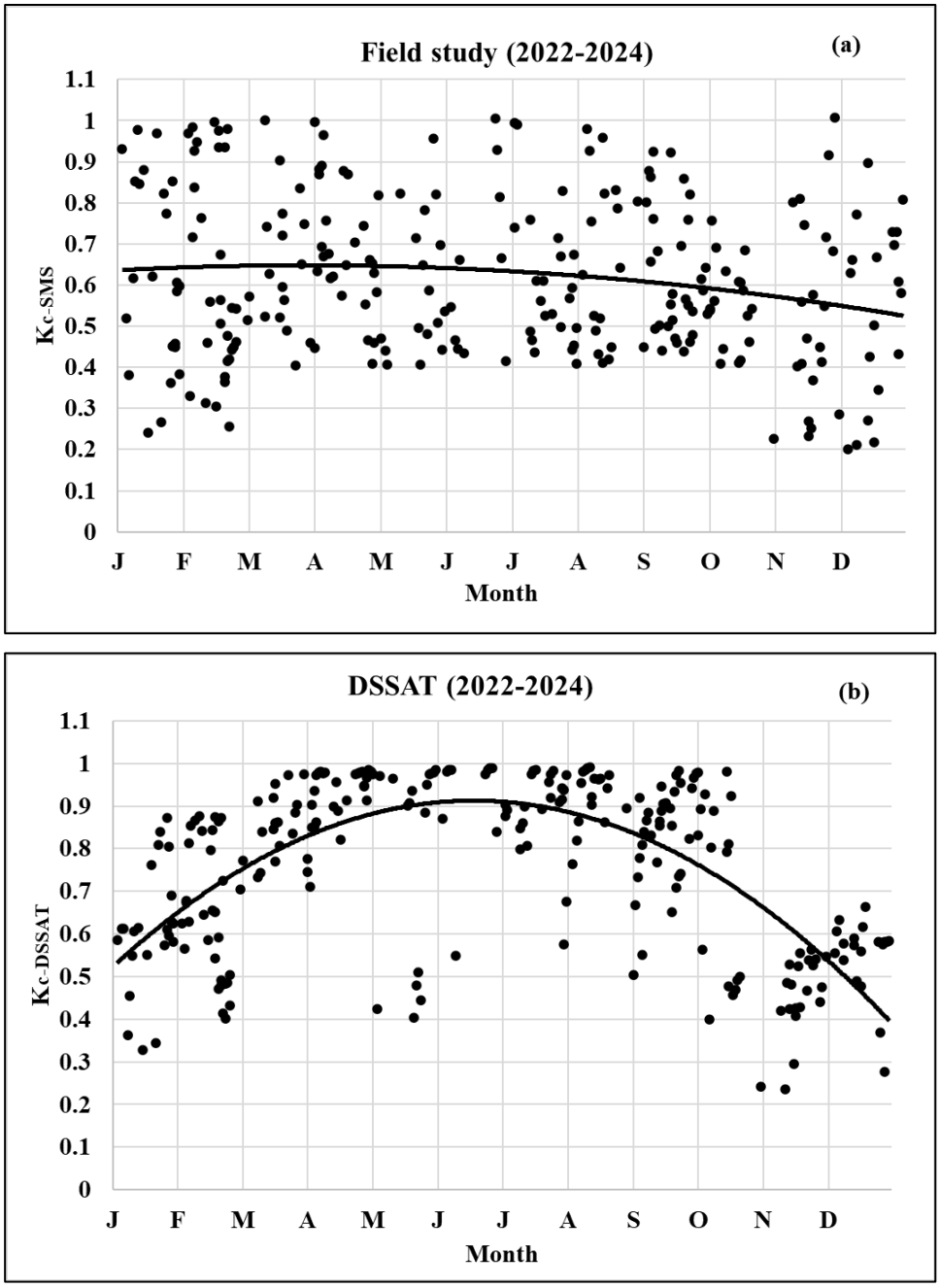

Figure 4.10 Polynomial curves developed using the daily mean of (a) empirically derived crop coefficient ($K_{C\text{-}SMS}$) and (b) simulated derived crop coefficient values using FAO-56 method ($K_{C\text{-}DSSAT}$) of "Alicia" and "Tifton 85" from 2022 to 2024.

Conclusions

The empirically derived K_C curves for rainfed bermudagrass reflected growing conditions during the three years for which data were collected. The primary factor affecting daily and monthly K_C values was precipitation, and to a lesser extent, the management of the two plots includes fertilization, pest and disease management, and hay cuttings. Fitting a polynomial to the daily $K_{C\text{-}SMS}$ values from all three years resulted in a smooth $K_{C\text{-}SMS}$ curve that likely underrepresents K_C values of rainfed bermudagrass in southern Georgia because of the conditions under which these data were collected.

Understanding the limitations of the empirically derived data, the CSM-CROPGRO-Perennial-Forage model was used to simulate the daily crop water use of rainfed bermudagrass. The 12 data points available per cultivar for model calibration (3 years × 4 harvests per year) were not sufficient to develop genetic coefficients and calibrate the model. Instead, the calibration for "Tifton 85" bermudagrass already available in the model was used. Although performance metrics were lower than those published in other uses of the model, the trends of the simulated variables matched those of the observed variables, including K_C. To develop a generic curve that can be applied regionally for bermudagrass cultivars, all the simulated daily $K_{C\text{-}DSSAT}$ values for the 3-year period that was simulated were plotted on one graph, and a polynomial curve was fit to the data. This resulted in a classic K_C curve for a perennial crop with lower crop water use during the winter months and water use approaching reference ET during the peak of the summer growing season. This DSSAT-derived $K_{C\text{-}DSSAT}$ curve can be integrated into SI CropFit as it represents the expected crop water use patterns of optimally managed rainfed forage bermudagrass in southern Georgia.

CHAPTER 5

CONCLUSIONS

Rainfed maize experienced flash drought at root zone soil water deficit (RZSWD) ≥60% on average at least once every growing season in Georgia, and at least 50% of the maize flash drought events occurred during the crop's reproductive phase. In Florida, this figure was as low as 12%. The reproductive phase accounted for 50% of cotton flash drought events in Florida and 75% in Georgia, even though the total number of cotton flash drought events in both states was smaller than for maize. One explanation for this is that September and October, when cotton is still in its reproductive phase, normally receive comparatively less precipitation than earlier in the growing season. So, when there are longer periods between precipitation events, flash drought occurs more rapidly.

Flash drought events of 15 days or longer that occur during the reproductive phase can result in significant yield reductions to rainfed crops. DSSAT-CSM modeling showed maize yield reductions exceeding 40% for Coastal Plain virtual fields in Georgia and exceeding 50% in Coastal Plain virtual fields in Florida for a flash drought event occurring during the first half of June. These reductions are a function of sandy soils with low water holding capacity and high air temperatures, typically associated with summer flash drought events. The impact of flash drought on cotton was not as severe, with maximum yield reductions of approximately 25% for events occurring from mid-July to mid-August.

For SI CropFit to be used to quantify flash drought for forage grass as was done for cotton and maize, it requires a forage grass model with a region-specific crop coefficient (K_C) curve. To

fulfill the objective, the empirically derived crop coefficient ($K_{C\text{-}SMS}$) curves for rainfed bermudagrass were developed, reflecting growing conditions during the three years for which data were collected. The primary factor affecting daily and monthly $K_{C\text{-}SMS}$ values was precipitation, and to a lesser extent, the management of the two fields includes fertilization, pest and disease management, and hay cuttings. Fitting a polynomial to the daily $K_{C\text{-}SMS}$ values from all three years resulted in a smooth $K_{C\text{-}SMS}$ curve that likely underrepresents K_C values of rainfed bermudagrass in southern Georgia because of the conditions under which these data were collected. To develop a generic curve that can be applied regionally for bermudagrass cultivars, all the simulated daily $K_{C\text{-}DSSAT}$ values for the 3-year period that was simulated were plotted on one graph, and a polynomial curve was fit to the data. This resulted in a classic K_C curve for a perennial crop with lower crop water use during the winter months and water use approaching reference ET during the peak of the summer growing season. This DSSAT-derived $K_{C\text{-}DSSAT}$ curve can be integrated into SI CropFit as it represents the expected crop water use patterns of optimally managed rainfed forage bermudagrass in southern Georgia.

The study presented on this dissertation is one of the first studies to quantify the frequency of flash drought and its effects on yield across different physiographic regions of the southeastern U.S. Overall, agencies that are responsible for administering state and federal disaster assistance programs for growers can use SI CropFit to quantify the occurrence of flash drought and, coupled with crop simulation models, can estimate the impact of the flash drought events on yield. Furthermore, policymakers and other stakeholders can more effectively allocate resources for drought mitigation and increase the regional resilience of agricultural systems by using spatial mapping of flash drought frequency.

REFERENCES

Abayechaw, D. (2021). Review on Decision Support System for Agrotechnology Transfer (DSSAT) Model. *International Journal of Intelligent Information Systems*, *10*(6), 117-124. https://doi.org/10.11648/j.ijiis.20211006.13

Adhikari, P., Ale, S., Bordovsky, J. P., Thorp, K. R., Modala, N. R., Rajan, N., & Barnes, E. M. (2016). Simulating future climate change impacts on seed cotton yield in the Texas High Plains using the CSM-CROPGRO-Cotton model. *Agricultural Water Management*, *164*, 317–330. https://doi.org/10.1016/j.agwat.2015.10.011

Alderman, P. D. (2011). Adapting the CROPGRO perennial forage model to predict growth of Brachiaria brizantha. *Field Crops Research*, *120*, 370–379.

Allen, R. G., Pereira, L. S., Raes, D., & Smith, M. (1998). Crop evapotranspiration –Guidelines for computing crop water requirements. *FAO Irrigation and Drainage Paper*, *56*. Rome, Italy: Food and Agriculture Organization of the United Nations. ISBN 92-5-104219-5

Allen, R. G., Pereira, L. S., Smith, M., Raes, D., & Wright, J. L. (2005). FAO-56 dual crop coefficient method for estimating evaporation from soil and application extensions. *J. Irrigation and Drainage Engineering*, *131*(1), 2–13.

Allen, R. G., Walter, I. A., Elliott, R. L., Howell, T. A., Itenfisu, D., Jensen, M. E., & Snyder, R. L. (Eds.). (2005). The ASCE Standardized Reference Evapotranspiration Equation. *Am. Soc. Civil Eng*, 59. *Am. Soc. Civil Eng*, *59*.

Amiri, E., Irmak, S., & Araji, H. A. (2022). Assessment of CERES-Maize model in simulating maize growth, yield, and soil water content under rainfed, limited, and full irrigation. *Agricultural Water Management*, *259*, 107271, https://doi.org/10.1016/j.agwat.2021.107271.

Araya, A., Kisekka, I., Prasanna, H., & Gowda, P. V. (2017). Evaluation of water-limited cropping systems in a semi-arid climate using DSSAT-CSM. *Agricultural Systems*, *150*, 86-98. https://doi.org/10.1016/j.agsy.2016.10.007.

ASCE.-EWRI. (2005). The ASCE Standardized Reference Evapotranspiration Equation. *Environment and Water Resources Institute (EWRI) of ASCE, Standardization of Reference Evapotranspiration Task Committee Final Rep*. http://www. kimberly.uidaho.edu/water/asceewri/ascestzdetmain2005.pdf

Aslam, M., Maqbool, M. A., & Cengiz, R. (2015). Effects of Drought on Maize. In *Drought Stress in Maize (Zea mays L.): Effects, Resistance Mechanisms, Global Achievements and Biological Strategies for Improvement* (pp. 5–17). Springer International Publishing. https://doi.org/10.1007/978-3-319-25442-5_2

Ayankojo, I. T., Morgan, K. T., & Ozores-Hampton, M. (2018). Effects of real-time location-specific drip irrigation scheduling on water use, plant growth, nutrient accumulation, and

yield of Florida fresh-market tomato. *HortScience*, *53*, 1372–1378. https://doi.org/10.21273/HORTSCI13183-18

Basara, J., & Christian, J. (2023). Farming and the Risk of Flash Droughts. *American Scientist*, *111*, 238. https://doi.org/10.1511/2023.111.4.238

Baxter, L. L., Anderson, W. F., Gates, R. N., Rios, E. F., & Hancock, D. W. (2022). Moving warm-season forage bermudagrass (Cynodon spp.) into temperate regions of North America. *Grass and Forage Science*, *77*(2), 141–150. https://doi.org/10.1111/gfs.12568

Baxter, L. L., Anderson, W. F., Gates, R. N., Rios, E. F., & Burt, J. C. (2024). Challenges in bermudagrass production in the southeastern USA. *Grassland Research*, *3*(2), 123-131.

Bedwell, E. (2025). *Developing a data-driven decision support tool to enhance irrigation water use efficiency and fresh market quality of sweet corn in the southeastern United States*. Doctoral dissertation, University of Georgia.

Bijalwan, P., Sharma, M., & Kaushik, P. (2022). *Review of the Effects of Drought Stress on Plants: A Systematic Approach*. https://doi.org/10.20944/preprints202202.0014.v1

Borges, B.M.M.N., Silveira, M.L., Cardoso, S.S., Moline, E.F.V., Coutinho Neto, A.M., Lucas, F.T., Muraoka, T., and Coutinho, E.L.M. (2017). Growth, Herbage Accumulation, and Nutritive Value of 'Tifton 85' Bermudagrass as Affected by Nitrogen Fertilization Strategies. *Crop Science*, *57*, 3333–3342. https://doi.org/10.2135/cropsci2016.10.0890

Bozorov, T. A., Usmanov, R. M., Yang, H., Hamdullaev, S. A., Musayev, S., Shavkiev, J., Nabiev, S., Zhang, D., & Abdullaev, A. A. (2018). Effect of water deficiency on relationships between metabolism, physiology, biomass, and yield of upland cotton (Gossypium hirsutum L. *J. Arid Land*, *10*, 441–456. https://doi.org/10.1007/s40333-018-0009-y

Brown, P. W., Mancino, C. F., Young, M. H., Thompson, T. L., Wierenga, P. J., & Kopec, D. M. (2001). Penman Monteith Crop Coefficients for Use with Desert Turf Systems. *Crop Sci*, *41*, 1197–1206. https://doi.org/10.2135/cropsci2001.4141197x

Castaño-Sánchez, J. P., Rotz, C. A., Karsten, H. D., & Kemanian, A. R. (2020). Elevated atmospheric carbon dioxide effects on maize and alfalfa in the Northeast US: A comparison of model predictions and observed data. *Agricultural and Forest Meteorology*, *291*, 108093.

Chen, L. G., Hartman, A., Pugh, B., Gottschalck, J., & D, M. (2020). Real-time prediction of areas susceptible to flash drought development. *Atmosphere (Basel*, *11*, 10 3390 11101114.

Chisanga, C. B., Phiri, E., & Chinene, V. R. N. (2021). Evaluating APSIM and DSSAT-CERES-Maize Models under Rainfed Conditions Using Zambian Rainfed Maize Cultivars. *Nitrogen*, *2*, 392–414. https://doi.org/10.3390/nitrogen2040027

Christian, J. I., Basara, J. B., Otkin, J. A., & Hunt, E. D. (2019). Regional characteristics of flash droughts across the United States. *Environ. Res. Commun*, *1*, 12.

Crookston, M. A. (2016). Seasonal Kc Curves for Turfgrass Using FAO-56 Dual Crop Coefficient Method. *2016 ASABE International Meeting*. https://doi.org/10.13031/aim.20162461635.

Daniel, J. L. P., Queiroz, O. C. M., Arriola, K. G., Staples, C. R., Romero, J. J., Shin, J. H., & Adesogan, A. T. (2016). Effects of maturity at ensiling of bermudagrass and fibrolytic enzyme application on the performance of early-lactation dairy cows. *Journal of Dairy Science*, *99*(12), 9716–9723.

Deepa, R., & Vijayan, L. (2025). Flash Droughts in the Southern United States: A Driver-Impact-Response (DRI) Framework. *Water*, *17*(5), 615. https://doi.org/10.3390/w17050615

DeJonge, K. C., & Thorp, K. R. (2017). Implementing standardized reference evapotranspiration and dual crop coefficient approach in the DSSAT cropping system model. *Transactions of the ASABE*, *60*(6), 1965–1981.

DeJonge, K. C., Thorp, K. R., & Marek, G. W. (2020). The apples and oranges of reference and potential evapotranspiration: Implications for agroecosystem models. *Agric Environ Lett*, *5*, 20011. https://doi.org/10.1002/ael2.20011

Edris, S. G., Basara, J. B., Christian, J. I., Hunt, E. D., Otkin, J. A., Salesky, S. T., & Illston, B. G. (2023). Analysis of the critical components of flash drought using the standardized evaporative stress ratio. *Agricultural and Forest Meteorology*, *330*, 109288. https://doi.org/10.1016/j.agrformet.2022.109288.

Elliott, J., Glotter, M., Ruane, A. C., Boote, K. J., Hatfield, J. L., Jones, J. W., Rosenzweig, C., Smith, L. A., & Foster, I. (2018). Characterizing agricultural impacts of recent large-scale US droughts and changing technology and management. *Agricultural Systems*, *159*, 275–281. https://doi.org/10.1016/j.agsy.2017.07.012.

Farhangfar, S., Bannayan, M., Khazaei, H. R., & Baygi, M. M. (2015). Vulnerability assessment of wheat and maize production affected by drought and climate change. *International Journal of Disaster Risk Reduction*, *13*, 37-51. https://doi.org/10.1016/j.ijdrr.2015.03.006.

FAWN. (2025). *Florida Automated Weather Network*. https://fawn.ifas.ufl.edu/

Fodor, N., Challinor, A., Droutsas, I., Ramirez-Villegas, J., Zabel, F., Koehler, A.-K., & Foyer, C. H. (2017). Integrating Plant Science and Crop Modeling: Assessment of the Impact of Climate Change on Soybean and Maize Production. *Plant and Cell Physiology*, *58*(11), 1833–1847. https://doi.org/10.1093/pcp/pcx141

Ford, T. W., Otkin, J. A., Quiring, S. M., Lisonbee, J., Woloszyn, M., Wang, J., & Zhong, Y. (2023). Flash Drought Indicator Intercomparison in the United States. *J. Appl. Meteor. Climatol*, *62*, 1713–1730. https://doi.org/10.1175/JAMC-D-23-0081.1.

Fortin, J. (2019). Flash Drought in the South Brings Record Heat Without Rain. *The New York Times*. https://www.nytimes.com/2019/10/04/us/flash-drought-monitor.html

Gallios, I. (2023). *Decision Support Tools For Irrigation Scheduling In Peanut [University of Georgia*. https://esploro.libs.uga.edu/esploro/outputs/graduate/DECISION-SUPPORT-TOOLS-FOR-IRRIGATION-SCHEDULING/9949575227602959#file-0

Gao, M., Snider, J. L., Bai, H., Hu, W., Wang, R., Meng, Y., Wang, Y., Chen, B., & Zhou, Z. (2020). Drought effects on cotton (*Gossypium hirsutum L.*) fiber quality and fiber sucrose metabolism during the flowering and boll-formation period. *Journal of Agronomy and Crop Science*, *206*, 309–321.

Garcia, A. G. Y., Persson, T., Paz, J. O., Fraisse, C., & Hoogenboom, G. (2010). ENSO-based climate variability affects water use efficiency of rainfed cotton grown in the southeastern USA. *Agriculture, Ecosystems & Environment*, *139*, 629–635. https://doi.org/10.1016/j.agee.2010.10.009.

Geng, S. M., Yan, D. H., Zhang, Z. B., L., W. Z., & A, G. (2017). Performance assessment and application of the DSSAT-CERES-Maize model for simulating maize yield under water stress conditions. *IOP Conf. Ser.: Earth Environ. Sci*, *82*, 012030. https://doi.org/10.1088/1755-1315/82/1/012030

Ghiat, I., Mackey, H. R., & Al-Ansari, T. (2021). A Review of Evapotranspiration Measurement Models, Techniques and Methods for Open and Closed Agricultural Field Applications. *Water*, *13*(18), 2523. https://doi.org/10.3390/w13182523

Gibbons, K., Gooch, M., Mills, C., & Deppert, Q. (2023). *Southeast U.S. Agriculture Evaluating the Spatial and Temporal Distribution of Flash Droughts within Agricultural Areas and Regional Crop Calendars in the Southeast using Earth Observations*. NASA DEVELOP National Program. https://ntrs.nasa.gov/api/citations/20230006899/downloads/2023Spring_MSFC_SoutheastUSAg_TechPaper_FDv3-final.pdf

Goche, T., Shargie, N. G., Cummins, I., Brown, A. P., Chivasa, S., & Ngara, R. (2020). Comparative physiological and root proteome analyses of two sorghum varieties responding to water limitation. *Scientific Reports*, *10*, 1–18. https://doi.org/10.1038/s41598-020-68735-3.

Godwin, D. C., & Singh, U. (1998). Nitrogen balance and crop response to nitrogen in upland and lowland cropping systems. In G. Y. Tsuji, G. Hoogenboom, & P. K. Thornton (Eds.), *Understanding Options for Agricultural Production. System Approaches for Sustainable Agricultural Development* (pp. 55–77). Springer. https://doi.org/10.1007/978-94-017-3624-4_4

Gopinath, L., Moss, J. Q., Wu, Y., & Schwartz, B. M. (2022). Drought response of 10 bermudagrass genotypes under field and controlled environment conditions. *Agrosystems, Geosciences & Environment*, *5*, 20300. https://doi.org/10.1002/agg2.20300

Haigh, T. R., Otkin, J. A., Mucia, A., Hayes, M., & Burbach, M. E. (2019). Drought early warning and the timing of range manager's drought response. *Adv. Meteor*, 1-14,. https://doi.org/10.1155/2019/9461513

Hailegnaw, N. S., Bayabil, H. K., Berihun, M. L., Teshome, F. T., Shelia, V., & Getachew, F. (2024). Integrating machine learning and empirical evapotranspiration modeling with

DSSAT: implications for agricultural water management. *Sci. Total Environ*, *912*(169403). https://doi.org/10.1016/j.scitotenv.2023.169403

Hancock, D. W., Edwards, N. R., Green, W., & Rehberg, D. M. (2013). *Selecting a Forage Bermudagrass Variety*. University of Georgia extension.

Hand, C., Culpepper, S., Harris, G., Kemerait, B., Liu, Hall, D., Lyons, D., Mallard, J., Edwards, P., Y., Perry, C., Porter, W., Roberts, P., Smith, A., Virk, S., Bag, S., Sintim, H. & Singleton, T. (2024). *University of Georgia cotton production Guide*. University of Georgia.

Hejnák, V., Tatar, Ö., Atasoy, G. D., Martinková, J., Çelen, A. E., Hnilička, F., & Skalický, M. (2015). Growth and photosynthesis of Upland and Pima cotton: Response to drought and heat stress. *CAAS Agricultural Journals*, *61*, 507–514. https://doi.org/10.17221/512/2015-PSE.

Hemati, A., Moghiseh, E., Amirifar, A., Mofidi-Chelan, M., & Asgari Lajayer, B. (2022). Physiological Effects of Drought Stress in Plants. *Plant Stress Mitigators*, 113–124. https://doi.org/10.1007/978-981-16-7759-5_6

Hendricks, T. J., Tucker, J. J., & Hancock, D. W. (2020). Forage accumulation and nutritive value of bermudagrass and alfalfa–bermudagrass mixtures when harvested for baleage. *Crop Science*, *60*, 2792–2801. https://doi.org/10.1002/csc2.20222

Himanshu, S. K., Ale, S., & Bordovsky, J. P. (2021). Assessing the impacts of irrigation termination periods on cotton productivity under strategic deficit irrigation regimes. *Sci Rep*, *11*, 20102. https://doi.org/10.1038/s41598-021-99472-w

Himanshu, S. K., Ale, S., Bell, J., Fan, Y., Samanta, S., Bordovsky, J. P., Gitz III, D. C., Lascano, R. J. & Brauer, D. K. (2023). Evaluation of growth-phase-based variable deficit irrigation strategies for cotton production in the Texas High Plains. *Agricultural Water Management*, *280*, 0378-3774. https://doi.org/10.1016/j.agwat.2023.108222.

Hobbins, M. T., Wood, A., McEvoy, D. J., Huntington, J. L., Morton, C., Anderson, M., & Hain, C. (2016). The Evaporative Demand Drought Index. Part I: Linking Drought Evolution to Variations in Evaporative Demand. *Journal of Hydrometeorology*, *17*(6), 1745–1761. https://doi.org/10.1175/JHM-D-15-0121.1

Hoogenboom, G., Jones, J. W., Wilkens, P. W., Porter, C. H., Boote, K. J., Hunt, L. A., & Koo, J. (2010). Decision support system for agrotechnology transfer (DSSAT. *Version*, *4*(5).

Hoogenboom, G., Porter, C. H., Boote, K. J., Shelia, V., Wilkens, P. W., Singh, U., White, J. W., Asseng, S., Lizaso, J. I., Moreno, L. P., Pavan, W., Ogoshi, R., Hunt, L. A., Tsuji, G. Y., & Jones, J. W. (2019). The DSSAT crop modeling ecosystem. In K. J. Boote (Ed.), *Advances in Crop Modeling for a Sustainable Agriculture* (pp. 173–216). https://doi.org/10.19103/AS.2019.0061.10.

Hoogenboom, G., Porter, C. H., Shelia, V., Boote, K. J., Singh, U., White, J. W., Pavan, W., Oliveira, F. A. A., Moreno-Cadena, L. P., Lizaso, J. I., Asseng, S., Pequeno, D. N. L., Kimball, B. A., Alderman, P. D., Thorp, K. R., Jones, M. R., Cuadra, S. V., Vianna, M. S., Villalobos, F. J., Ferreira, T.B., Batchelor, W.D., Koo, J., Hunt, L.A. & Jones, J.W.

(2023). *Decision Support System for Agrotechnology Transfer (DSSAT) Version 4.8.2 (DSSAT.net).* DSSAT Foundation, Gainesville, Florida, USA. https://dssat.net/

Hoogenboom, G., Porter, C.H., Shelia, V., Boote, K. J., Singh, U., Pavan, W., Oliveira, F.A.A., Moreno-Cadena, L.P., Ferreira, T.B., White, J.W., Lizaso, J.I., Pequeno, D.N.L., Kimball, B.A., Alderman, P.D., Thorp, K.R., Cuadra, S.V., Vianna, M.S., Villalobos, F.J., Batchelor, W.D., Asseng, S., Jones, M.R., Hopf, A., Dias, H.B., Jintrawet, A., Jaikla, R., Memic, E., Hunt, L.A. and Jones, J.W. (2024). *Decision Support System for Agrotechnology Transfer (DSSAT) Version 4.8.5 (www.DSSAT.net).* DSSAT Foundation, Gainesville, Florida, USA. https://dssat.net/

Huang, C., Zhang, Y. & Liu, G. (2011) Nutrition value evaluation of *Cynodon dactylon* germplasm resource. *Chin. J. Trop. Crops, 32*, 1418–1425.

Huang, B., DaCosta, M., & Jiang, Y. (2014). Research advances in mechanisms of turfgrass tolerance to abiotic stress: From physiology to molecular biology. *CRC Crit. Rev. Plant Sci*, *33*, 141–189.

Husmoen, D., Vietor, D. M., Rouquette, F. M., & Cothren, J. T. (2012). Variation of responses to water stress between 'Tifton 85' and 'Tifway' or 'Coastal' bermudagrass. Crop Science, 52(5), 2153–2160. https://doi.org/10.2135/cropsci2012.01.0019

Ingrao, C., Strippoli, R., Lagioia, G., & Huisingh, D. (2023). Water scarcity in agriculture: An overview of causes, impacts and approaches for reducing the risks. *Heliyon*, *9*(8), 2405–8440. https://doi.org/10.1016/j.heliyon.2023.e18507.

Iqbal, M., Ul-Allah, S., Naeem, M., Ijaz, M., Sattar, A., & Sher, A. (2017). Response of cotton genotypes to water and heat stress: From field to genes. *Euphytica*, *213*, 131.

Jensen, M. E. (1968). Water consumption by agricultural plants. In Kozlowski, T.T. (Ed.), *Water Deficits and Plant Growth, Vol. II* (pp. 1–22). Academic Press, Inc., New York, NY.

Jespersen, D., Leclerc, M., Zhang, G., & Raymer, P. (2019). Drought Performance and Physiological Responses of Bermudagrass and Seashore Paspalum. *Crop Science*, *59*, 778–786. https://doi.org/10.2135/cropsci2018.07.0434

Jin, C., Luo, X., Xiao, X., Dong, J., Li, X., Yang, J., & Zhao, D. (2019). The 2012 Flash Drought Threatened US Midwest Agroecosystems. *Chinese Geographical Science*, *29*(5), 768–783. https://doi.org/10.1007/s11769-019-1066-7

Jones, J. W., Tsuji, G. Y., Hoogenboom, G., Hunt, L. A., Thornton, P. K., Wilkens, P. W., Imamura, D. T., Bowen, W. T., Singh, U., Gijsman, A. J., & Ritchie, J. T. (2003). The DSSAT cropping system model. *Europ. J. Agronomy*, *18*, 235–265.

Kaniewski, C. (2021). Understanding Flash Drought Spatial Extent, Duration, and Meteorological Drivers. OpenSIUC. https://opensiuc.lib.siu.edu/theses/2876/

Kaur, R., & Arora, V. K. (2018). Assessing spring maize responses to irrigation and nitrogen regimes in north-west India using CERES-Maize model. *Agricultural Water Management*, *209*, 171–177. https://doi.org/10.1016/j.agwat.2018.07.022.

Keating, B. A., Carberry, P. S., Hammer, G. L., Probert, M. E., Robertson, M. J., Holzworth, D., Huth, N. I., Hargreaves, J. N. G., Meinke, H., Hochman, Z., McLean, G., Verburg, K., Snow, V., Dimes, J. P., Silburn, M., Wang, E., Brown, S., Bristow, K. L., Asseng, S., & Chapman, S. (2003). An overview of APSIM, a model designed for farming systems simulation. European Journal of Agronomy, 18(3), 267–288. https://doi.org/10.1016/S1161-0301(02)00108-9

Khan, A., Pan, X., Najeeb, U., Tan, D. K. Y., Fahad, S., Zahoor, R., & Luo, H. (2018). Coping with drought: Stress and adaptive mechanisms, and management through cultural and molecular alternatives in cotton as vital constituents for plant stress resilience and fitness. *Biol Res*, *51*, 47. https://doi.org/10.1186/s40659-018-0198-z

Kim, K. H., & Lee, B. M. (2023). Effects of Climate Change and Drought Tolerance on Maize Growth. *Plants*, *12*(20), 3548. https://doi.org/10.3390/plants12203548

Kimball, B. A., Boote, K. J., Hatfield, J. L., Ahuja, L. R., Stockle, C., Archontoulis, S., & Williams, K. (2019). Simulation of maize evapotranspiration: An inter-comparison among 29 maize models. *Agricultural and Forest Meteorology*, *27*, 264–284. https://doi.org/10.1016/j.agrformet.2019.02.037

Kiniry, J. R., Burson, B. L., Evers, G. W., Williams, J. R., Sanchez, H., Wade, C., Featherston, J. W., & Greenwade, J. (2007). Coastal Bermudagrass, Bahiagrass, and Native Range Simulation at Diverse Sites in Texas. *Agron. J*, *99*, 450–461. https://doi.org/10.2134/agronj2006.0119

Kisekka, I., Aguilar, J., Rogers, D., Holman, J., O'Brien, D. M., & Klocke, N. (2016). Assessing Deficit Irrigation Strategies for Corn Using Simulation. *Transactions of the ASABE*, *59*, 303–317. https://doi.org/10.13031/trans.59.11206.

Koo, J. (2016). *DSSAT listed as one of the greatest accomplishments of the UF-IFAS - DSSAT.net*. DSSAT.net. https://dssat.net/2164/

Kumar, R., Mishra, S. K., Singh, K., Al-Ashkar, I., Iqbal, M. A., Muzamil, M. N., Habib Ur Rahman, M., & El Sabagh, A. (2023). Impact analysis of moisture stress on growth and yield of cotton using DSSAT-CROPGRO-cotton model under semi-arid climate. *PeerJ*, *11*, 16329. https://doi.org/10.7717/peerj.16329

Kumawat, K. R., & Sharma, N. K. (2018). Effect of Drought Stress on Plants Growth. *Popular Kheti*, *6*, 239–241.

Kuwayama, Y., Thompson, A., Bernknopf, R., Zaitchik, B., & Vail, P. (2019). Estimating the Impact of Drought on Agriculture Using the U.S. *Drought Monitor. American Journal of Agricultural Economics*, *101*, 193–210. https://doi.org/10.1093/ajae/aay037

Lee, R. D., Harris, G., & Murphy, T. R. (2017). *Bermudagrass in Georgia*. University of Georgia extension.

Leeper, R. D., Bilotta, R., Petersen, B., Stiles, C. J., Heim, R., Fuchs, B., Prat, O. P., Palecki, M., & Ansari, S. (2022). Characterizing U.S. drought over the past 20 years using the U.S. drought monitor. *International Journal of Climatology*, *42*, 6616–6630. https://doi.org/10.1002/joc.7653

Lesinger, K., & Tian, D. (2022). Trends, variability, and drivers of flash droughts in the contiguous United States. *Water Resources Research*, *58*, 2022 032186. https://doi.org/10.1029/2022WR032186.

Li, J., Wang, Z., Wu, X., Chen, J., Guo, S., & Zhang, Z. (2020). A new framework for tracking flash drought events in space and time. *Catena*, *194*, 104763. https://doi.org/10.1016/j.catena.2020.104763

Li, M., Du, Y., Zhang, F., Fan, J., Ning, Y., Cheng, H., & Xiao, C. (2020). Modification of CSM-CROPGRO-Cotton model for simulating cotton growth and yield under various deficit irrigation strategies. *Computers and Electronics in Agriculture*, *179*, 105843. https://doi.org/10.1016/j.compag.2020.105843.

Lin, M., Wang, L., Gaoqiang Lv, Gao, C., Zhao, Y., Li, X., He, L., & Sun, W. (2024). Deficit Irrigation Effects on Cotton Growth Cycle and Preliminary Optimization of Irrigation Strategies in Arid Environment. *Plants*, *13*(10), 1403–1403. https://doi.org/10.3390/plants13101403

Liu, X., Yu, Y., Huang, S., Xu, C., Wang, X., Gao, J., Meng, Q., & Wang, P. (2022). The impact of drought and heat stress at flowering on maize kernel filling: Insights from the field and laboratory. *Agricultural and Forest Meteorology*, *312*, 0168–1923. https://doi.org/10.1016/j.agrformet.2021.108733.

Luo, H. H., Zhang, Y. L., & Zhang, W. F. (2016). Effects of water stress and rewatering on photosynthesis, root activity, and yield of cotton with drip irrigation under mulch. *Photosynthetica*, *54*, 65–73. https://doi.org/10.1007/s11099-015-0165-7

Luo, L., Sun, S., Xue, J., Gao, Z., Zhao, J., Yin, Y., Gao, F., & Luan, X. (2023). Crop yield estimation based on assimilation of crop models and remote sensing data: A systematic evaluation. *Agricultural Systems*, *210*, 103711–103711. https://doi.org/10.1016/j.agsy.2023.103711

Maktabi, S. (2022). *Developing a soil moisture Decision Support Tool to quantify the occurrence of flash droughts and saturated soil conditions for pasture grasses in the southeast of the United States,* UNIVERSITÀ DEGLI STUDI DI PADOVA [Thesis]. https://thesis.unipd.it/bitstream/20.500.12608/32685/1/Maktabi_Sara.pdf

Malik, W., Boote, K. J., Hoogenboom, G., Cavero, J., & Dechmi, F. (2018). Adapting the CROPGRO Model to Simulate Alfalfa Growth and Yield. *Agronomy Journal*, *110*, 1777–1790. https://doi.org/10.2134/agronj2017.12.0680

Malik, W., & Dechmi, F. (2019). DSSAT modeling for best irrigation management practices assessment under Mediterranean conditions. *Agricultural Water Management*, *216*, 27-43. https://doi.org/10.1016/j.agwat.2019.01.017.

Manuel, J. (2008). Drought in the Southeast: Lessons for Water Management. *Environ. Health Perspect*, *116*, 168–171.

Marek, G. W., Marek, T. H., Xue, Q., Gowda, P. H., Evett, S. R., & Brauer, D. K. (2017). Simulating Evapotranspiration and Yield Response of Selected Corn Varieties under Full

and Limited Irrigation in the Texas High Plains Using DSSAT-CERES-Maize. *Transactions of the ASABE*, *60*(3), 837–846. https://doi.org/10.13031/trans.12048.

McNider, R. T., Christy, J. R., Moss, D., Doty, K., Handyside, C., Limaye, A., Garcia, G., A., & Hoogenboom, G. (2011). A Real-Time Gridded Crop Model for Assessing Spatial Drought Stress on Crops in the Southeastern United States. *Journal of Applied Meteorology and Climatology*, *50*, 1459–1475. https://doi.org/10.1175/2011JAMC2476.1

Meeks, C. D., Snider, J. L., Babb-Hartman, M. E., & Barnes, T. L. (2019). Evaluating the Mechanisms of Photosynthetic Inhibition under Growth-Limiting, Early-Season Water Deficit Stress in Cotton. *Crop Science*, *59*, 1144–1154. https://doi.org/10.2135/cropsci2018.07.0432

Menefee, D., Rajan, N., Cui, S., Bagavathiannan, M., Schnell, R., & West, J. (2021). Simulation of dryland maize growth and evapotranspiration using DSSAT-CERES-Maize model. *Agronomy Journal*, *113*, 1317–1332. https://doi.org/10.1002/agj2.20524

Mi, N., Cai, F., Zhang, Y., Ji, R., Zhang, S., & Wang, Y. (2018). Differential responses of maize yield to drought at vegetative and reproductive phase. *Plant Soil Environ*, *64*, 260–267. https://doi.org/10.17221/141/2018-PSE.

Migliaccio, K. W., Morgan, K. T., Fraisse, C., Vellidis, G., & Andreis., J. H. (2015a). Performance evaluation of urban turf irrigation smartphone app. *Computers and Electronics in Agriculture*, *118*, 136–142.

Migliaccio, K. W., Morgan, K. T., Fraisse, C., Vellidis, G., Zotarelli, L., Fraisse, C., Zurweller, B. A., Andreis, J. H., Crane, J. H., & Rowland, D. (2015b). Smartphone apps for irrigation scheduling. *Trans of the ASABE*, *59*, 291–301.

Miller, L., Vellidis, G., & Coolong, T. (2018a). Comparing a smartphone irrigation scheduling application with water balance and soil moisture-based irrigation methods: Part II—Plasticulture-grown watermelon. *HortTechnology*, *28*, 362–369.

Miller, L., Vellidis, G., Mohawesh, O., & Coolong, T. (2018b). Comparing a smartphone irrigation scheduling application with water balance and soil moisture-based irrigation methods: Part I—Plasticulture-grown tomato. *HortTechnology*, *28*, 354–361.

Mo, K. C., & Lettenmaier, D. P. (2015). Heat wave flash droughts in decline. *Geophys. Res. Lett*, *42*, 2823–2829. https://doi.org/10.1002/ 2015GL064018

Modala, N. R., Ale, S., Rajan, N., Musnter, C., DeLaune, P., Thorp, K., Nair, S., & Barnes, E. (2015). Evaluation of the CSM-CROPGRO-Cotton model for the Texas Rolling Plains region and simulation of deficit irrigation strategies for increasing water use efficiency. *American Society of Agricultural and Biological Engineers*, *58*, 685–696.

Mozny, M., Trnka, M., Zalud, Z., Hlavinka, P., Nekovar, J., Potop, V., & Virag, M. (2012). Use of a soil moisture network for drought monitoring in the Czech Republic. *Theor. Appl. Climatol*, *107*, 99-111. https://doi.org/10.1007/s00704-011-0460-6.

Muir, J. P., Lambert, B. D., Greenwood, A., Lee, A., & Riojas, A. (2010). Comparing repeated forage bermudagrass harvest data to single, accumulated bioenergy feedstock harvests. *Bioresource Technology*, *101*(1), 200–206.

National Integrated Drought Information System. (2024). Drought in Georgia. https://www.drought.gov/states/georgia

Newman, Y. (2007). Costal vs. “Tifton 85” bermudagrass for horses. Facts & myths. In *University of Florida, IFAS Extension*. http://cflag.ifas.ufl.edu/documents/2007EquineInstit/CoastalvsT-85.pdf

Nguyen, H., Thompson, A., & Costello, C. (2023). Impacts of historical droughts on maize and soybean production in the southeastern United States. *Agricultural Water Management*, *281*, 0378–3774. https://doi.org/10.1016/j.agwat.2023.108237.

Ngwira, A. R., Jens, B., & Thierfelder, A. C. (2014). DSSAT modelling of conservation agriculture maize response to climate change in Malawi. *Soil and Tillage Research*, *143*, 85–94. https://doi.org/10.1016/j.still.2014.05.003

NOAA. (2022). *Flash Drought. National Integrated Drought Information System*. https://www.drought.gov/what-is-drought/flash-drought

Noguera, I., Domínguez-Castro, F., & Vicente-Serrano, S. M. (2020). Characteristics and trends of flash droughts in Spain, 1961–2018. *Annals of the New York Academy of Sciences*, *1472*(1), 155–172. https://doi.org/10.1111/nyas.14365

Onyekwelu, I., & Sharda, V. (2024). Root proliferation adaptation strategy improved maize productivity in the US Great Plains: Insights from crop simulation model under future climate change. *Science of The Total Environment*, *927*, 172205, 0048–9697. https://doi.org/10.1016/j.scitotenv.2024.172205.

Orfanou, A. (2023). *Management and simulation of agronomic practices for pursuing high maize yields in Georgia.* Doctoral dissertation, University of Georgia. https://esploro.libs.uga.edu/esploro/outputs/doctoral/MANAGEMENT-AND-SIMULATION-OF-AGRONOMIC-PRACTICES/9949365847802959#file-0

Otkin, J. A., Svoboda, M., Hunt, E. D., Ford, T. W., Anderson, M. C., Hain, C., & Basara, J. B. (2018). Flash droughts: A review and assessment of the challenges imposed by rapid-onset droughts in the United States. *Bulletin of the American Meteorological Society*, *99*, 911–919. https://doi.org/10.1175/BAMS-D-17-0149.1

Otkin, J. A., Woloszyn, M., Wang, H., Svoboda, M., Skumanich, M., Pulwarty, R., Lisonbee, J., Hoell, A., Hobbins, M., Haigh, T., & Cravens, A. E. (2022). Getting ahead of flash drought: From early warning to early action. *Bull. Amer. Meteor. Soc*, *103*, 2188-2202. https://doi.org/10.1175/BAMS-D-21-0288.1.

Oury, V., Caldeira, C. F., Prodhomme, D., Pichon, J. P., Gibon, Y., Tardieu, F., & Turc, O. (2016a). Is Change in Ovary Carbon Status a Cause or a Consequence of Maize Ovary Abortion in Water Deficit during Flowering? *Plant Physiology*, *171*, 997-1008. https://doi.org/10.1104/pp.15.01130

Oury, V., Tardieu, F., & Turc, O. (2016b). Ovary Apical Abortion under Water Deficit Is Caused by Changes in Sequential Development of Ovaries and Silk Growth Rate in Maize. *Plant Physiol*, *171*, 986-996. https://doi.org/10.1104/pp.15.00268

Paredes, P., Rodrigues, G. J., Petry, M. T., Severo, P. O., Carlesso, R., & Santos Pereira, L. (2018). Evapotranspiration Partition and Crop Coefficients of "Tifton 85" Bermudagrass as Affected by the Frequency of Cuttings. Application of the FAO-56 Dual Kc Model. *Water*, *10*(5), 558. https://doi.org/10.3390/w10050558

Parkash, V., Snider, J. L., Virk, G., Dhillon, K. K., & Lee, J. M. (2024). Diffusional and Biochemical Limitations to Photosynthesis Under Water Deficit for Field-Grown Cotton. *Physiologia Plantarum*, *176*, 14281. https://doi.org/10.1111/ppl.14281

Parton, W.J., Ojima, D.S., Cole, C.V. and Schimel, D.S. (1994). A General Model for Soil Organic Matter Dynamics: Sensitivity to Litter Chemistry, Texture and Management. In Quantitative Modeling of Soil Forming Processes (eds R.B. Bryant and R.W. Arnold). https://doi.org/10.2136/sssaspecpub39.c9

Parton, W. J., Stewart, J. W. B., & Cole, C. V. (1988). Dynamics of C, N, P and S in grassland soils: a model. *Biogeochemistry*, *5*(1), 109–131. https://doi.org/10.1007/bf02180320

Paz, J. O., Woli, P., Garcia, A. G. Y., & Hoogenboom, G. (2012). Cotton yields as influenced by ENSO at different planting dates and spatial aggregation levels. *Agricultural Systems*, *111*, 45-52. https://doi.org/10.1016/j.agsy.2012.05.004.

Pendergrass, A. G., Meehl, G. A., Pulwarty, R., Hobbins, M., Hoell, A., AghaKouchak, A., Bonfils, C. J., Gallant, A. J., Hoerling, M., Hoffmann, D., Kaatz, L., Lehner, F., Llewellyn, D., Mote, P., Neale, R. B., Overpeck, J. T., Shefplot, A., Stahl, K., Svoboda, M., Wheeler, M. C., Wood, A. W. and Woodhouse, C. A. (2020). Flash droughts present a new challenge for subseasonal-to-seasonal prediction. *Nature Climate Change*, *10*(3), 191–199. https://doi.org/10.1038/s41558-020-0709-0

Pequeno, D. N. L., Pedreira, C. G. S., Boote, K. J., Alderman, P. D., & Faria, A. F. G. (2018). Species-genotypic parameters of the CROPGRO Perennial Forage Model: Implications for comparison of three tropical pasture grasses. *Grass Forage Sci*, *73*, 440–455. https://doi.org/10.1111/gfs.12329

Pequeno, D. N. L., Pedreira, C. G. S., Boote, K. J., Alderman, P. D., & Faria, A. F. G. (2018). Species-genotypic parameters of the CROPGRO Perennial Forage Model: Implications for comparison of three tropical pasture grasses. *Grass Forage Sci*, *73*, 440–455. https://doi.org/10.1111/gfs.12329

Perkins, H. F. (1987). *Characterization data for selected Georgia soils*. Georgia Agricultural Experiment Stations, College of Agriculture, University of Georgia.

Peters, T. R., Desta, K., & Nelson, L. (2013). *Practical use of soil moisture sensors and their data for irrigation scheduling*. Washington State University Extension Fact Sheet.

Pinnix, G. D., & Miller, G. L. (2019). Crop Coefficients for Tall Fescue and Hybrid Bermudagrass in the Transition Zone. *Crop, Forage & Turfgrass Management*, *5*, 1-7 190013. https://doi.org/10.2134/cftm2019.02.0013

Price, K. (2017). Thirsty City: Politics, Greed, and the Making of Atlanta's Water Crisis by Skye Borden. *Southeast. Geogr*, *57*, 322–326.

Priestley, C. H. B., & Taylor, J. (1972). On the assessment of surface heat flux and evaporation using large-scale parameters. *Mon. Weather Rev*, *100*, 81–92.

R Core Team. (2023). R: A language and environment for statistical computing. R Foundation for Statistical Computing. https://www.R-project.org/

Ritchie, J. T. (1972). Model for predicting evaporation from a row crop with incomplete cover. *Water Resour. Res*, *8*(5), 1204–1213.

Ritchie, J. T. (1998). Soil water balance and plant stress. In G. Y. Tsuji, G. Hoogenboom, & P. K. Thornton (Eds.), *Understanding options for agricultural production. System approaches for sustainable agricultural development* (pp. 41–54). Kluwer Academic Publishers.

Ritchie, J. T., & Otter, S. (1985). Description and performance of CERES-Wheat: A user-oriented wheat yield model. *ARS Wheat Yield Project*, *38*, 159–175.

Rouquette, F. M., Jr, Anderson, W. F., Harris-Shultz, K. R., & Smith, G. R. (2011). Stand maintenance and genetic diversity of bermudagrass pastures under different grazing management strategies during a 38-year period. *Crop Sci*, *51*(6), 2886–2894.

Rymph, S. J., Boote, K. J., Irmak, A., Mislevy, P., & Evers, G. W. (2004). Adapting the CROPGRO model to predict growth and composition of tropical grasses: Developing physiological parameters. *Soil Crop Sci. Soc. Fla. Proc*, *63*, 37–51.

Sah, R. P., Chakraborty, M., Prasad, K., Pandit, M., Tudu, V. K., Chakravarty, M. K., Narayan, S. C., Rana, M., & Moharana, D. (2020). Impact of water deficit stress in maize: Phenology and yield components. *Sci Rep*, *10*, 2944. https://doi.org/10.1038/s41598-020-59689-7

Sanches, A. C., Souza, D. P., Jesus, F. L. F., Mendonça, F. C., & Gomes, E. P. (2019). Crop coefficients of tropical forage crops, single cropped and overseeded with black oat and ryegrass. *Scientia Agrícola*, *76*(6), 448–458. https://doi.org/10.1590/1678-992x-2017-0386

Scherer, T.F., and Steele, D. D. (2024). Irrigation scheduling by the checkbook method. AE792, North Dakota State University Extension, Fargo, North Dakota, https://www.ndsu.edu/agriculture/sites/default/files/2024-02/ae792.pdf

Sekmen, A. H., Ozgur, R., Uzilday, B., & Turkan, I. (2014). Reactive oxygen species scavenging capacities of cotton (Gossypium hirsutum) cultivars under combined drought and heat induced oxidative stress. *Environ. Exp. Bot*, *99*, 141-149. https://doi.org/10.1016/j.envexpbot.2013.11.010

Seleiman, M. F., Al-Suhaibani, N., Ali, N., Akmal, M., Alotaibi, M., Refay, Y., Dindaroglu, T., Abdul-Wajid, H. H., & Battaglia, M. L. (2021). Drought Stress Impacts on Plants and Different Approaches to Alleviate Its Adverse Effects. *Plants (Basel*, *10*, 259. https://doi.org/10.3390/plants10020259.

Sharda, V., Handyside, C., Cordoba, B., C., & McNider, R. (2017). The Impact of Spatial Soil Variability on Simulation of Regional Maize Yield. *Transactions of the ASABE*, *60*, 2137–2148. https://doi.org/10.13031/trans.12374.

Sharma, V. (2019). *Soil moisture sensors for irrigation scheduling*. University of Minnesota Extension. https://extension.umn.edu/irrigation/soil-moisture-sensors-irrigation-scheduling#sources-1871060

Shen, H., Chen, Y., Wang, Y., Xing, X., & Ma, X. (2020). Evaluation of the Potential Effects of Drought on Summer Maize Yield in the Western Guanzhong Plain, China. *Agronomy*, *10*(8). https://doi.org/10.3390/agronomy10081095

SI CropFit. (2025). SmartIrrigation CropFit app. https://smartirrigationapps.org/cropfit-app/

Smith, H. D., Wilson, C. H., Rymph, S. J., Santos, E. R. S., & Boote, K. J. (2023). Adapting the CROPGRO Perennial Forage model to predict growth and development of Pensacola bahiagrass. *Field Crops Research*, *302*, 109095–109095. https://doi.org/10.1016/j.fcr.2023.109095

Snowden, M. C., Ritchie, G. L., Simao, F. R., & Bordovsky, J. P. (2014). Timing of Episodic Drought Can Be Critical in Cotton. *Agronomy Journal*, *106*, 452–458.

Srinivasan, G., Pazhanivelan, S., Krishnasamy, S. M., Sudarmanian, N. S., Rajeswari, S., & Kannan, B. (2021). Estimating Genetic Parameters for DSSAT CROPGRO-Cotton Model Calibration and Validation. *International Journal of Plant & Soil Science*, 165–172. https://doi.org/10.9734/ijpss/2021/v33i2430764

Steinke, K., Chalmers, D., Thomas, J., & White, R. (2011). Bermudagrass and Buffalograss Drought Response and Recovery at Two Soil Depths. *Crop Sci*, *51*, 1215–1223. https://doi.org/10.2135/cropsci2010.08.0469

Stewart, L., Worley, J. W. and Hancock, D. W., (n.d.). (2014). *Forage systems for stocker cattle*. UGA Cooperative Extension. https://extension.uga.edu/publications/detail.html?number=B1392&title=forage-systems-for-stocker-cattle

Steduto, P., Hsiao, T. C., Raes, D., & Fereres, E. (2009). AquaCrop—The FAO crop model to simulate yield response to water: I. Concepts and underlying principles. *Agronomy journal*, *101*(3), 426-437.

Stone, K. C., Bauer, P. J., Andrae, J., Busscher, W. J., Millen, J. A., Strickland, E. E., & Evans, D. E. (2012). Irrigation and nitrogen impact on bermudagrass yield response in the southeastern coastal plains. *Trans. Am. Soc. Agric. Biol. Eng*, *55*(3), 969–978.

Thorp, K. R., Mareck, G. W., DeJonge, K. C., & Evett, S. R. (2020). Comparison of evapotranspiration methods in the DSSAT Cropping System Model: II. *Algorithm Performance. Computer and Electronics in Agriculture*, *177*, 105679. https://doi.org/10.1016/j.compag.2020.105679.

Tokel, D., Genc, B. N., & Ozyigit., I. I. (2022). Economic impacts of Bt (Bacillus thuringiensis) cotton. *J. Nat. Fibers*, *19*, 4622–4639.

Tubbs, R. S., Harris, G., Sintim, H., Porter, W., Prostco, E., Buntin, D., Kemerait, B., Towes, M., & Smith, A. (2024). *Georgia Corn Production Guide*. University of Georgia Extension. https://grains.caes.uga.edu/content/dam/caes-subsite/grains/docs/corn/2024-Corn-Production-Guide.pdf

Turf.js. (2025). Turf - advanced geospatial analysis for browsers and Node.js. https://turfjs.org/

Tyagi, S., Zhang, X., Saraswat, D., Sahany, S., Mishra, S. K., & Niyogi, D. (2022). Flash drought: Review of concept, prediction and the potential for machine learning, deep learning methods. *Earth's Future*, *10*, 2022 002723. https://doi.org/10.1029/2022EF002723

UGAWN. (2025). *University of Georgia Weather Network*. http://weather.uga.edu

Ullah, A., Sun, H., Yang, X., & Zhang, X. (2017). Drought coping strategies in cotton: Increased crop per drop. *Plant Biotechnol J*, *15*, 271–284. https://doi.org/10.1111/pbi.12688.

USDA-ERS. (2025). *Feed Grains Database*. USDA Economic Research Service. https://data.ers.usda.gov/FEED-GRAINS-custom-query.aspx#ResultsPanel

USDA-ERS. (2025). *Feed Grains Database*. USDA Economic Research Service. https://data.ers.usda.gov/FEED-GRAINS-custom-query.aspx#ResultsPanel

USDA-NASS (2017). *Census of Agriculture*. USDA National Agricultural Statistics Service. https://www.nass.usda.gov/Publications/AgCensus/2017/Full_Report/Volume_1,_Chapter_1_US/usv1.pdf

USDA-NASS (2022). *Census of Agriculture*. USDA National Agricultural Statistics Service. https://www.nass.usda.gov/Publications/AgCensus/2022/Full_Report/Volume_1,_Chapter_1_US/usv1.pdf

USDA-NRCS. (2024). *Web soil survey: USDA natural resources conservation service*. USDA Natural Resources Conservation Service.

Vellidis, G., Liakos, V., Andreis, J. H., Perry, C. D., Porter, W. M., Barnes, E. M., Morgan, K. T., Fraisse, C., & Migliaccio, K. W. (2016). Development and assessment of a smartphone application for irrigation scheduling in cotton. *Computers and Electronics in Agriculture*, *127*, 249–259.

Vellidis, G. (2022). BMPs & precision ag tools in GA: Reducing inputs while maintaining yields. Informational flyer. http://floridanwater.research.ufl.edu/wp-content/uploads/5_GeorgiaBMPsAndPrecisionAg_Infographic2022_Vellidas.pdf.

Voiland, A. (2019). *A Flash Drought Dries the Southeast. NASA Earth Observatory*. https://earthobservatory.nasa.gov/images/145762/a-flash-drought-dries-the-southeast

Volterrani, M., Minelli, A., Gaetani, M., Grossi, N., Magni, S., & Caturegli, L. (2017). Reflectance, absorbance and transmittance spectra of bermudagrass and manilagrass turfgrass canopies. PLOS ONE, 12(11), e0188080. https://doi.org/10.1371/journal.pone.0188080

Walker, D. W., Vergopolan, N., Cavalcante, L., Smith, K. H., Agoungbome, S. M. D., Almagro, A., Apurv, T., Dahal, N. M., Hoffmann, D., Singh, V., & Xiang, Z. (2023). Flash Drought Typologies and Societal Impacts: A. *Worldwide Review of Occurrence, Nomenclature, and Experiences of Local Populations. Wea. Climate Soc*, *16*, 3–28. https://doi.org/10.1175/WCAS-D-23-0015.1.

Wang, L., & Yuan, X. (2018). Two Types of Flash Drought and Their Connections with Seasonal Drought. *Adv. Atmos. Sci*, *35*, 1478–1490. https://doi.org/10.1007/s00376-018-8047-0.

Wang M, Li Y, Ye W, Bornman JF, Yan X (2011). Effects of climate change on maize production, and potential adaptation measures: a case study in Jilin Province, China. Clim Res 46:223–242

Wherley, B., Dukes, M. D., Cathey, S., Miller, G., and Sinclair, T. (2015). Consumptive water use and crop coefficients for warm-season turfgrass species in the southeastern United States. *Agricultural Water Management*, *156*, 10–18. https://doi.org/10.1016/j.agwat.2015.03.020

Woli, P., Jones, J. W., Ingram, K. T., & Fraisse, C. W. (2012). Agricultural Reference Index for Drought (ARID. *Agron. J*, *104*, 287–300. https://doi.org/10.2134/agronj2011.0286

Woli, P., Rouquette, F. M., Jr., Long, C. R., Gowda, P., & Pequeno, D. N. L. (2017). Simulated Bermudagrass Production and Nitrate Leaching Affected by El Niño-Southern Oscillation, Soil, and Clipping Frequency. *Agronomy Journal*, *109*, 2649–2661. https://doi.org/10.2134/agronj2017.05.0268

Woloszyn, M., Skumanich, M., Lisonbee, J., Deheza, V., Hobbins, M., Hoell, A., Otkin, J., Svoboda, M., & Wang, H. (2021). Flash Drought: Current Understanding and Future Priorities. In *Report of the 2020 NIDIS Flash Drought Virtual Workshop. NOAA National Integrated Drought Information System*.

Wright, D., Marois, J., & Rich, J. (2003). Cotton Cultural Practices and Fertility Management: SS-AGR-194/AG200, 9/2003. *EDIS*, *2003*(15). https://doi.org/10.32473/edis-ag200-2003

Wright, D., Small, I., Mackowiak, C., Grabau, Z., Devkota, P., & Paula Moraes, S. (2020). FIELD CORN PRODUCTION GUIDE. University of Florida Extension. https://edis.ifas.ufl.edu/publication/AG202

Yakoub, A., Lloveras, J., Biau, A., Lindquist, J. L., & Lizaso, J. I. (2017). Testing and improving the maize models in DSSAT: Development, growth, yield, and N uptake. *Field Crops Research*, *212*, 95–106. https://doi.org/10.1016/j.fcr.2017.07.002.

You, E., & Vue.js Contributors. (2024). Vue.js [Computer software]. https://vuejs.org/

Yuan, X., Wang, Y., Ji, P., Wu, P., Sheffield, J., & Otkin, J. A. (2023). A global transition to flash droughts under climate change. *Science*, 380,187-191. https://doi.org/10.1126/science.abn630

Zhang, F., Chen, Y., Zhang, J., Guo, E., Wang, R., & Li, D. (2019). Dynamic drought risk assessment for maize based on crop simulation models and multi-source drought indices. *Journal of Cleaner Production*, *233*, 100–114.

Zhou, Y., Lambrides, C. J., & Fukai, S. (2013). Drought resistance of bermudagrass (Cynodon spp.) ecotypes collected from different climatic zones. *Environ. Exp. Bot*, *85*, 22–29.

Zhou, Y., Lambrides, C. J., & Fukai, S. (2014). Drought resistance and soil water extraction of a perennial C4 grass: Contributions of root and rhizome traits. *Funct. Plant Biol*, *41*, 505–519.

Zonta, J. H., Brandao, Z. N., Rodrigues, J. I. D. S., & Sofiatti, V. (2017). Cotton response to water deficits at different growth phase. *Revista Caatinga*, *30*, 980–990.